APPENDIX 13-C
2011 GLACIER MONITORING SUMMARY REPORT

Seabridge Gold Inc.

KSM PROJECT
2011 Glacier Monitoring Summary Report

SEABRIDGE GOLD

Rescan™ Environmental Services Ltd.
Rescan Building, Sixth Floor - 1111 West Hastings Street
Vancouver, BC Canada V6E 2J3
Tel: (604) 689-9460 Fax: (604) 687-4277

November 2012

Executive Summary

The KSM (Kerr-Sulphurets-Mitchell) Project is located in the glacierized Boundary Ranges of the northern Coast Mountains of British Columbia. Rugged topography, high elevations, proximity to the ocean, and location in relation to a robust winter storm track combine to create conditions which support the growth of large alpine glaciers and ice fields.

The ultimate boundaries of the proposed Mitchell pit in the KSM Project area extend under the current terminus of Mitchell Glacier. Assuming glacial recession rates remain constant, it is anticipated that the glacier terminus will be upslope of the proposed Mitchell pit location by the time construction begins. Access to the eastern edge of the Mitchell deposit is currently obstructed by the glacier, and glacier melt will supply substantial runoff over the area of the proposed Mitchell pit. Although Mitchell Glacier has the greatest potential influence on project development and operations, several other proposed project infrastructure components would also be located within glacierized watersheds. In total, thirteen glaciers (or ice fields), including Mitchell Glacier, were identified upstream of proposed Project infrastructure. The glaciers range in size from 0.9 km^2 to 132 km^2 and in elevation from approximately 700 metres above sea level (masl) to near 2,500 masl.

The focus of the 2011 Glacier Monitoring Program was to continue mass balance and glacier dynamic studies initiated on Mitchell Glacier in 2008, and complete the first year of direct mass balance measurements on McTagg South and West, McTagg East, Gingras North and South, and Kerr glaciers. This program included field measurements of end-of-winter accumulation, mid- and end-of-summer ablation, surface velocity measurements, and glacier terminus mapping of Mitchell Glacier. Terminus measurements were conducted for McTagg South and West, McTagg East, Gingras North and South, and Kerr Glaciers in September 2010, and ablation stake networks were installed to allow mass balances to be calculated in 2011. In the 2010 mass balance year (September 2009 - September 2010), the mass balance relationships derived for Mitchell Glacier were extended to estimate seasonal and net mass balance on McTagg South and West, McTagg East, Gingras North and South, and Kerr glaciers. Given that one full year of mass balance data is now available for these glaciers, the first year of direct mass balance measurements can be completed. In addition, the third full year of mass balance measurements are available for Mitchell Glacier.

End-of-winter accumulation on Mitchell Glacier ranged from +0.3 m of water equivalence (w.e.) near to the glacier terminus to +2.4 m w.e. on the upper glacier accumulation zone. Summer ablation was observed to range more than -8 m water equivalence (w.e.) near the terminus of the glacier to -0.6 m w.e. at high elevations. Over the 2011 mass balance year, a glacier-averaged net mass balance of -0.22 m w.e., calculated from point observations made at 27 sites, indicates that the Mitchell Glacier was in disequilibrium, (i.e., negative mass balance) in 2011. This value is more positive than for the 2010 mass balance year (-1.33 m w.e.) and closer to the 2009 glacier-averaged mass balance (-0.04 m w.e.).

Available evidence suggests that Mitchell Glacier is actively flowing, but that recent melt rates at the terminus are sufficient to cause a retreat rate of approximately 48 m/y from September 2010 to September 2011. This rate is greater than the average 2004 to 2008 retreat rate estimated from satellite imagery, and the rates calculated from terminus surveys for the 2009 and 2010 mass balance years. Comparison of historic glacier surface elevation data to current surface elevations suggests that the glacier terminus has thinned by over 100 m since the provincial TRIM I mapping data were created in the early 1990s. A comparison of current areal extent to historical data prior to the early 1990's suggests that the glacier size has remained relatively unchanged in the upper elevations but has been shrinking in the lower elevations.

Annually-averaged glacier velocities were computed from repeat surveys of the ablation stake network on Mitchell Glacier in September 2010 and September 2011. Velocities ranged from approximately 21 m/y at 1,000 masl elevation to 101 m/y at 1,400 m. These flow speeds are very close to those observed in the 2010 mass balance year. Relatively low flow velocities near the terminus indicate that ice loss is primarily due to downwasting of the glacier surface rather than accelerated flow (resulting from the input of summer melt water and basal sliding).

Measurements of glacier mass balance and dynamics at McTagg South and West, McTagg East, Gingras North and South and Kerr glaciers were conducted between September 2010 and September 2011. McTagg East Glacier had the lowest glacier-averaged net mass balance of all glaciers in the monitoring program (-0.66 m w.e.). An estimated 43% of the glacier gained mass over the 2011 mass balance year, and measured summer ablation was more than -4 m w.e. near the terminus. As for Mitchell Glacier, surface velocities are relatively low near the terminus of this glacier, suggesting that this loss of mass occurred primarily due to downwasting of the ice surface.

McTagg South and West, Gingras and Kerr glaciers all had glacier-averaged net mass balances close to neutral (ranging from -0.15 to 0.13 m w.e.). Measured ice loss at low elevations was less at these sites than at Mitchell and McTagg East glaciers, with a net balance of -2.8 m w.e. at McTagg South and West Glacier (at 1,200 masl); -2.7 m w.e. at Gingras North and South Glacier (at 1,425 masl) and -2.0 m w.e. at Kerr Glacier (at 1,425 masl).

Ablation stake velocities were calculated for these glaciers between September 2010 and September 2011. McTagg South and West Glacier had high surface velocities, ranging from 21 to 104 m/yr, which is comparable to Mitchell Glacier. However, unlike Mitchell Glacier, it also has high terminus velocities, which suggests that this glacier responds rapidly to the input of summer melt water, which would lubricate the bed and cause basal sliding. Gingras North and South and Kerr glaciers have low surface velocities, with maximum speeds of only 10 - 14 m/yr.

2011 Glacier Monitoring Summary Report

TABLE OF CONTENTS

LIST OF APPENDICES

LIST OF FIGURES

Figure **Page**

LIST OF TABLES

Table **Page**

LIST OF PLATES

Plate **Page**

Glossary and Abbreviations

Terminology used in this document is defined where it is first used. The following list will assist readers who may choose to review only portions of the document.

$\Delta \mathbf{h_i}$	Net Change in Ice Surface
$\mathbf{B_n}$	Mean Specific Net Balance
$\mathbf{b_n}$	Specific Net Mass Balance
$\mathbf{B_s}$	Mean Specific Summer Balance
$\mathbf{b_s}$	Specific Summer Balance
$\mathbf{B_w}$	Mean Specific Winter Balance
$\mathbf{b_w}$	Specific Winter Balance
$\mathbf{M_i}$	Ice Melt
$\mathbf{M_s}$	Snow Melt
$\boldsymbol{\rho_i}$	Ice Density
$\boldsymbol{\rho_w}$	Water Density
AAR	Accumulation Area Ratio
DEM	Digital Elevation Model
DGPS	Differential Global Positioning Satellite
ELA	Equilibrium Line Altitude
KSM	Kerr-Sulphurets-Mitchell
Landsat	Land Remote Sensing Satellite
LiDAR	Light Detection and Ranging
m w.e.a^{-1}	Metres of water equivalent per year

NAD83	North American Datum 1983
PVC	Polyvinyl Chloride
SPOT 5	Système Pour l'Observation de la Terre (Satellite managed by Spot Image in Toulouse, France)
TRIM	Terrain Resource Information Management
UTM	Universal Transverse Mercator
w.e.	Water Equivalent

1. Introduction

1.1 Project Proponent

The proponent for the KSM (Kerr-Sulphurets-Mitchell) Project is Seabridge Gold Inc. (Seabridge), a publicly traded junior gold company headquartered in Toronto, Ontario, with common shares trading on the Toronto Stock Exchange in Canada and on the New York Stock Exchange in the United States.

1.2 KSM Project Location

The KSM Project is a proposed gold/copper project located in the mountainous terrain of northwestern British Columbia, approximately 950 km northwest of Vancouver, British Columbia, and approximately 65 km north of Stewart, British Columbia (Figure 1.2-1). The proposed Project lies approximately 20 km southeast of Barrick Gold's recently-closed Eskay Creek Mine and 30 km northeast of the Alaska border. The proposed processing plant and Tailing Management Facility (TMF) will be located about 15 km southwest of Bell II on Highway 37.

1.3 KSM Project Description

The proposed Project as defined for the purposes of this environmental baseline study will be comprised of two distinct and geographically separate areas (the Mining Area, Process Plant and TMF; Figure 1.3-1).

The proposed Mining Area is located in the drainage basin of Sulphurets Creek, a major tributary of the Unuk River. It will be accessed by a new road, the Coulter Creek Access Road, to be constructed from the current Eskay Creek Mine road. Four deposits will be mined, the Kerr, Sulphurets, Mitchell and Iron Cap. Ore will be crushed and then transported through one of two parallel 23 km long tunnels to the Process Plant. Non-ore mined (waste) rock will be stored in engineered facilities (rock storage facilities or RSFs) to be located in the Mitchell and McTagg valleys. Surface water that contacts disturbed areas will be collected and treated at a Water Treatment Plant.

The Process Plant and TMF will be located in the upper tributaries of Teigen and Treaty creeks, which flow to the Bell-Irving River. It will be accessed from Highway 37 by a new road parallel to Treaty Creek of which the first three kilometres is an old forest service road. The Process Plant will process up to 130,000 tonnes per day of ore to produce an average of 1,200 tonnes per day of concentrate that will be transported to the port of Stewart by truck. The tailings will be pumped to the TMF, to be located in headless valley situated in the upper reaches of a southern tributary of Teigen Creek and a northern tributary of Treaty Creek.

Figure 1.2-1

SEABRIDGE GOLD
KSM PROJECT

KSM Project Location

Rescan
Engineers & Scientists

PROJECT # 0868-016-06-01 GIS No. KSM-15-263 October 5, 2012

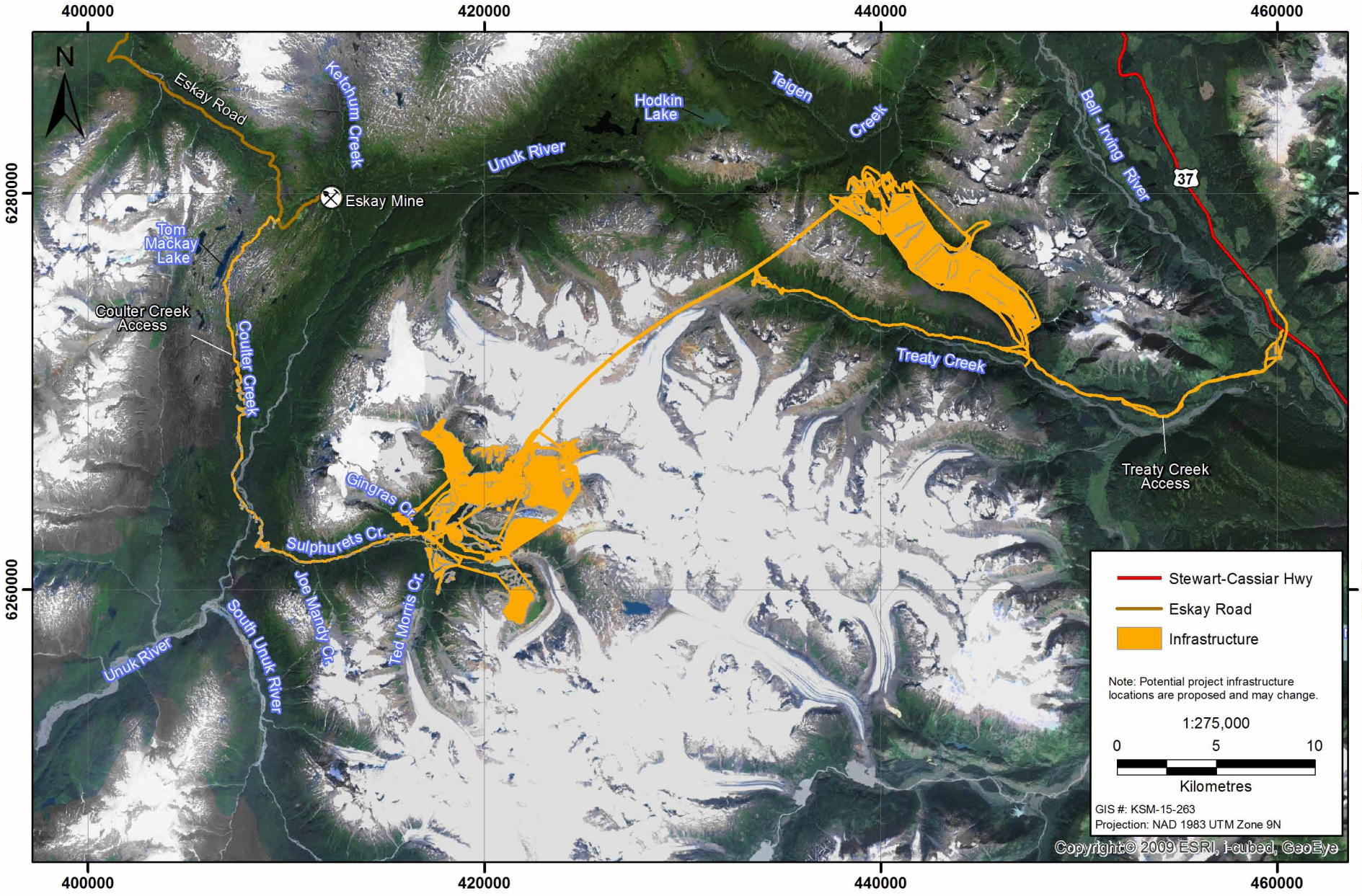

Figure 1.3-1

SEABRIDGE GOLD
KSM PROJECT

2011 KSM Project Layout

Figure 1.3-1

Rescan
Engineers & Scientists

1.4 Glacier Monitoring Program

The KSM Project is located in the glacierized Boundary Ranges of the northern Coast Mountains of British Columbia. Rugged topography, high elevations, proximity to the ocean, and location in relation to a robust winter storm track combine to create conditions which support the growth of large alpine glaciers and ice fields.

The ultimate boundaries of the proposed Mitchell pit in the KSM Project area extend under the current terminus of Mitchell Glacier. Assuming glacial recession rates remain constant, it is anticipated that the glacier terminus will be upslope of the proposed Mitchell pit location by the time construction begins.

Access to the eastern edge of the Mitchell deposit is currently obstructed by the glacier, and glacier melt will supply substantial runoff over the area of the proposed Mitchell open pit. Glaciers can be described as dynamic reservoirs that store water mainly in the form of snow and ice. By considering the inputs (in the form of snow) and the outputs (in the form of melt) of a glacier system on an annual timescale, a glacier mass balance can be assessed. The dynamic behaviour of a glacier, such as patterns of advance and retreat, are linked to the observed mass balance, but operate on longer timescales, and are affected by a number of other factors, such as bedrock topography, accumulation rates, and ice temperatures.

Mountain glaciers experience two seasons during each year: the accumulation season, where snow accumulation, snow redistribution, and avalanches add to the mass of the glacier, and the ablation (or melt) season, where warm temperatures and solar radiation inputs reduce the mass of the glacier through melting and runoff. The mean specific winter balance (B_w) is the total winter accumulation (mass gained) averaged over the entire surface of the glacier. The mean specific summer balance (*Bs*) is the total ablation (mass lost) averaged over the surface of the glacier (B_s is negative by convention). The net mass balance of the glacier (B_n) is the sum of B_w and B_s. While internal accumulation (refreezing of rain and melt water within the snowpack) may contribute to the glacier mass balance, it is difficult to measure. For the 2010 Mitchell Glacier mass balance calculations presented here, internal accumulation is assumed to be negligible in comparison to the magnitude of the surface processes.

Glacier mass balance represents the annual change in glacier mass in response to the temperature and precipitation patterns of a particular year. The long-term response of a glacier to perturbations in the climate/mass balance is the dynamic response, which can be observed through measurements of surface flow velocities, glacier topography, and terminus positions. Glacier flow rates are a product of gravity and mass: snow and ice accumulates at higher elevations, thickens, and eventually flows downhill. However, flow rates are affected by bedrock topography, surface topography, ice thickness, temperature, and melt water drainage systems. Glacier response time is the delay between perturbations in the climate/mass balance and the dynamic response at the terminus. Maritime alpine glaciers are thought to have a fairly rapid response time (Josberger et al. 2007), given their high rate of mass turnover; therefore, glaciers in the vicinity of the KSM Project are expected to have response times on the order of 5 to 50 years.

The KSM Glacier Monitoring Program was initiated in 2008 to provide information on the rates of down-wasting and retreat of Mitchell Glacier, seasonal and annual mass balance estimates and flow velocities. Nearby glaciers were catalogued and hypsometries generated for 12 glaciers that are located upstream or proximal to proposed development. The first annual mass balance was calculated for the Mitchell Glacier in 2009, as well as an annual rate of terminus retreat (Rescan 2009). Multiple linear regression analysis was used to determine the primary meteorological controls on peak stream discharges resulting from high glacier melt rates in 2008 and 2009. Air temperature was found to be the dominant control, with early season (May to July) melt events having a more muted response in comparison with late season (August to September) melt events. The mass balance monitoring program was continued in 2010 (Rescan 2010) and the relationships derived for Mitchell Glacier from the 2010 mass balance year were used to estimate mass balance on the other glaciers in the KSM area.

The following sections present the methods and results from the 2011 Glacier Monitoring Program for the KSM Project area, which included both glacier mass balance and glacier dynamic components.

1.5 Study Objectives

The Project area is located in a glacierized region, and the proposed ultimate boundaries of the Mitchell pit extend slightly beneath the current terminus of Mitchell Glacier. The primary focus of the 2010/2011 field season was to maintain the Glacier Monitoring Program initiated in 2008 through mass balance measurements, surface velocity measurements, and glacier terminus mapping at the Mitchell Glacier. In addition, mass balance measurements were made on four other glaciers upstream of the Project area. McTagg East and McTagg South and West glaciers are located to the west and north-east (respectively) of the proposed Mitchell-McTagg rock storage facility. Gingras North and South Glaciers are located to the west of the Project area, and melt water from this glacier flows south-west, towards the Sulphurets Creek access road. Kerr Glacier is located to the south-west of the proposed Kerr Pit.

Development and maintenance of a monitoring program requires considerable knowledge of the glacier environment and its climatic conditions and the Glacier Monitoring Program continues to evolve in response to new information gained with each field visit. Continuity in glacier monitoring is essential, given the dynamic response times of glaciers and the possibility that observations in any given year may not be representative of general trends.

Objectives of the mass balance component of the Glacier Monitoring Program for 2011 were as follows:

- measure the winter balance in April 2011
- measure the summer balance in September 2011
- determine the net mass for each glacier balance based on these measurements

The 2011 mass balance measurements and calculations (September 2010-September 2011) will provide three consecutive years of data for Mitchell Glacier and the first direct year of observations on the McTagg South and West, Gingras North and South and Kerr Glaciers.

Objectives of the glacier dynamic study for the 2011 season were to repeat the glacier terminus survey conducted in 2008, 2009 and 2010 on Mitchell Glacier and to continue tracking the location of the ablation stake network on all glaciers in order to compute glacier surface velocities.

The potential for rapid advance of glaciers in the KSM region is of particular concern for the proposed mine infrastructure, and the surface velocity and terminus monitoring will provide some indication of the potential for such advance.

2. Study Area

2.1 Monitored Glaciers

In 2010, Mitchell Glacier continued to be the primary study site for the KSM Glacier Monitoring Program. However, in 2010 glacier monitoring was initiated on several additional glaciers within the Sulphurets Creek watershed including the McTagg South and West, McTagg East, Gingras North and South, and Kerr glaciers. The McTagg South and West glaciers share the same glacier terminus, and were considered as one glacier for this report. Similarly, the Gingras North and South glaciers were grouped together. The studied glaciers span the western part of the Project area, and their combined surface area is 29.3 km^2 (Figure 2.1-1).

2.2 Mitchell Glacier

Mitchell Glacier is a medium-sized alpine glacier (approximately 16 km^2) that forms part of what is known as the Unuk Icefield or the Sulphurets Icefield, in north-western British Columbia. Mitchell Glacier was chosen for glacier monitoring due to the location of the proposed Mitchell pit and the potential for glacier-related impacts on mine water diversions, access ramps and related infrastructure. The size and elevation range of Mitchell Glacier is also representative of other glaciers in the region, which will be useful for estimating glacier changes throughout the study area. A ground view of the lower ablation zone of Mitchell Glacier is shown in Plate 2.2-1.

Plate 2.2-1. Ground view across the lower ablation zone of Mitchell Glacier, August 2011.

Mitchell Glacier has two main accumulation basins where new ice is formed from accumulated snowpack and from an inflow of glacial ice from higher-elevation basins. Ice outflow from these main basins coalesce into a westward-flowing valley glacier with a total elevation range of 1,000 to 2,460 masl (Figure 2.1-1). Plateau regions in the upper elevations of Mitchell Glacier join with other glaciers to the north and the south; the unnamed glacier connected through the south-eastern saddle was formerly a tributary of Sulphurets Glacier, located in the valley which contains Sulphurets Lake.

At its terminus, Mitchell Glacier is characterized by ice-cliffs, with an estimated height of approximately 40 to 80 m (Plate 2.2-2). Recent ground penetrating radar surveys support these estimates and indicate an ice thickness of up to 210 m approximately 1.5 km upglacier from the terminus. The ice cliffs are undercut at the base by former and current sub-glacial melt channels, and several calving events (the sudden breaking away of ice) were observed during late-summer field visits between 2009 and 2011.

Plate 2.2-2. Aerial view of the terminus of Mitchell Glacier, September 2010.

Middle sections of Mitchell Glacier are heavily crevassed, and contain numerous icefalls, which are both difficult and hazardous to traverse. Although safe passage is relatively straightforward in spring when several metres of snow cover the glacier, helicopter support is required to access the upper portions of the glacier in summer and fall. The bottom portions can be safely travelled at all times of year by an alert and adequately prepared team, provided that snow and visibility conditions are good. For this reason, ablation stakes were installed along the lower half of Mitchell Glacier, where the absence of substantial crevasses allowed for safe glacier access and travel by field personnel. Similarly, DGPS surveys of glacier extent were focused near the glacier terminus for safety reasons.

PROJECT # 0868-016-06-01 GIS No. KSM-10-147_T November 22, 2012

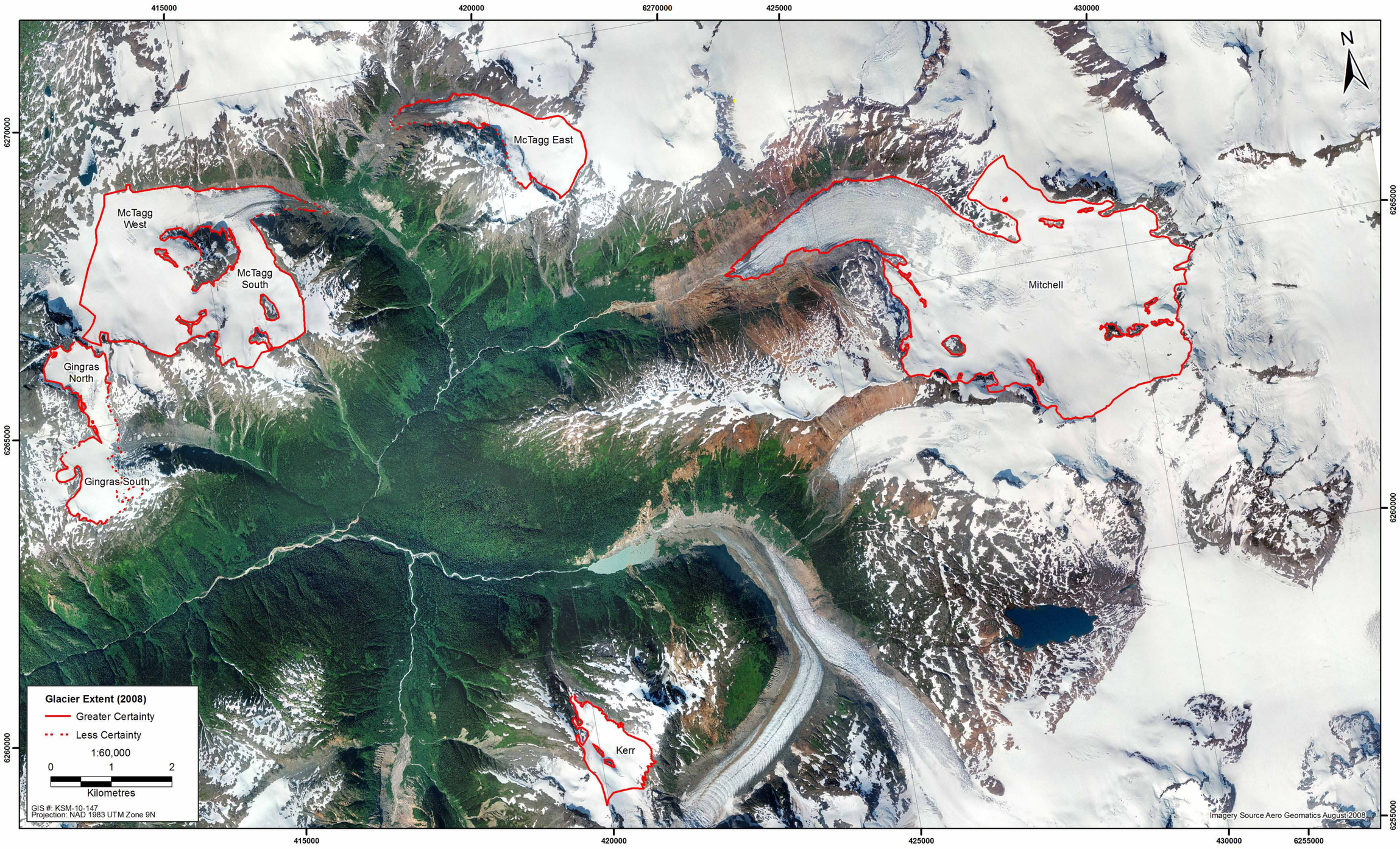

Figure 2.1-1

SEABRIDGE GOLD
KSM PROJECT

Rescan Engineers & Scientists

KSM Project 2011
Glacier Study Area

2.3 McTagg, Gingras and Kerr Glaciers

McTagg South and West Glacier is approximately 7.6 km^2 in area, ranging in elevation from 960 to 2,000 masl, with the proportional area within each elevation band increasing steadily up to 1,800 masl. The two glacier arms converge near the terminus at approximately 1,250 masl (Plate 2.3-1). An icefall is located at approximately 1,600 masl, and a steep roll-over at 1,500 masl results in a heavily crevassed zone.

McTagg East Glacier is approximately 2.1 km^2 in area, ranging in elevation from 1,010 to 1,900 masl, with the majority of this area located between 1,500 and 1,800 masl. No major icefalls are located on this glacier; however, the steep south-facing slopes above the glacier will increase the avalanche hazard during the spring (Plate 2.3-2).

Plate 2.3-1. Aerial view of McTagg South (left) and West (right) Glaciers, August 2010.

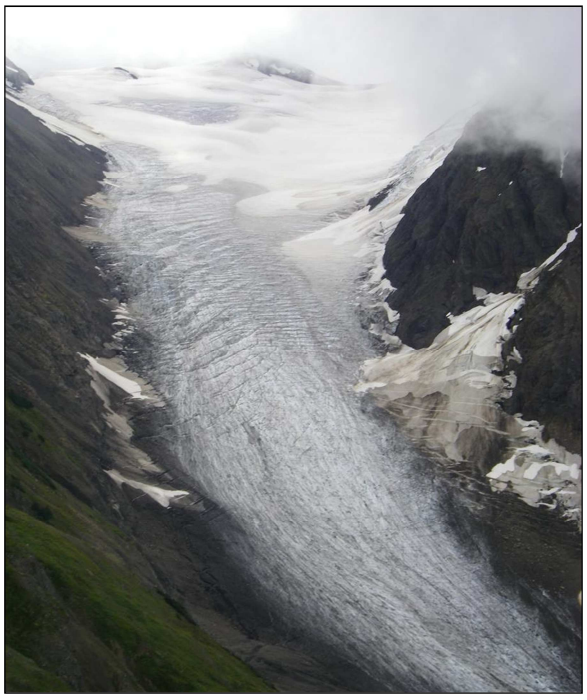

Plate 2.3-2. Aerial view of McTagg East Glacier, August 2010.

Gingras North and South Glacier is approximately 2.1 km^2 in area, ranging from 1,390 masl at the terminus to 2,100 masl at the highest elevations. The glacier comprises a north arm that is heavily crevassed between 1,640 and 1,780 masl (Plate 2.3-3) and a larger south arm with moderate slope (Plate 2.3-4).

Kerr Glacier is approximately 1.1 km^2 in area, ranging from 1,320 masl at the terminus to 2,050 masl at the highest elevations. It is a steep north-facing pocket glacier located west of and above Sulphurets Glacier (Plate 2.3-5).

Plate 2.3-3. Aerial view of the north arm of Gingras Glacier, August 2010.

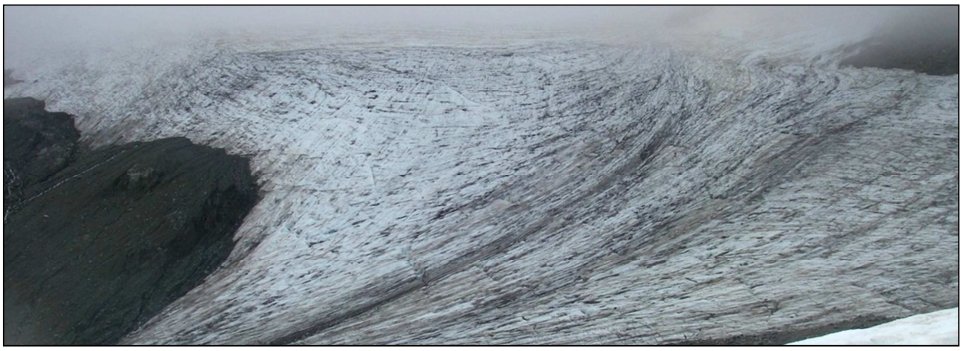

Plate 2.3-4. Gingras South Glacier viewed from Gingras North, September 2010.

Plate 2.3-5. View south on Kerr Glacier from approximately 1,575 masl elevation, September 2010.

3. Methods

3.1 Glacier Delineation

In 2008, the extent of the Mitchell Glacier was delineated from a composite of Landsat and SPOT 5 images taken in 2002 and 2004, respectively. Surface hydrological divides and operator discretion were used to map the extents of the Mitchell Glacier at high elevations, and a digital elevation model (DEM) of the Mitchell Glacier at 20 m resolution was extracted from TRIM data using the digitized glacier extents. From the DEM a glacier hypsometry (i.e., distribution of surface area by elevation) was generated. The original TRIM DEM was updated in 2009 by adjusting the glacier surface elevations based on the 2009 DGPS survey of the ablation stake locations and in 2010 by adjusting the glacier extent based on the 2010 DGPS survey of the terminus position.

The TRIM DEMs for the McTagg South and West, McTagg East, Gingras North and South and Kerr Glaciers were adjusted using the 2010 DGPS terminus surveys in order to calculate glacier hypsometries, as well as to provide the basis for the distributed mass balance estimates for 2011.

3.2 Glacier Mass Balance

Elevation exerts an important control on accumulation and ablation processes, due to the dependence of both temperature and precipitation on elevation. Snow accumulation is generally greatest at high elevations due to orographic enhancement and the frontal dynamics of weather systems in the study area. Melt is generally greatest at low elevations due to warmer temperatures and the earlier exposure of glacier ice after melting of the winter snowpack; glacier ice absorbs more than twice as much solar radiation as fresh snow, resulting in enhanced melt rates. While variations in accumulation and ablation will occur in horizontal directions, a monitoring network that exploits their dependence on elevation is sufficient to describe the majority of the spatial variability in mass balance.

There are several methods for measuring glacier mass balance, each with its own benefits and drawbacks. A brief summary is shown in Table 3.2-1. Most glacier mass balance monitoring conducted in Canada uses the glaciological method of measurement (Østrem and Brugman 1991), and this was the primary method selected for the KSM Glacier Study. However, components of the geodetic and index methods were also incorporated to provide some perspective on the historical mass balance of glaciers studied, and help place results from the current observation program in perspective.

The glaciological method used for determining the mass balance of Mitchell Glacier involved measuring the accumulation of snow during the winter and the change in snow depths and ice surface heights over the summer. As Mitchell Glacier is an elongated valley glacier where mass balance is primarily controlled by elevation, monitoring locations were distributed along the vertical mid-line of the glacier. A glaciological year runs from October to September of the

following year, and the mass balance year from October 2009 to September 2010, for example, is referred to as the 2010 balance year.

Table 3.2-1. Summary of Glacier Mass Balance Measurement Methods

Method	Details	Summary
Index Methods: Terminus position, area changes, equilibrium line altitude (ELA)	Ground surveys, air photos, remote sensing	Changes in mass balance and ice flow can be observed through changes in the terminus position, though the relationship is complex and it requires extensive knowledge of the glacier flow dynamics. The equilibrium line altitude (ELA) is also a response to mass balance conditions, and knowledge of the relationship between the two is necessary before it can be used as an index.
Glaciological Method	Ablation stake network, snow depth probing, and density pits	Measurements of surface lowering (ice melt) are made at ablation stakes installed across a range of elevations in the ablation zone, and end-of-summer snow depth and density sampling at the higher elevations yields an estimate of the summer balance. Winter accumulation totals are sampled over the entire elevation range of the glacier using snow probing and density measurements in early- to mid-May.
Hydrological Method	Measurement of precipitation, evaporation, groundwater, and runoff for glacier watershed.	Measurements of water input and output allow for the calculation of net storage within the glacier system. Accurate precipitation and groundwater measurements are difficult or impossible to obtain, and changing morphology of pro-glacial streams makes stream flow measurements challenging.
Geodetic Method	Ground surveys, topographic maps, air photos, remote sensing, LiDAR	Measurement of the topographic change of the glacier surface to determine volumetric change. Sufficiently accurate methods require expensive high-resolution data such as LiDAR.

At any point on the glacier, the specific net mass balance (b_n) is the sum of the winter accumulation (b_w) and summer ablation (b_s, negative by convention), all with units of metres of water equivalent (m w.e.):

$$b_n = b_w + b_s \qquad [1]$$

Point mass balance observations are denoted by a lower-case *b*. Winter accumulation is affected by avalanching, wind redistribution, changes in precipitation type (rain versus snow), and orographic enhancement. Accumulation can thus exhibit a high spatial variability, with the majority of the variability due to elevation. Summer ablation is determined primarily by air temperature and absorbed solar radiation. Spatial patterns of melt are dominated by the decrease in temperature with elevation, as well as variations in radiation absorption related to shading, albedo, surface slope and aspect. Initial distributions of snow can also play a large role; before ice melt can begin,

the snow cover must be completely removed, and the high reflectivity (albedo) of snow reduces the absorption of solar radiation.

3.2.1 Winter Balance

Winter balances are calculated through observations of snow depth (d_s) and snow density (ρ_s), from which a snow water equivalent (SWE, in m) can be calculated:

$$b_w = d_s \bullet \rho_s / \rho_w \qquad [2]$$

where ρ_w is the density of water (1.000 kg/m^3).

Field observations of snow depth and density were collected on each glacier in April 2011 (Plates 3.2-1 and 3.2-2). Snow pits were excavated between the terminus and the upper basins and snow densities were continuously sampled throughout the entire depth of each pit and integrated to determine the total SWE at each pit location. Snow densities below 2 m were measured with a Federal Snow Tube. As density varies with snow depth, a function describing the relationship between depth and density was determined so that snow density could be estimated over the entire glacier surface.

Plate 3.2-1. Measuring snow density at McTagg West Glacier (1,700 masl) in April 2011.

Snow depths were probed at numerous locations in the upper basins of each glacier (see Chapter 4, Figures 4.2-1 to 4.2-5 for maps indicating all snow depth sites). Between three and six depth measurements were made at each location and the average snow depth computed.

A relation between elevation and snow depth was determined based on these field observations in order to estimate snow depth over the entire glacier surface.

Plate 3.2-2. Probing snow depths in the upper accumulation basin of McTagg West Glacier, April 2011.

With established relations between 1) snow depth and elevation and 2) snow depth and density, winter balance b_w was estimated over the glacier surface from Equation [2] and the DEMs of each glacier. The glacier averaged winter balance B_w was then calculated by integrating the estimated specific winter balance for each DEM grid cell, and dividing by the total area of the glacier (A):

$$B_w = \frac{1}{A}\int b_w \qquad [3]$$

3.2.2 Summer Balance

Summer ablation is the combined loss of both snow and ice during the melt season, which typically lasts from May to September. Snow melt (M_s) is calculated by subtracting the observed end-of-summer SWE from the observed winter balance (b_w) at a given location. If the ice surface has been exposed, then $M_s = b_w$. Above the end-of-summer snowline, $M_s < b_w$, and observations of end-of-summer snow depth and density are required to estimate the remaining SWE.

Ice melt (M_i) is measured using stakes (referred to as ablation stakes) which are drilled into the ice. The base of the stake remains fixed relative to changes in the height of the surface (Figure 3.2-1). Total ice melt (in m w.e.) is calculated by converting the depth of ice melt (Δd_i in m) to water equivalence following:

$$M_i = \Delta d_i \frac{\rho_i}{\rho_w} \quad [4]$$

where ρ_i is the density of ice (900 kg/m^3; Paterson 1994).

Ablation stakes consist of two 2 m PVC poles were attached with cable ties and placed in holes at each ablation stake location (Plates 3.2-3 and 3.2-4). Ablation stake holes were hand-drilled to a depth of approximately 4 m on each site visit. These stakes were measured and re-drilled where necessary in both July and September 2011. In September 2011, snow depth measurements were conducted above the end-of-summer snowline and density pits were excavated to estimate summer snow melt.

Plate 3.2-3. Ablation stake, MI-1000, in August 2011 before re-drilling (after a substantial amount of surface lowering).

The summer balance (b_s) at a specific point was calculated by:

$$b_s = M_s + M_i \quad [5]$$

Glacier-averaged summer mass balance (B_s) was calculated by integrating the specific summer mass balance estimated for each DEM grid cell and dividing by the total area A, as in Equation [3].

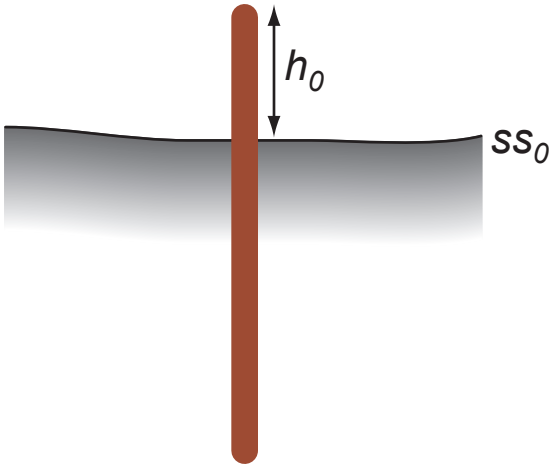

1. When the ablation stake is installed, its intial height (h_0) above the end-of-summer surface (ss_0) is measured.

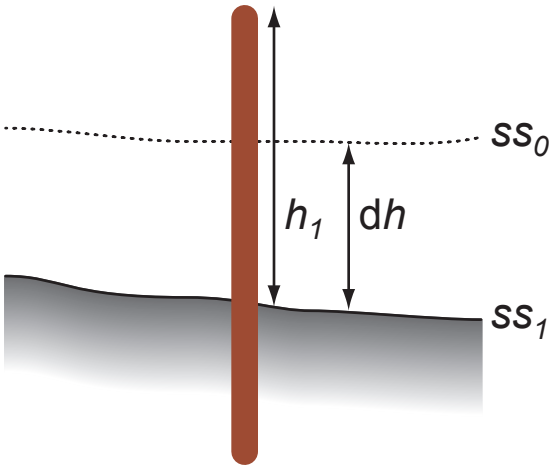

2. On subsequent visits, the new height of the stake (h_1) is measured, allowing for the calculation of net surface lowering (dh = h_1 - h_0). The stake will then be redrilled, and a new intial height above the surface will be recorded.

SEABRIDGE GOLD
KSM PROJECT

Use of Ablation Stakes in Measuring Summer Mass Balance

Figure 3.2-1

Rescan™ Engineers & Scientists

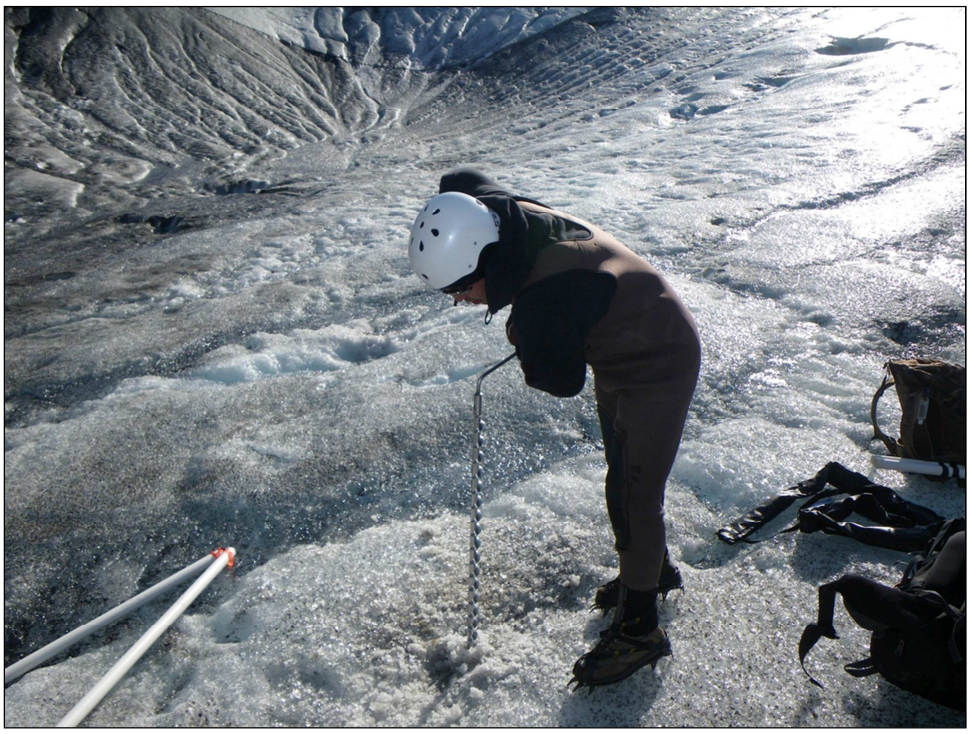

Plate 3.2-4. Ablation stake, MI-900 being redrilled level with the ice surface in August 2011.

3.2.3 Summary of Ablation Stake Sites

In September 2008, ablation stakes were installed at eight sites on Mitchell Glacier and two additional stakes were added in July 2009 and September 2010 (Table 3.2-2). In September 2010, 10 additional stakes were installed on McTagg West and South Glaciers between 1,040 and 1,625 m; six ablation stakes were installed between 1,150 and 1,600 masl on McTagg East Glacier; five stakes were installed on Gingras North and South Glacier between 1,400 and 1,600 masl, and four stakes were installed between 1,425 and 1,650 masl on Kerr Glacier (Table 3.2-2). All stakes are located below the end-of-summer snowline, also known as the equilibrium line altitude (ELA), and maps of ablation stake locations are provided in Chapter 4 (see Figures 4.2-1 to 4.2-5).

3.2.4 Glacier-averaged Mass Balance

Mass balance values estimated for each grid cell (in m w.e.) were multiplied by the area of each grid cell (20 by 20 m) to calculate a volume (in m^3 w.e.). Volumes for b_w, b_s, and b_n in each grid cell were then summed over the entire glacier and divided by the total area of the glacier to obtain the glacier-averaged mass balance. Although the total glacier mass balance is frequently expressed as a volume, the glacier-averaged mass balance is more intuitive, and it allows for comparisons between glaciers and time periods.

Table 3.2-2. Overview of Ablation Stake Network from 2008 to 2011

Glacier	Ablation Stake	Installation	Comments
Mitchell	MI-900	Sep 2010	New installation in 2010
	MI-925	Sep 2008	Could not be located in 2009, presumed lost due to avalanche
	MI-960	Sep 2008	Replaced MI-925 in July 2009, Melted out in summer 2009, reinstalled Sep 2009
	MI-1000	Jul 2009	Melted out in 2009
	MI-1100	Sep 2008	Located in crevasse in 2009, reinstalled Sep 2009
	MI-1200	Sep 2008	No issues to comment on
	MI-1300	Sep 2008	No issues to comment on
	MI-1400	Sep 2008	No issues to comment on
	MI-1450	Sep 2008	No issues to comment on
	MI-1525	Sep 2008	Relocated locally in 2010 due to crevasses formation
McTagg South	MS-1440	Sep 2010	No issues to comment on
	MS-1500	Sep 2010	No issues to comment on
McTagg West	MW-1040	Sep 2010	No issues to comment on
	MW-1200	Sep 2010	No issues to comment on
	MW-1250	Sep 2010	No issues to comment on
	MW-1325	Sep 2010	No issues to comment on
	MW-1440	Sep 2010	No issues to comment on
	MW-1500	Sep 2010	No issues to comment on
	MW-1575	Sep 2010	No issues to comment on
	MW-1625	Sep 2010	No issues to comment on
McTagg East	ME-1150	Sep 2010	No issues to comment on
	ME-1225	Sep 2010	No issues to comment on
	ME-1300	Sep 2010	No issues to comment on
	ME-1400	Sep 2010	No issues to comment on
	ME-1550	Sep 2010	Stake not located in Sep 2011
	ME-1600	Sep 2010	No issues to comment on
Gingras	GS-1400	Sep 2010	No issues to comment on
	GN-1425	Sep 2010	No issues to comment on
	GS-1500	Sep 2010	No issues to comment on
	GS-1600A	Sep 2010	No issues to comment on
	GS-1600B	Sep 2010	No issues to comment on
Kerr	KG-1425	Sep 2010	No issues to comment on
	KG-1500	Sep 2010	No issues to comment on
	KG-1575	Sep 2010	No issues to comment on
	KG-1650	Sep 2010	No issues to comment on

3.3 Glacier Dynamics

A primary safety concern in heavily glacierized terrain is the possibility of rapid glacial advances, such as surges (where velocities are orders of magnitude greater than normal velocities), that could affect infrastructure located near glacier termini. The factors contributing to alpine glacier surges are complex: glacier bed topography, subsurface hydrological drainage characteristics, and antecedent mass balance conditions are all contributing factors (Raymond 1987), but these parameters are difficult or impossible to measure. Surging glaciers are also not limited to a particular geographic region: they have been identified in Alaska, the Yukon, and northwest British Columbia, as well as the Arctic, South America, and in the Himalayas (Benn and Evans 1998).

Surface features that are indicative of surge-type glaciers include heavy crevassing, intense folding visible at the surface and looped medial moraines (Copland et al. 2003). Other investigators have suggested that long glaciers with low slope angles have a higher probability of being surge-type glaciers in comparison with short glaciers, which will generally have a greater slope angle (Clarke 1991). These generalizations are useful in the context of examining the potential for glacier surges in the KSM region, but cannot be considered as rules.

In order to quantify the rate of retreat or ablation of Mitchell, McTagg South and West, McTagg East, Gingras North and South, and Kerr Glaciers, the following methods were used:

- annual differential GPS (DGPS) surveys of the terminus
- annual DGPS surveys of the ablation stake network
- field-based evidence for glacier flow
- TRIM data analysis

Surveys of Mitchell Glacier terminus using DGPS were conducted in September 2008, 2009, 2010, and 2011. Surveys of McTagg South and West, McTagg East, Gingras North and South, and Kerr glaciers were also conducted in September 2010. Using a sampling interval of one second, location coordinates were recorded as a surveyor walked along the terminus margins. Safety concerns of collapsing ice cliffs limited the extent to which the terminus was mapped in all years, but the data collected provide a benchmark for future terminus mapping and comparison. To reduce some of the uncertainty introduced by the safety concerns, a rangefinder was used in 2010 to determine the distance to the glacier snout where it was unsafe to walk immediately along the terminus.

To estimate glacier flow velocities, the locations of ablation stakes were surveyed after initial installation in July and September of each year (Plate 3.3-1). The DGPS unit was operated for approximately one minute at each stake using a sampling interval of one second, yielding approximately 60 points for each site.

The DGPS data collected in the field was post-processed and corrected using an off-site base station. From the corrected data at each stake, an average location was calculated. The change in stake position (in the easting and northing directions, in metres) was calculated by subtracting

the 2010 coordinates from the 2011 coordinates. Total displacements (and flow velocities) were calculated using trigonometry, with an estimated horizontal error of one metre.

Plate 3.3-1. Conducting ablation stake maintenance near the terminus of Mitchell Glacier, June 2011.

4. Results

4.1 Glacier Delineation and Hypsometries

4.1.1 Delineation

The TRIM DEM for each glacier was adjusted using the methodology described in the 2009 KSM Glaciology Report (Rescan 2010). Mitchell Glacier extent and adjusted DEM are presented in Figures 4.1-1 and 4.1-2. The adjusted DEM has a minimum elevation of 928 masl and a maximum elevation of 2,461 masl (Figure 4.1-2). The terminus of Mitchell Glacier (Plate 4.1-1) represents a relatively small amount of the total area. The terminus area (east of the UTM 426000 grid line) was 11% of the total glacier area in 2009. Recent glacier thinning and terminus retreat has reduced the terminus area compared to previous years (see Section 4.3-1 and Figure 4.3-1).

Plate 4.1-1. Lower Mitchell Glacier, July 2011.

In 2010, the same delineation methods were used for McTagg South and West (Figure 4.1-3), McTagg East (Figure 4.1-4), Gingras North and South (Figure 4.1-5) and Kerr (Figure 4.1-6) glaciers.

4.1.2 Hypsometries

Glacier hypsometry describes the elevation distribution by unit area and plays an important role in determining glacier-averaged mass balance. The glacier hypsometries calculated from the adjusted DEMs are presented in Figures 4.1-7 and 4.1-8.

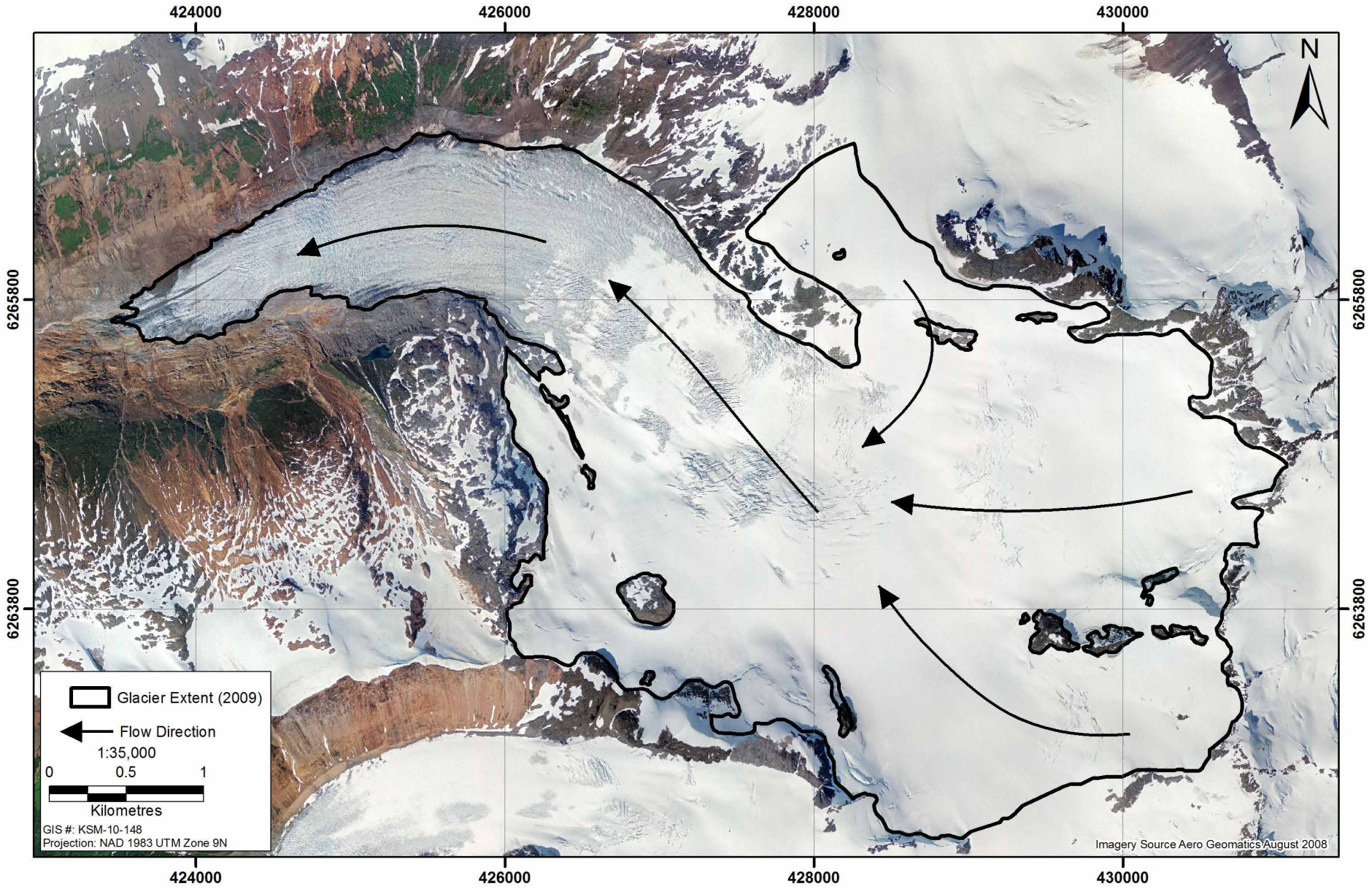

Figure 4.1-1

SEABRIDGE GOLD
KSM PROJECT

Mitchell Glacier Flow Divisions and Mapped Extent

Figure 4.1-1

Rescan
Engineers & Scientists

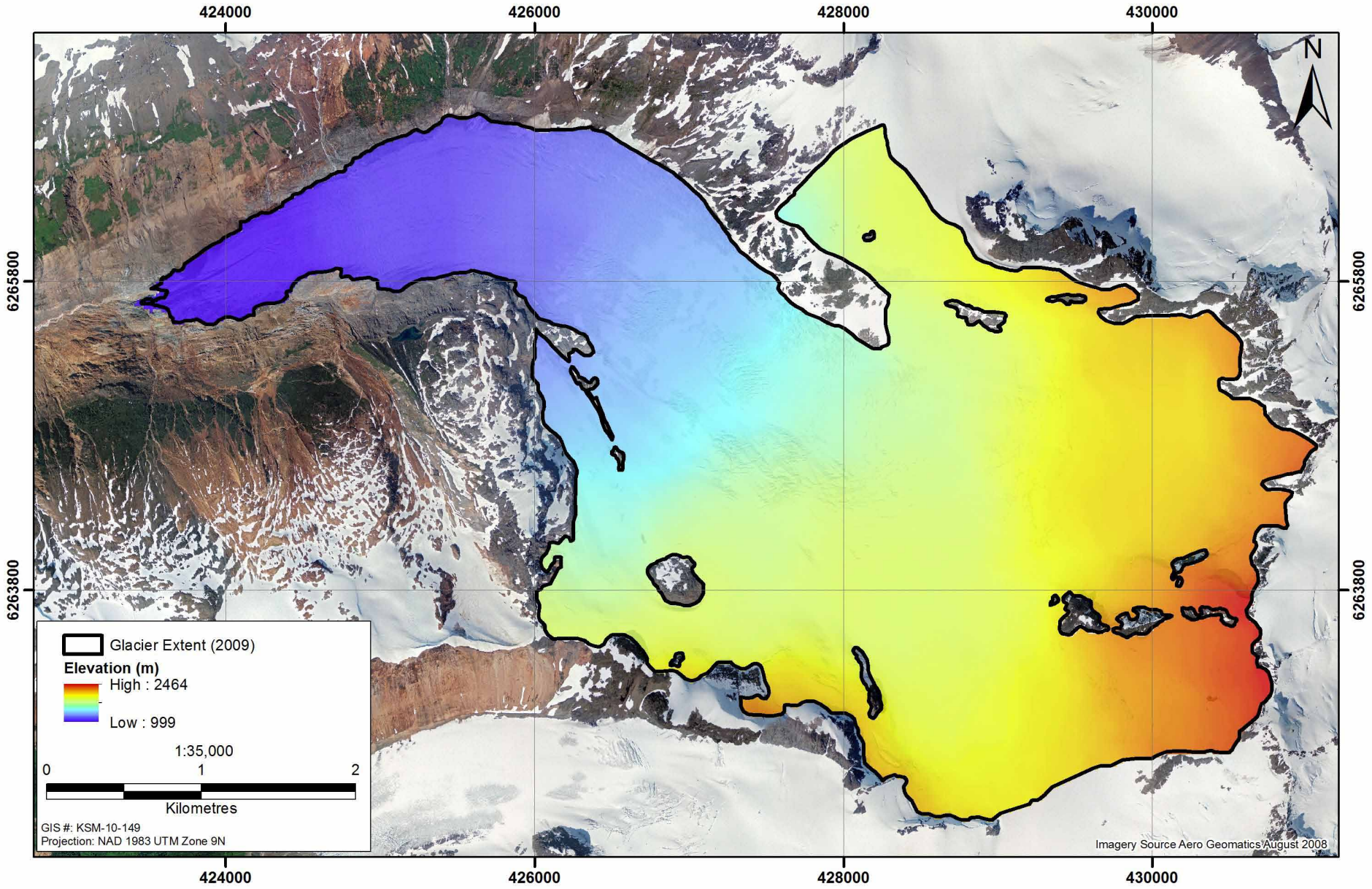

Figure 4.1-2

SEABRIDGE GOLD
KSM PROJECT

Mitchell Glacier Adjusted Digital Elevation Model

Figure 4.1-2

Rescan Engineers & Scientists

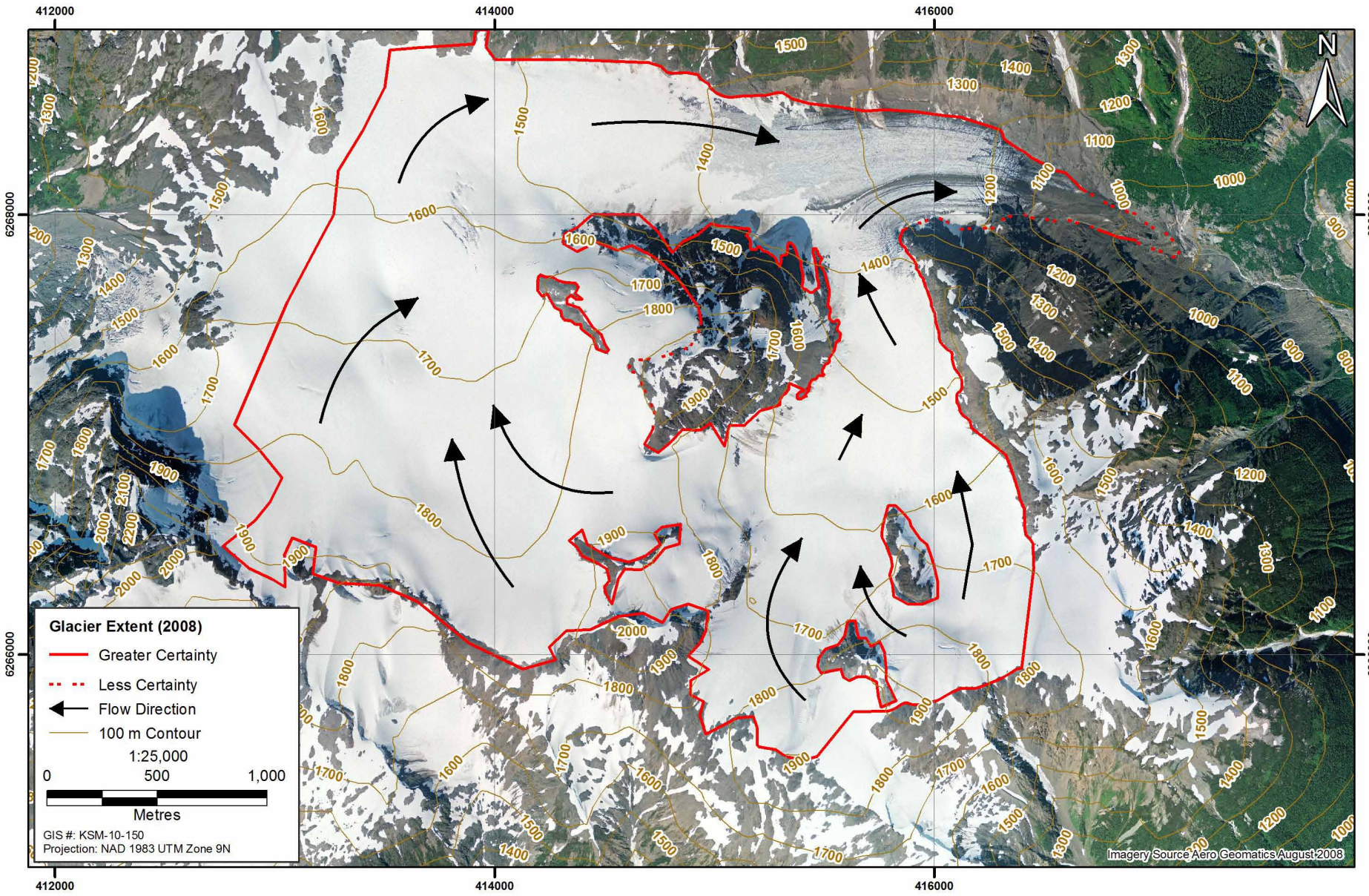

Figure 4.1-3

SEABRIDGE GOLD
KSM PROJECT

McTagg South and West Glacier Flow Divisions and Mapped Extent

Figure 4.1-3

Rescan
Engineers & Scientists

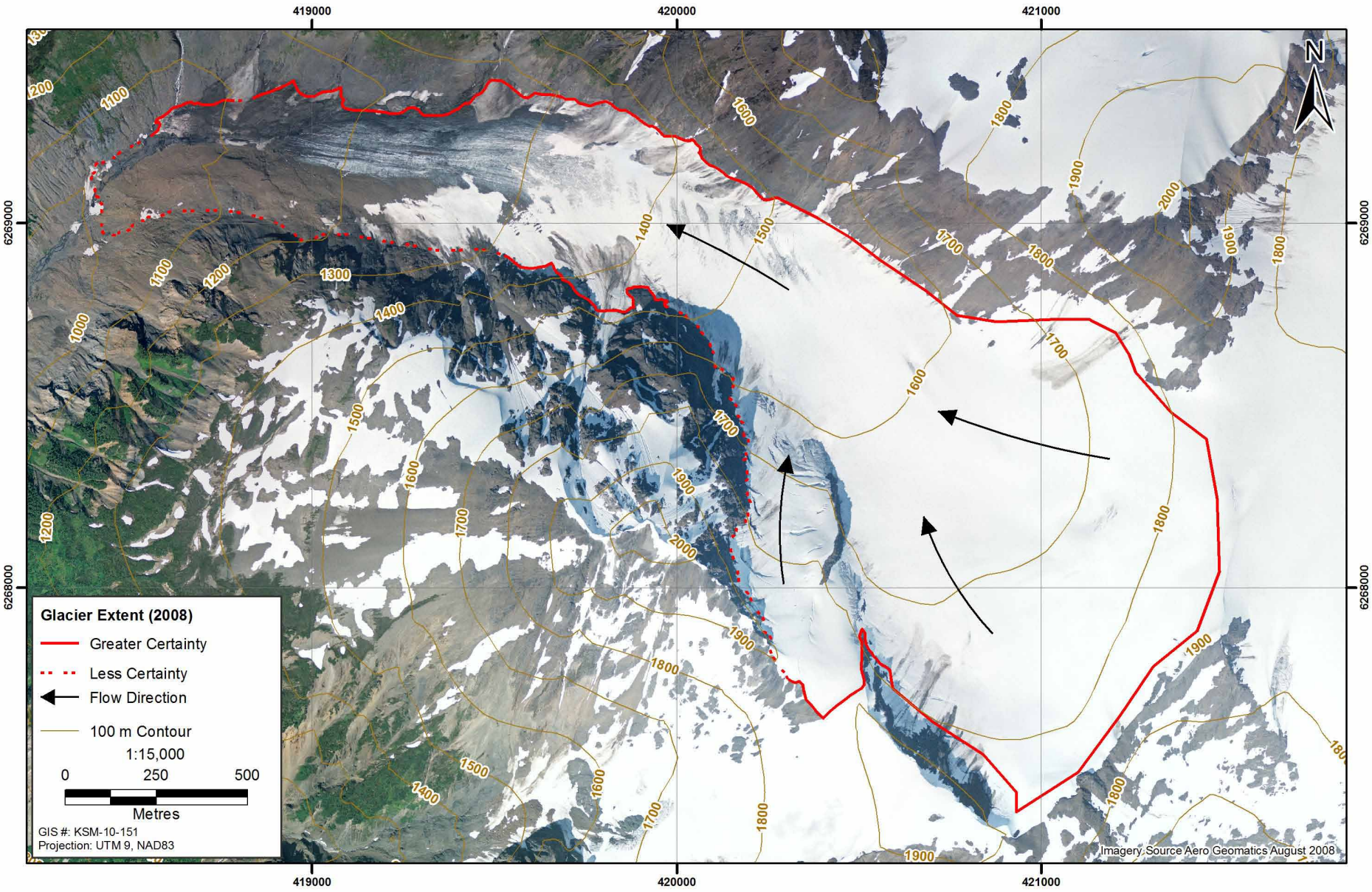

Figure 4.1-4

SEABRIDGE GOLD
KSM PROJECT

McTagg East Glacier Flow Divisions and Mapped Extent

Figure 4.1-4

Rescan
Engineers & Scientists

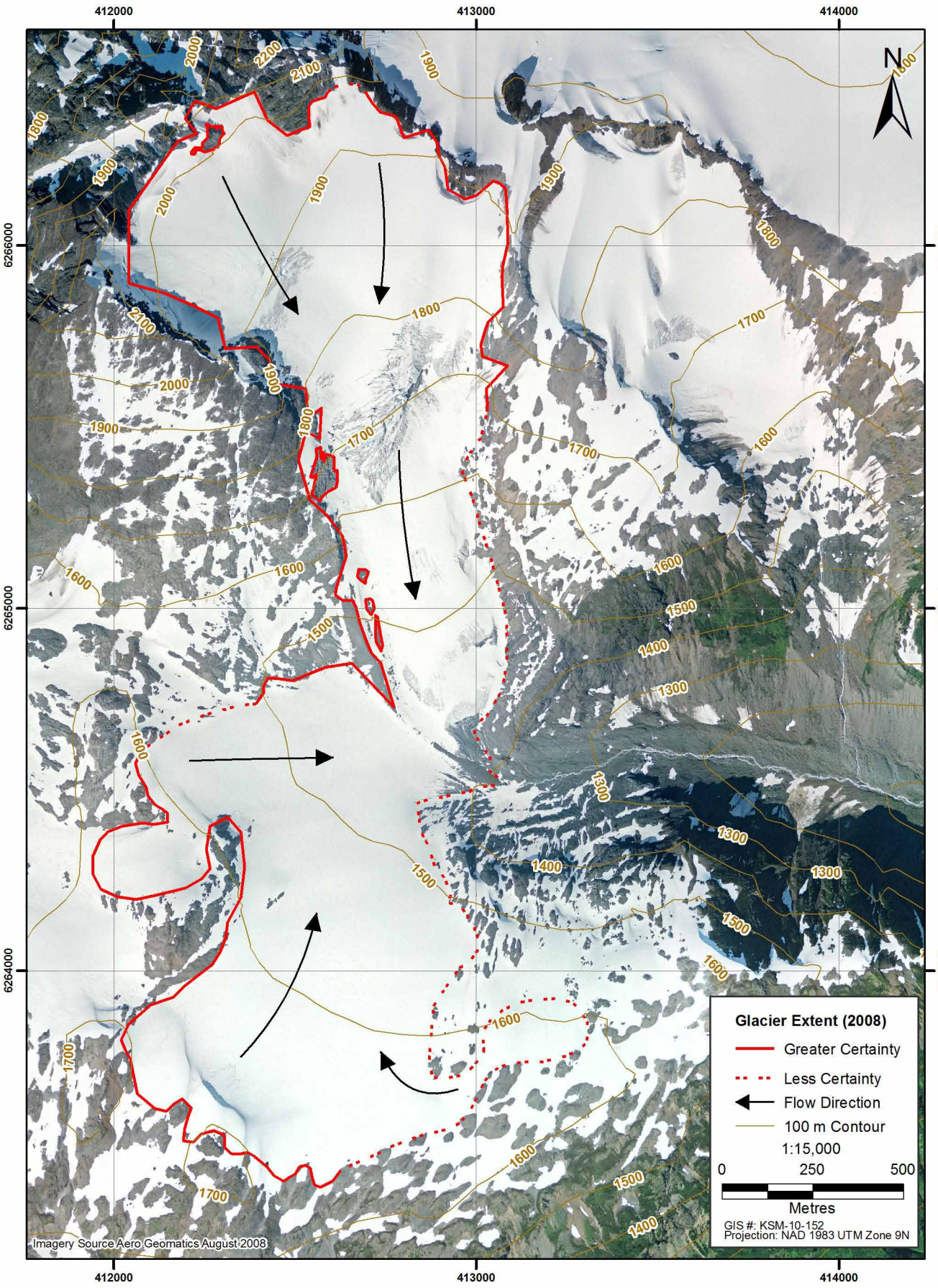

Figure 4.1-5

Gingras North and South Glacier Flow Divisions and Mapped Extent

SEABRIDGE GOLD
KSM PROJECT

Rescan
Engineers & Scientists

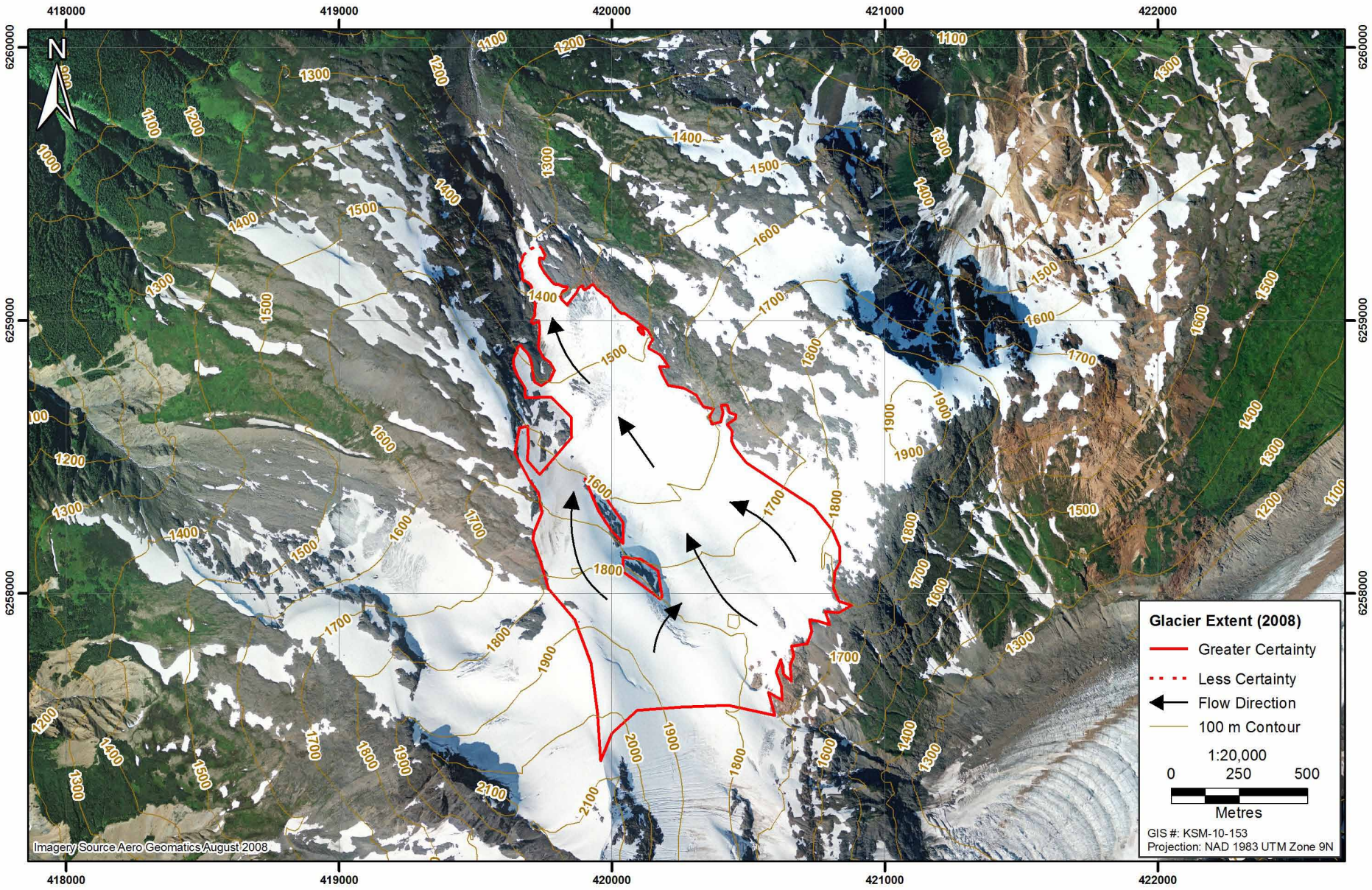

Figure 4.1-6

SEABRIDGE GOLD
KSM PROJECT

Kerr Glacier Flow Divisions and Mapped Glacier Extent

Figure 4.1-6

Rescan
Engineers & Scientists

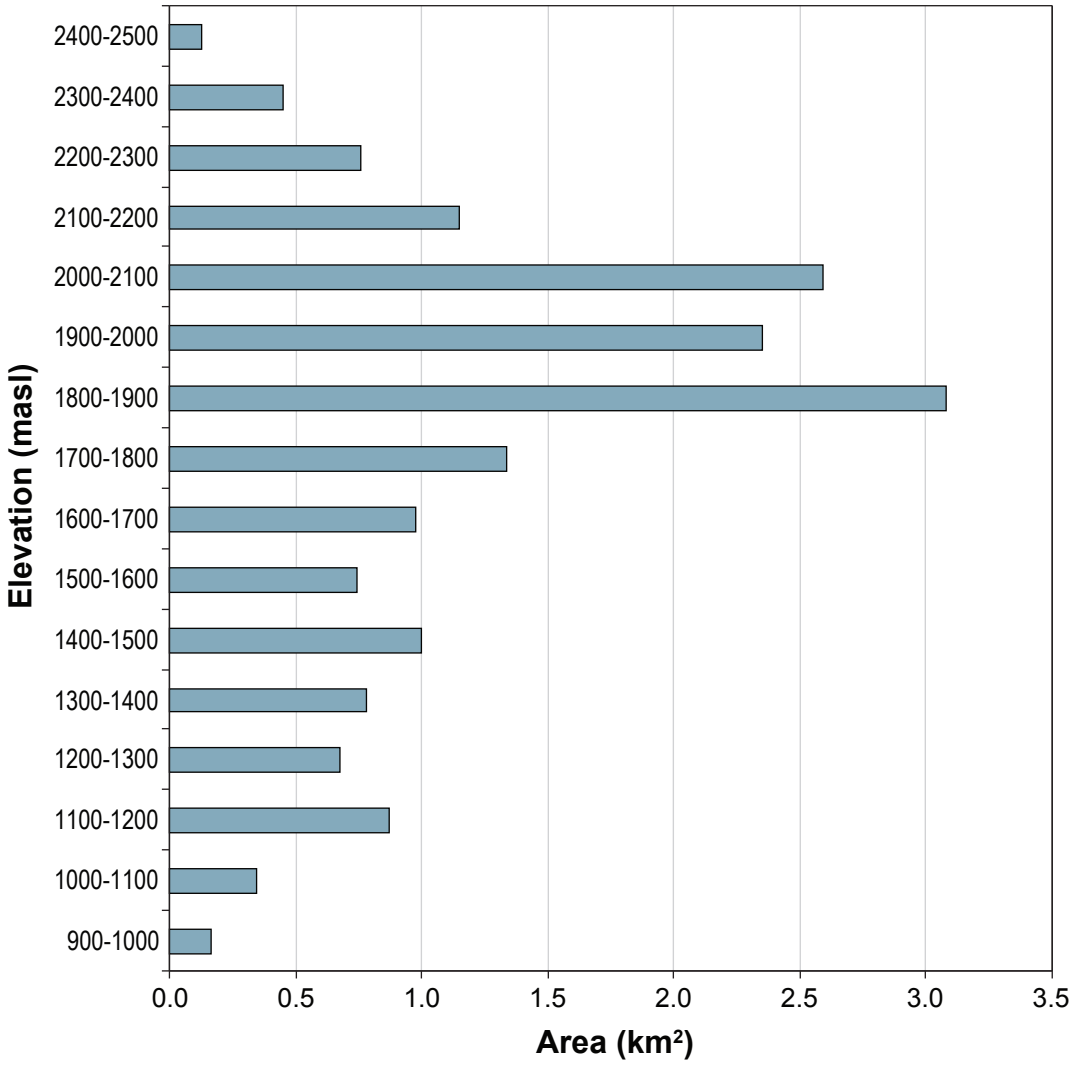

SEABRIDGE GOLD
KSM PROJECT

Mitchell Glacier
Adjusted Hypsometry

Figure 4.1-7

Rescan™ Engineers & Scientists

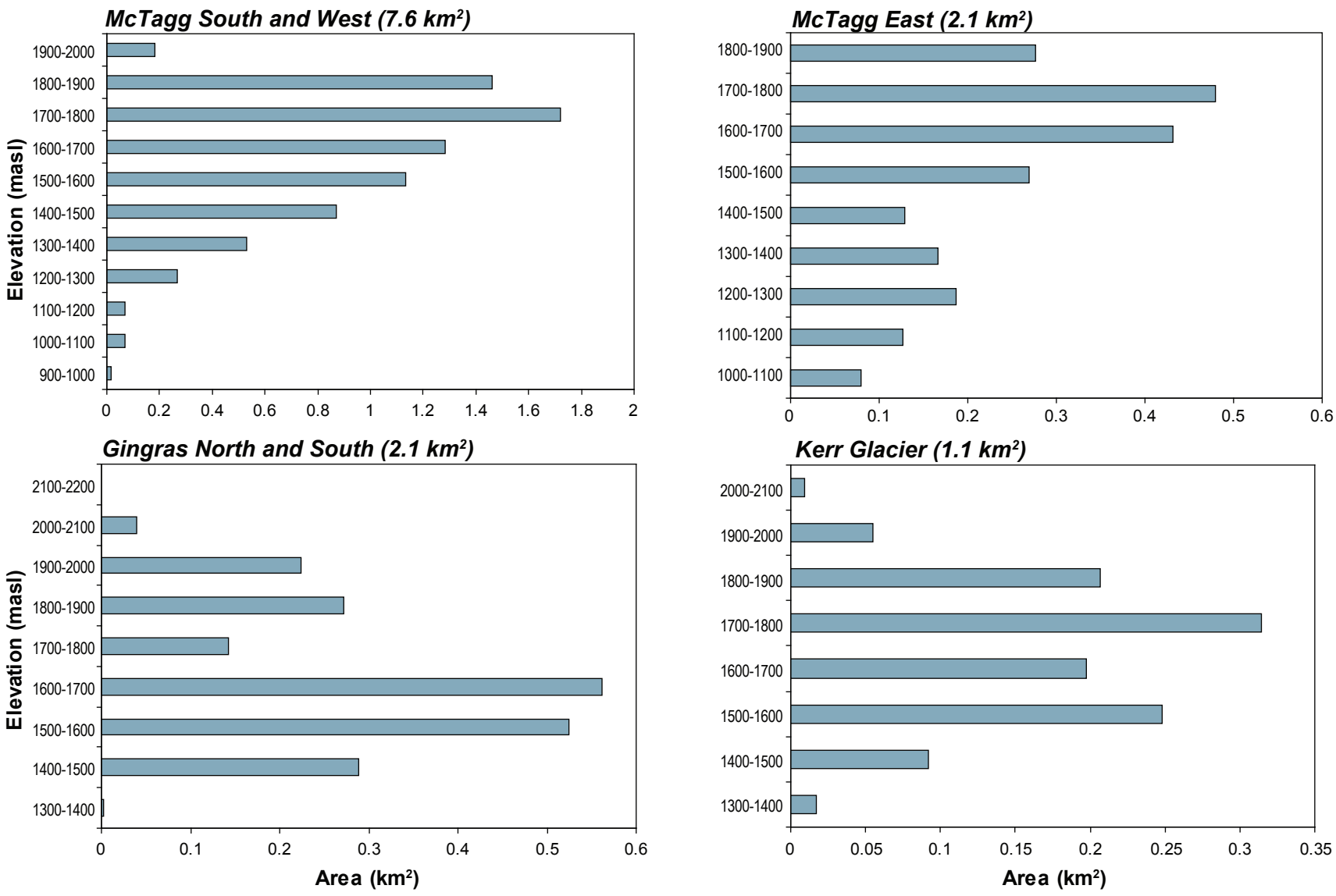

Figure 4.1-8

SEABRIDGE GOLD
KSM PROJECT

Hypsometry of McTagg, Gingras, and Kerr Glaciers

Figure 4.1-8

Rescan™ Engineers & Scientists

4.2 Glaciological Mass Balance

4.2.1 Monitoring Sites

Monitoring locations (ablation stakes and snow depth sites) for the 2011 mass balance year for all glaciers in the monitoring program are summarized in Table 4.2-1 and shown spatially in Figures 4.2-1 to 4.2-5. Table 4.2-2 gives mass balance measurements at each site between September 2010 and September 2011.

Table 4.2-1. Coordinates for Mitchell Glacier Ablation Stake and Snow Depth Sites, 2010-2011

Glacier	Site	Easting	Northing	Elevation	Site Type
Mitchell	**MI-900***	423780	6265699	883	s,d
	MI-960*	423969	6265799	943	s,ρ,d
	MI-1000*	424117	6265953	986	s,d
	MI-1100*	424646	6266022	1081	s,d
	MI-1200*	425452	6266357	1169	s,d
	MI-1300*	425987	6266386	1256	s,d
	MI-1400*	426711	6266049	1381	ρ,d
	MI-1450*	426774	6265420	1437	s,d
	MI-1525*	426965	6265174	1483	s,d
	MIB1-1700^	428108	6264676	1695	d
	MIB1-1800^	428613	6264632	1780	d
	MIB1-1820^	428763	6265272	1822	d
	MIB2-1850#	427719	6263819	1846	d
	MIB0-1900^	428564	6265882	1916	d
	MIB2-1900#	428365	6263736	1890	d
	MIB1-1975^	430207	6263353	1977	d
	MIB1-2000^	429439	6263920	2007	d
	MIB2-2000#	429265	6263157	2022	ρ,d
	MIB1-2050A^	430062	6264635	2064	d
	MIB1-2050B^	429601	6264782	2045	d
	MIB1-2050C^	429645	6264907	2038	d
	MIB1-2050D#	429693	6264139	2065	d
	MIB1-2075#	429701	6264270	2075	d
	MIB1-2100^	430394	6264694	2100	ρ,d
	MIB2-2200^	429912	6263159	2200	d
	MIB2-2300A^	430869	6264349	2296	d
	MIB2-2300B^	430223	6263299	2300	d
	MIB2-2400^	430514	6263251	2395	d

(continued)

Table 4.2-1. Coordinates for Mitchell Glacier Ablation Stake and Snow Depth Sites, 2010-2011 (continued)

Glacier	Site	Easting	Northing	Elevation	Site Type
McTagg South	**MS-1440***	415792	6267432	1429	s,d
	MS-1500*	415717	6267064	1486	s,d
	MS-1450^	415887	6267447	1450	d
	MS-1500^	415813	6267098	1500	d
	MS-1550^	415621	6266784	1547	d
	MS-1600^	415486	6266559	1600	ρ,d
	MS-1700^	415291	6266116	1700	d
	MS-1800^	415216	6265809	1800	d
McTagg West	**MW-1040***	416643	6268124	956	s,d
	MW-1200*	416112	6268291	1192	s,ρ,d
	MW-1250*	415785	6268286	1246	s,d
	MW-1325*	415370	6268314	1307	s,d
	MW-1440*	414755	6268419	1414	s,d
	MW-1500*	414122	6268455	1485	s,d
	MW-1575*	413551	6268240	1565	s,d
	MW-1625*	413368	6267822	1614	s,d
	MW-1650^	413747	6267710	1647	d
	MW-1700A^	413797	6267333	1700	ρ,d
	MW-1700B^	414025	6267306	1702	d
	MW-1750^	413961	6266889	1750	d
	MW-1825^	414221	6266381	1825	d
McTagg East	ME-1040^	418726	6269232	1043	d
	ME-1150*	419112	6269223	1142	s,ρ,d
	ME-1200^	419256	6269181	1203	d
	ME-1225*	419388	6269218	1225	s,d
	ME-1300*	419655	6269159	1290	s,d
	ME-1400*	419914	6269020	1387	s,d
	ME-1450^	420015	6268904	1448	d
	ME-1550#	420515	6268719	1551	s,d
	ME-1600*	420631	6268570	1589	s,d
	ME-1650^	420932	6268346	1650	ρ,d
	ME-1700^	421127	6268444	1700	d
	ME-1750^	421235	6268489	1743	d
	ME-1800^	421380	6268451	1794	d

(continued)

Table 4.2-1. Coordinates for Mitchell Glacier Ablation Stake and Snow Depth Sites, 2010-2011 (completed)

Glacier	Site	Easting	Northing	Elevation	Site Type
Gingras North	**GN-1425***	412913	6264824	1420	s,d
	GN-1500^	412802	6265046	1500	d
	GN-1550^	412762	6265219	1550	d
	GN-1600^	412807	6265331	1592	d
	GN-1800^	412988	6265878	1800	d
	GN-1850^	412921	6266049	1855	d
Gingras South	**GS-1400***	412767	6264604	1399	s,ρ,d
	GS-1450^	412587	6264607	1448	d
	GS-1500*	412671	6264268	1506	s,d
	GS-1525^	412315	6264512	1525	d
	GS-1550A^	412722	6264082	1550	d
	GS-1550B^	412480	6264216	1551	d
	GS-1600A^	412775	6263758	1596	d
	GS-1600B^	412345	6263917	1618	d
	GS-1625^	412545	6263642	1630	ρ,d
	GS-1650A^	412692	6263557	1652	d
	GS-1650B^	412496	6263585	1652	d
	GS-1600A*	412769	6263758	1596	s,d
	GS-1600B*	412349	6263918	1602	s,d
Kerr	**KG-1425***	419919	6259009	1419	s,d
	KG-1500*	420008	6258816	1496	s,ρ,d
	KG-1525^	419973	6258719	1524	d
	KG-1575*	420247	6258486	1568	s,d
	KG-1650A*	420433	6258293	1634	ρ,d
	KG-1650B^	420563	6258318	1654	d
	KG-1675^	420503	6258235	1675	d

Note: Site in bold are ablation stakes
UTM coordinates given in UTM 9N, NAD83
*** Sept 2011**
^ April 2011
 # Sept 2010
s = stake
ρ = density
d = depth

4.2.2 Winter Balance

4.2.2.1 Point Water Balance

End-of-winter (April, 2011) snow accumulation was measured at 27 sites on Mitchell Glacier, 18 sites at McTagg South and West Glaciers, 13 sites at McTagg East Glacier, 17 sites at Gingras North and South Glacier and 6 sites at Kerr Glacier (Table 4.2-2).

PROJECT # 0868-016-06-01 GIS No. KSM-10-154 November 22, 2012

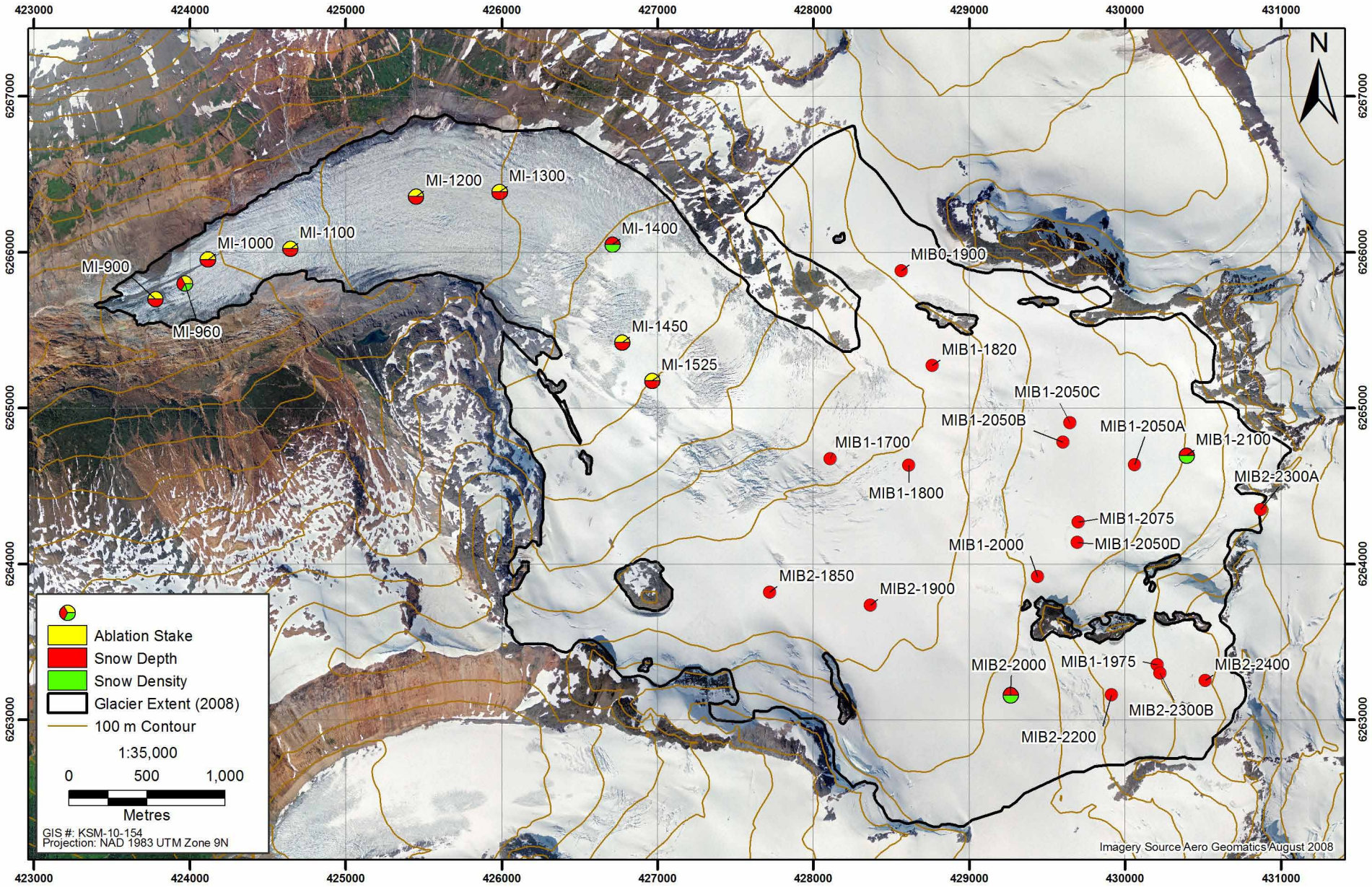

Figure 4.2-1

SEABRIDGE GOLD
KSM PROJECT

Mitchell Glacier 2011
Monitoring Sites

Figure 4.2-1

Rescan
Engineers & Scientists

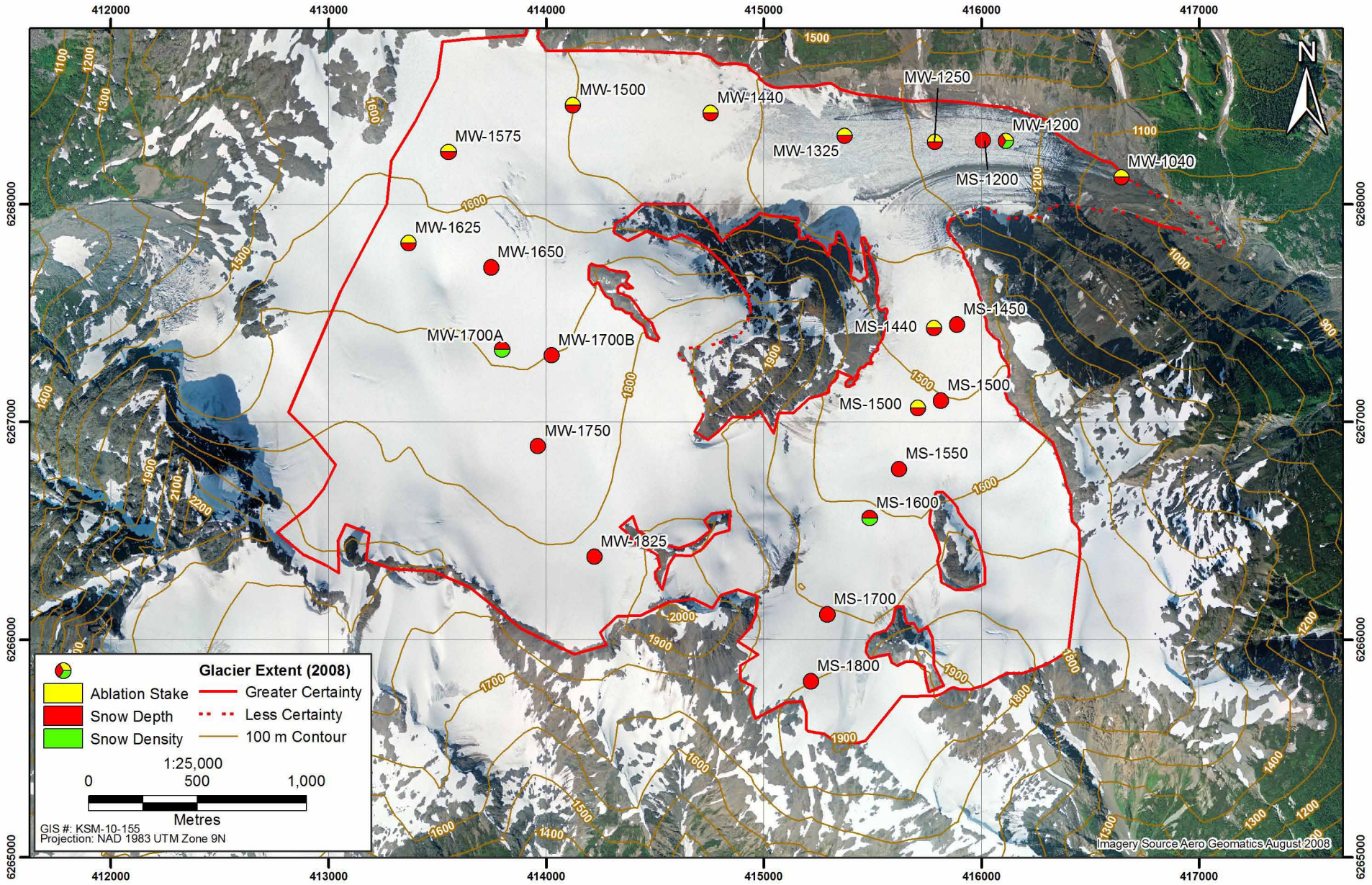

Figure 4.2-2

SEABRIDGE GOLD
KSM PROJECT

McTagg South and West Glacier
2011 Monitoring Sites

Figure 4.2-2

Rescan
Engineers & Scientists

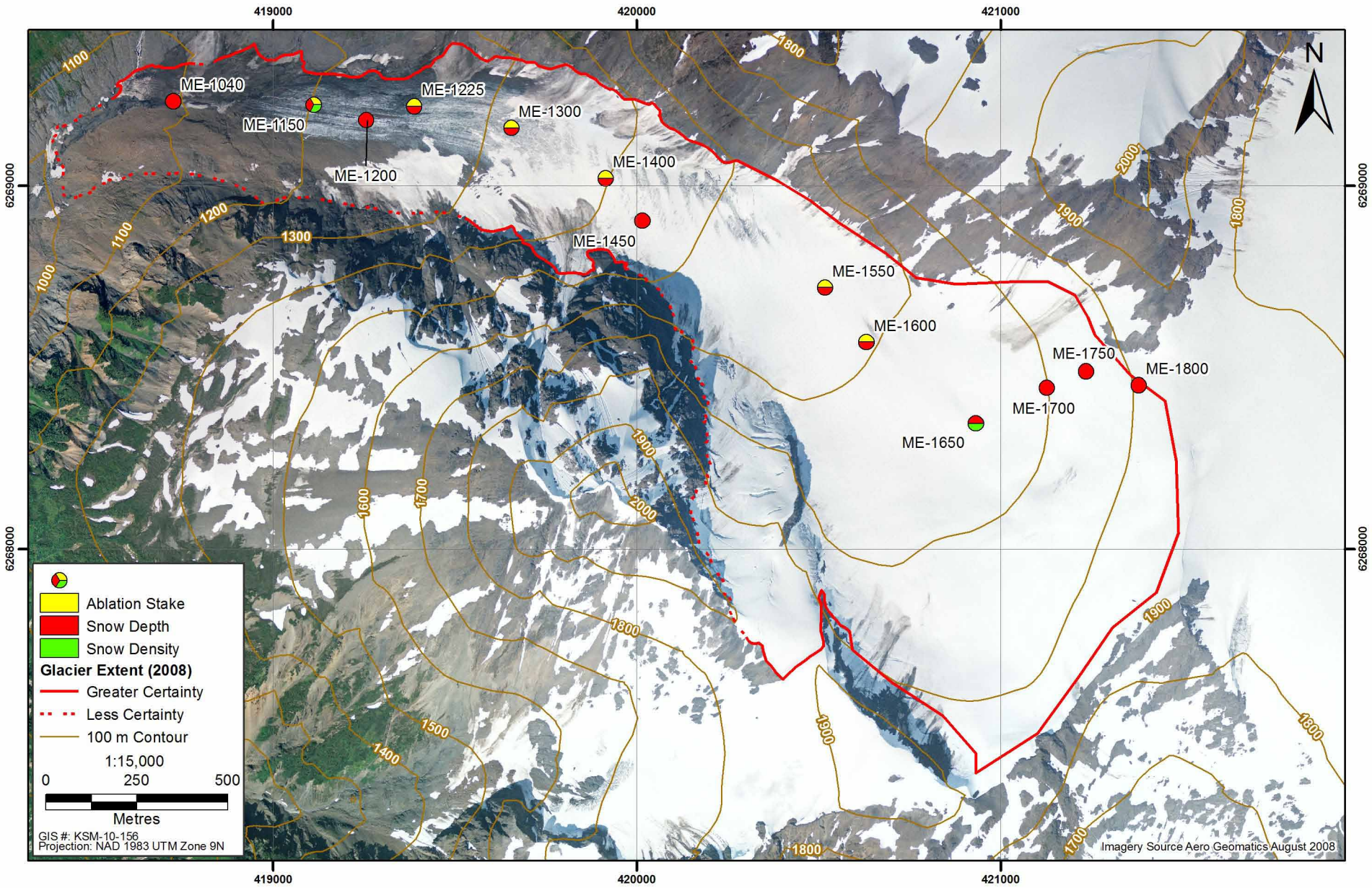

Figure 4.2-3

SEABRIDGE GOLD
KSM PROJECT

McTagg East Glacier
2011 Monitoring Sites

Figure 4.2-3

Rescan
Engineers & Scientists

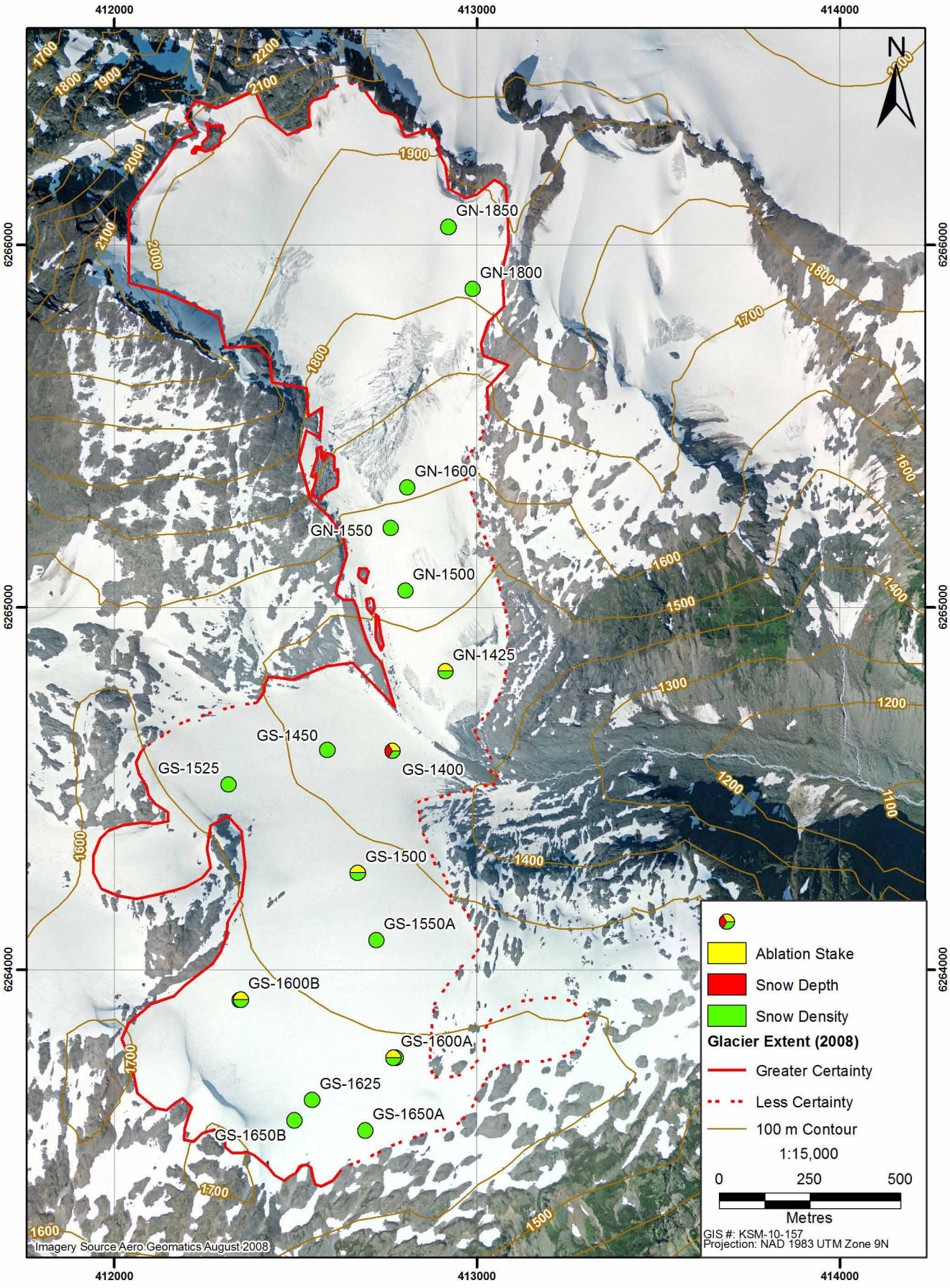

SEABRIDGE GOLD
KSM PROJECT

Gingras North and South Glacier 2011 Monitoring Sites

Figure 4.2-4

Rescan Engineers & Scientists

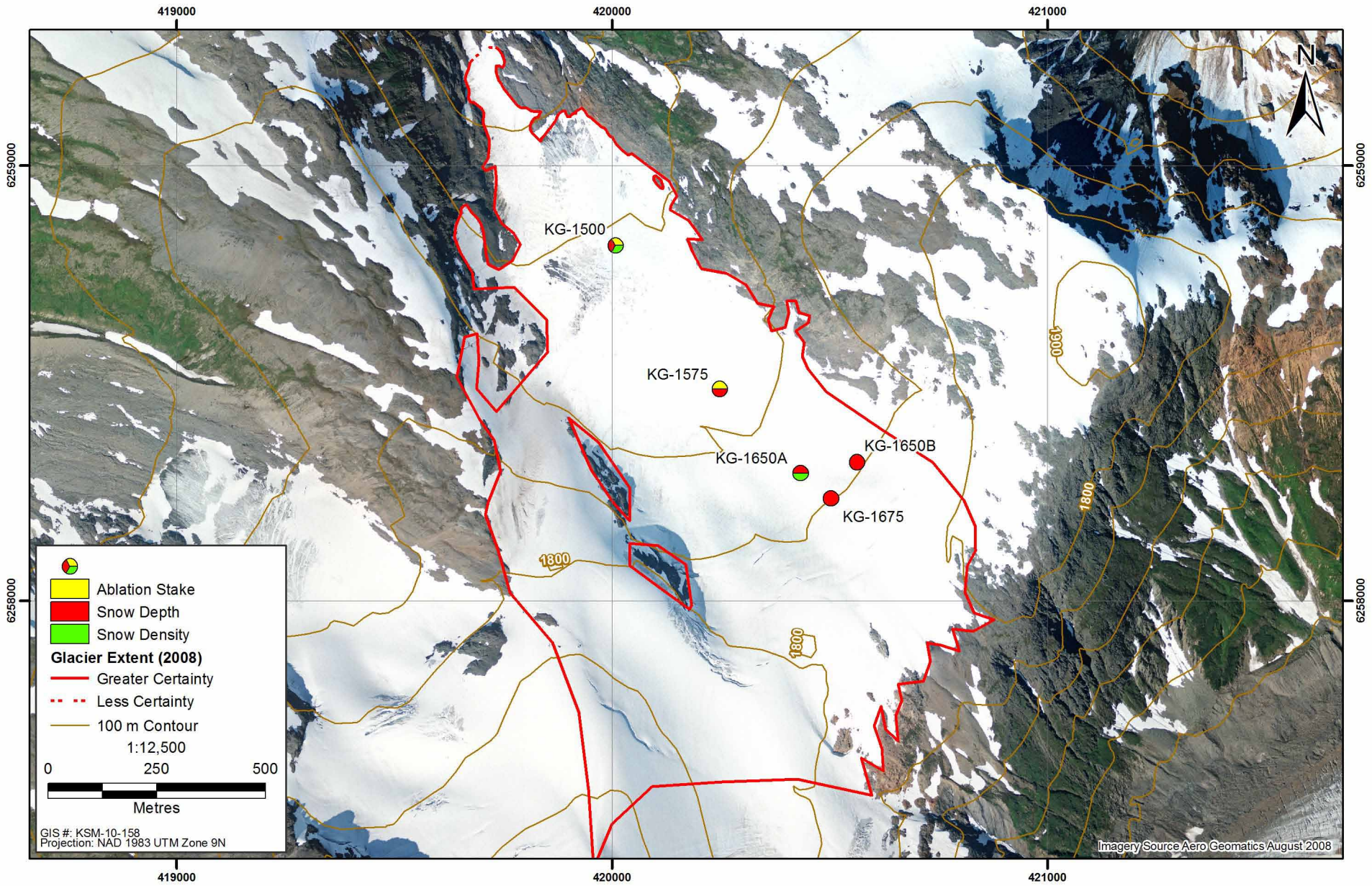

Figure 4.2-5

SEABRIDGE GOLD
KSM PROJECT

Kerr Glacier 2011 Monitoring Sites

Figure 4.2-5

Rescan
Engineers & Scientists

Table 4.2-2. Summary of Measurements and Mass Balance Results, 2010-2011

Glacier	Site	ds (m) Apr	ds (m) Sep	Δdi (m)	SWE Apr (bw m w.e.)		SWE Sep (m w.e.)		Ms (m w.e.)	Mi (m w.e.)	bs (m w.e)	bn (m w.e)	
Mitchell	MI-900	1.23	0.00	7.27	0.32		0.00		0.32	6.54	-6.86	-6.54	
	MI-960	2.40	0.00	8.77	0.59	b	0.00		0.59	7.89	-8.48	-7.89	
	MI-1000	1.34	0.00	8.77	0.35		0.00		0.35	7.89	-8.25	-7.89	
	MI-1100	2.00	0.00	4.55	0.58		0.00		0.58	4.10	-4.67	-4.10	
	MI-1200	2.67	0.00	3.87	0.83		0.00		0.83	3.48	-4.32	-3.48	
	MI-1300	2.47	0.00	3.94	0.75		0.00		0.75	3.55	-4.30	-3.55	
	MI-1400	3.35	0.00	2.50	0.80	b	0.00		0.80	2.25	-3.05	-2.25	
	MI-1450	2.47	0.00	2.78	0.75		0.00		0.75	2.50	-3.26	-2.50	
	MI-1525	2.96	0.00	2.87	0.95		0.00		0.95	2.58	-3.53	-2.58	
	MIB1-1700	3.28	N/A	0.00	1.09		N/A		N/A	0.00	N/A	N/A	
	MIB1-1800	3.21	N/A	0.00	1.06		N/A		N/A	0.00	N/A	N/A	
	MIB1-1820	3.47	N/A	0.00	1.17		N/A		N/A	0.00	N/A	N/A	
	MIB2-1850	5.37	N/A	0.00	2.09		N/A		N/A	0.00	N/A	N/A	
	MIB0-1900	4.11	N/A	0.00	1.46		N/A		N/A	0.00	N/A	N/A	
	MIB2-1900	5.81	N/A	0.00	2.31		N/A		N/A	0.00	N/A	N/A	
	MIB1-1975	4.86	N/A	0.00	1.83		N/A		N/A	0.00	N/A	N/A	
	MIB1-2000	4.26	N/A	0.00	1.54		N/A		N/A	0.00	N/A	N/A	
	MIB2-2000	3.95	2.53	0.00	1.51	b	1.34	a	0.17	0.00	-0.17	1.34	d
	MIB1-2050A	4.52	N/A	0.00	1.66		N/A		N/A	0.00	N/A	N/A	
	MIB1-2050B	4.22	N/A	0.00	1.52		N/A		N/A	0.00	N/A	N/A	
	MIB1-2050C	4.53	N/A	0.00	1.67		N/A		N/A	0.00	N/A	N/A	
	MIB1-2050D	4.50	N/A	0.00	1.65		N/A		N/A	0.00	N/A	N/A	
	MIB1-2100	3.72	3.30	0.00	2.39	b	1.75	a	0.64	0.00	-0.64	1.75	d
	MIB2-2100	5.75	N/A	0.00	2.28		N/A		N/A	0.00	N/A	N/A	
	MIB2-2200	4.82	N/A	0.00	1.81		N/A		N/A	0.00	N/A	N/A	
	MIB2-2300	5.21	N/A	0.00	2.00		N/A		N/A	0.00	N/A	N/A	
	MIB2-2400	3.91	N/A	0.00	1.37		N/A		N/A	0.00	N/A	N/A	

(continued)

Table 4.2-2. Summary of Measurements and Mass Balance Results, 2010-2011 (continued)

Glacier	Site	ds (m) Apr	ds (m) Sep	Δdi (m)	SWE Apr (bw m w.e.)		SWE Sep (m w.e.)		Ms (m w.e.)	Mi (m w.e.)	bs (m w.e)	bn (m w.e)	
McTagg South	MS-1440	3.56	0.00	1.53	1.29		0.00		1.29	1.38	-2.66	-1.38	
	MS-1500	3.96	0.00	1.28	1.49		0.00		1.49	1.15	-2.64	-1.15	
	MS-1550	3.75	0.00	N/A	1.38		0.00		1.38	N/A	N/A	N/A	
	MS-1600	3.67	0.00	N/A	1.43	b	0.00		1.43	N/A	N/A	N/A	
	MS-1700	2.53	1.30	0.00	0.82		0.69	a	0.14	0.00	-0.14	0.69	d
	MS-1800	3.93	N/A	0.00	1.48		N/A		N/A	0.00	N/A	N/A	
McTagg West	MW-1040	N/A	0.00	3.14	N/A		0.00		N/A	2.83	N/A	N/A	
	MW-1200	2.77	0.00	3.15	1.09	b	0.00		1.09	2.83	-3.92	-2.83	
	MW-1250	3.46	0.00	2.92	1.24		0.00		1.24	2.63	-3.87	-2.63	
	MW-1325	3.24	0.00	3.17	1.13		0.00		1.13	2.85	-3.99	-2.85	
	MW-1440	3.66	0.00	2.52	1.34		0.00		1.34	2.26	-3.60	-2.26	
	MW-1500	3.21	0.00	1.63	1.12		0.00		1.12	1.46	-2.58	-1.46	
	MW-1575	3.33	0.00	1.81	1.18		0.00		1.18	1.62	-2.80	-1.62	
	MW-1625	4.05	0.00	1.07	1.54		0.00		1.54	0.96	-2.50	-0.96	
	MW-1650	3.56	0.89	0.00	1.29		0.47	a	0.82	0.00	-0.82	0.47	d
	MW-1700A	4.02	N/A	0.00	1.47	b	N/A		N/A	0.00	N/A	N/A	
	MW-1700B	3.98	N/A	0.00	1.50		N/A		N/A	0.00	N/A	N/A	
	MW-1750	4.37	N/A	0.00	1.71		N/A		N/A	0.00	N/A	N/A	
	MW-1825	4.24	N/A	0.00	1.64		N/A		N/A	0.00	N/A	N/A	

(continued)

Table 4.2-2. Summary of Measurements and Mass Balance Results, 2010-2011 (continued)

Glacier	Site	ds (m) Apr	ds (m) Sep	Δdi (m)		SWE Apr (bw m w.e.)		SWE Sep (m w.e.)		Ms (m w.e.)	Mi (m w.e.)	bs (m w.e)	bn (m w.e)	
McTagg East	ME-1040	2.22	0.00	N/A		0.70		0.00		0.70	N/A	N/A	N/A	
	ME-1150	2.50	0.00	4.85		0.89	b	0.00		0.89	4.37	-5.26	-4.37	
	ME-1200	3.33	0.00	N/A		1.18		0.00		1.18	N/A	N/A	N/A	
	ME-1225	2.50	0.00	3.02		0.81		0.00		0.81	2.72	-3.53	-2.72	
	ME-1300	2.21	0.00	2.27		0.70		0.00		0.70	2.04	-2.74	-2.04	
	ME-1400	3.16	0.00	2.03		1.10		0.00		1.10	1.83	-2.92	-1.83	
	ME-1450	2.48	0.00	N/A		0.80		0.00		0.80	N/A	N/A	N/A	
	ME-1550	2.30	0.00	N/A	c	0.73		0.00		0.73	N/A	N/A	N/A	
	ME-1600	3.13	0.00	1.01		1.08		0.00		1.08	0.91	-1.99	-0.91	
	ME-1650	3.65	0.85	0.00		1.49	b	0.45	a	1.04	0.00	-1.04	0.45	d
	ME-1700	4.57	0.94	0.00		1.83		0.50	a	1.33	0.00	-1.33	0.50	d
	ME-1750	4.75	0.75	0.00		1.94		0.40	a	1.54	0.00	-1.54	0.40	d
	ME-1800	3.56	N/A	0.00		1.29		N/A		N/A	0.00	N/A	N/A	
Gingras North	GN-1425	3.70	0.0	2.98		1.29		0.0		1.29	2.68	-3.97	-2.68	
	GN-1500	3.79	0.0	N/A		1.33		0.0		1.33	N/A	N/A	N/A	
	GN-1550	3.73	0.0	0.92		1.30		0.0		1.30	0.83	-2.13	-0.83	
	GN-1600	4.01	0.0	N/A		1.46		0.0		1.46	N/A	N/A	N/A	
	GN-1800	4.91	N/A	0.00		2.01		N/A		N/A	0.00	N/A	N/A	
	GN-1850	5.10	N/A	0.00		2.14		N/A		N/A	0.00	N/A	N/A	

(continued)

Table 4.2-2. Summary of Measurements and Mass Balance Results, 2010-2011 (completed)

Glacier	Site	ds (m) Apr	ds (m) Sep	Δdi (m)	SWE Apr (bw m w.e.)		SWE Sep (m w.e.)		Ms (m w.e.)	Mi (m w.e.)	bs (m w.e)	bn (m w.e)	
Gingras South	GS-1400	3.67	0.0	2.40	1.43	b	0.0		1.43	2.16	-3.59	-2.16	
	GS-1450	4.23	0.0	N/A	1.58		0.0		1.58	N/A	N/A	N/A	
	GS-1500	3.85	0.0	1.31	1.37		0.0		1.37	1.18	-2.55	-1.18	
	GS-1525	4.38	0.0	N/A	1.67		0.0		1.67	N/A	N/A	N/A	
	GS-1550A	3.62	0.0	N/A	1.24		0.0		1.24	N/A	N/A	N/A	
	GS-1550B	3.08	0.0	1.33	0.98		0.0		0.98	1.20	-2.18	-1.20	
	GS-1600A	3.38	0.0	1.33	1.12		0.0		1.12	1.20	-2.32	-1.20	
	GS-1600B	4.20	0.0	0.92	1.56		0.0		1.56	0.83	-2.39	-0.83	
	GS-1625	3.20	0.0	N/A	1.13	b	0.0		1.13	N/A	N/A	N/A	
	GS-1650A	3.31	N/A	0.00	1.09		N/A		N/A	0.00	N/A	N/A	
	GS-1650B	4.36	N/A	0.00	1.66		N/A		N/A	0.00	N/A	N/A	
Kerr	KG-1425	3.46	0.00	2.24	1.16		0.00		1.16	2.02	-3.18	-2.02	
	KG-1500	2.82	0.00	2.48	0.87	b	0.00		0.87	2.23	-3.10	-2.23	
	KG-1525	2.53	0.00	N/A	0.74		N/A		N/A	N/A	N/A	N/A	
	KG-1575	3.54	0.00	1.24	1.20		0.00		1.20	1.12	-2.32	2.32	
	KG-1650	4.53	N/A	0.22	0.64	b	N/A		N/A	0.20	N/A	N/A	
	KG-1675	4.59	0.51	N/A	1.80		0.27	a	1.53	0.00	-1.53	0.27	d
	KG-1700	N/A	1.40	N/A	N/A		0.74	a	N/A	0.00	N/A	0.74	d

Note: end of summer snowline assumed to be between 1625 and 1650 m based on observations
N/A: No observation made or value cannot be computed
a: Values estimated using density of 529 kg/m^3
b: Measured directly from snow pits
c: Stake lost during summer melt
d: bn set as remaining SWE in Sept
m w.e.: metres of water equivalent
ds = snow depth
Δdi = change in depth of ice
bw = winter balance
SWE = snow water equivalence
Ms = snow melt
Mi = ice melt
bs = summer balance
bn = net balance

Snow depth measurements are plotted against elevation in Figure 4.2-6. Due to their geographical proximity and comparable depth-elevation relationships, McTagg South and West Glacier is combined with McTagg East Glacier (referred to as 'McTagg'). Similarly, Gingras North and South Glacier (referred to as 'Gingras') and Kerr Glacier data are combined due to the smaller number of observations and the similar size and elevation distributions of these glaciers (Figure 4.1-8). A quadratic fit is applied to each set of depth-density data and, using a least-squares regression technique, snow depth d_s is approximated as a function of elevation Z:

$$d_s = p_1 Z^2 + p_2 Z + p_3. \qquad [6]$$

The fitted parameters p_1, p_2 and p_3 for each dataset are given in Table 4.2-3 along with the coefficient of determination (R^2) and the root mean squared error (RMSE).

Table 4.2-3. Quadratic Fits for Snow Depth-elevation Relationships

Glacier	p_1	p_2	p_3	R^2	RMSE (m)
Mitchell	-1.105×10^{-7}	2.983×10^{-3}	-1.071	0.77	0.60
McTagg	4.256×10^{-8}	2.308×10^{-3}	-0.101	0.62	0.41
Gingras and Kerr	4.358×10^{-6}	-10.851×10^{-3}	10.317	0.71	0.25

For Mitchell Glacier all data were included in the regression analysis, but for McTagg Glacier two outliers were removed and are indicated in Figure 4.2-6. While Mitchell and McTagg Glaciers show a clear trend towards increased snow depths with elevation, snow depth data from Gingras and Kerr glaciers are more dispersed, particularly in the 1,500 - 1,650 masl elevation range (Figure 4.2-6). For this reason, six outliers were removed from the regression analysis, as these were anonymously low snow depths compared to the remainder of the dataset. The outliers in order of increasing elevation are KG-1500, KG-1525, GS- 1550B, GS-1600A, GS-1625, and GS-1650A.

The resulting coefficient of determination for these relationships ranges from 0.62 to 0.77, with a RMSE of between 0.41 and 0.60 m. However, it is of note that Gingras and Kerr glaciers show an overall weaker snow depth-elevation gradient compared to McTagg and Mitchell glaciers, and the quadratic curve tends to overestimate snow accumulation, particularly between 1,500 - 1,600 masl. The primary reason for this is thought to be the low elevation range of these glaciers and the impact of undulating surface topography on snow accumulation over this limited elevation range.

A quadratic formulation of the relation between snow depth and elevation is consistent with studies that indicate that maximum snow accumulation does not generally occur at mountain peaks (Barry 1992). While snow depth generally increases with elevation due to orographic enhancement and rain/snow temperature thresholds, wind speeds are also greatest at high elevations and strong winds act to redistribute snow to lower and more sheltered areas. In the case of Mitchell Glacier, the highest snow depths (5.81 m) were noted at 1,900 masl, and lower snow depths (5.21 m) were observed at the highest sampling site at 2,300 masl. Below 1,900 masl snow depths generally decreased with elevation to a local minimum of 1.2 m near the terminus (Figure 4.2-6).

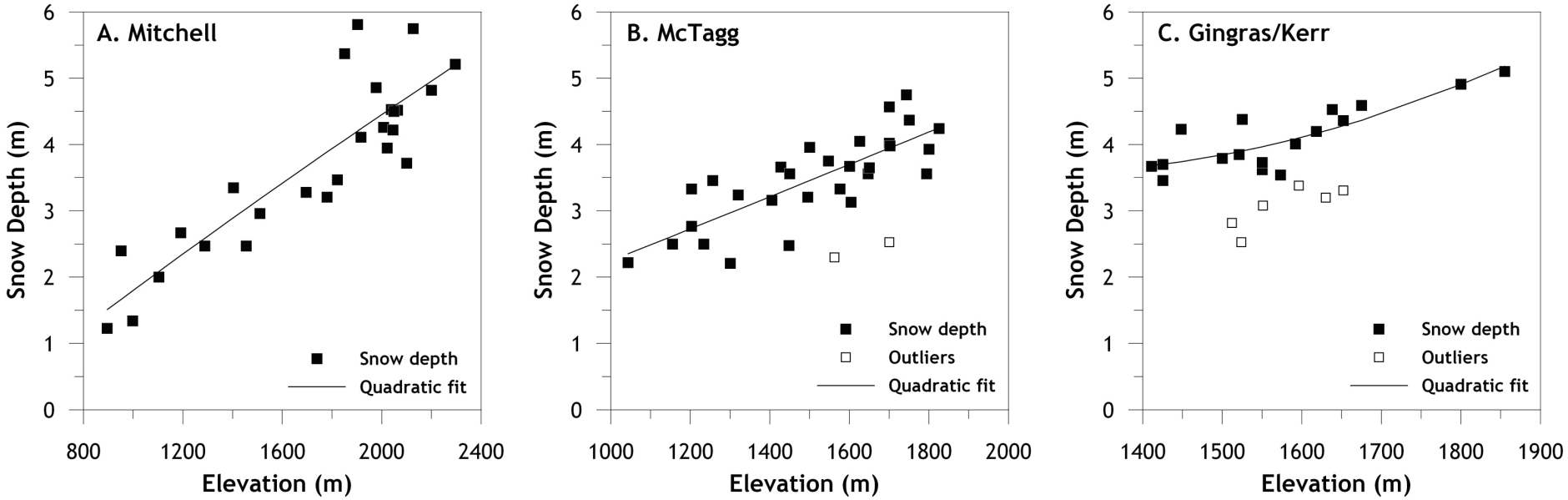

Figure 4.2-6

SEABRIDGE GOLD
KSM PROJECT

Snow Depth Change with Elevation, April 2011

Figure 4.2-6

Rescan™ Engineers & Scientists

Snow densities were measured in snow pits excavated at 13 locations in April 2011 (four on Mitchell Glacier, three on McTagg West and South Glacier, two on McTagg East Glacier, two on Gingras North and South Glacier and two on Kerr Glacier). Figure 4.2-7 shows all snow density measurements as a function of snow depth below the surface. It should be noted that the lower elevation snow pits (KG-1500 and GS-1400) were not included in the calculations of quadratic fit. This was due to the fact that the snow densities were relatively homogeneous with depth at the lower elevation sites. All measured snow densities are within the normal range expected for alpine snowpacks (Paterson 1994) and densities observed in pits at 1,600 masl and higher follow a typical winter pattern of densities increasing with depth. This occurs through densification processes (such as grain rounding and compaction) that occur as the overlying snowpack becomes deeper and heavier.

Winter snow density observations reveal systematic differences based on elevation. For snow pits between 950 and 1,500 masl, density was either uniform with depth (e.g., MW-1200) or was consistently greater than at higher-elevation sites (e.g., GS-1400). This is typical for snowpacks that are either melting or in a transitional state between winter conditions and the onset of summer melt.

Temperature profiles obtained from the snow pits provide further information regarding the state of the snowpack, and are shown in Figure 4.2-8. The loss of the winter snowpack generally begins when the entire snowpack has a temperature of approximately 0°C, and surface melt water no longer freezes as it percolates through the snow. For Mitchell Glacier snow pits, it is clear that the snowpack at MI-925 is melting, as evidenced by the consistent (isothermal) nature of the temperature profile (-0.1°C) and the high densities compared to the MIB2-2000 and MIB1-2100 snow pits (Figure 4.2-7). MI-1400 has a similar mean density to MI-925 (382 kg/m^3 at MI-1400 and 366 kg/m^3 at MI-925), but the temperature profile suggests that warming in the surface layers of the snow pit has not penetrated to the base.

Similarly, at McTagg South and West Glacier and McTagg East Glacier, snow pits at MW-1200 and ME-1150 are approaching an isothermal (melted) state, but MS-1600, ME-1650 and MW-1700 have not yet been melt-affected (Figure 4.2-8). The differentiation of melt-affected snowpacks from high-elevation (winter) snowpacks is not as clear on Gingras and Kerr Glaciers. The temperature profiles in Figure 4.2-8 show that by April all snow pits had warmed in the upper reaches. However, the isothermal layer is persistent until 0.6 m in the GS-1400 snow pit, but the temperatures decrease rapidly below 0.2 m in the higher-elevation snow pits.

The occurrence of snowmelt prior to the April 2010 field trip will not have a significant effect on the calculation of glacier mass balance. Snowmelt will be limited spatially to the lowest portions of the glacier, and the specific summer mass balance (b_s) at these low-elevation sites is dominated by ice melt (Table 4.2-2). It is also possible that higher elevation sites receive snowfall after the winter balance measurement, but again these amounts will likely be negligible in comparison with the total observed winter balances, and the timing of the winter balance trip aims to minimize these complications.

Based on the depth-density and depth-temperature data shown in Figures 4.2-7 and 4.2-8, snow pits that represent winter conditions (i.e., above 1,500 masl) were used to produce a least-squares regression of snow density (ρ_s) and snow depth (d):

$$\rho_s = p_4 Z^2 + p_5 Z + p_6. \qquad [7]$$

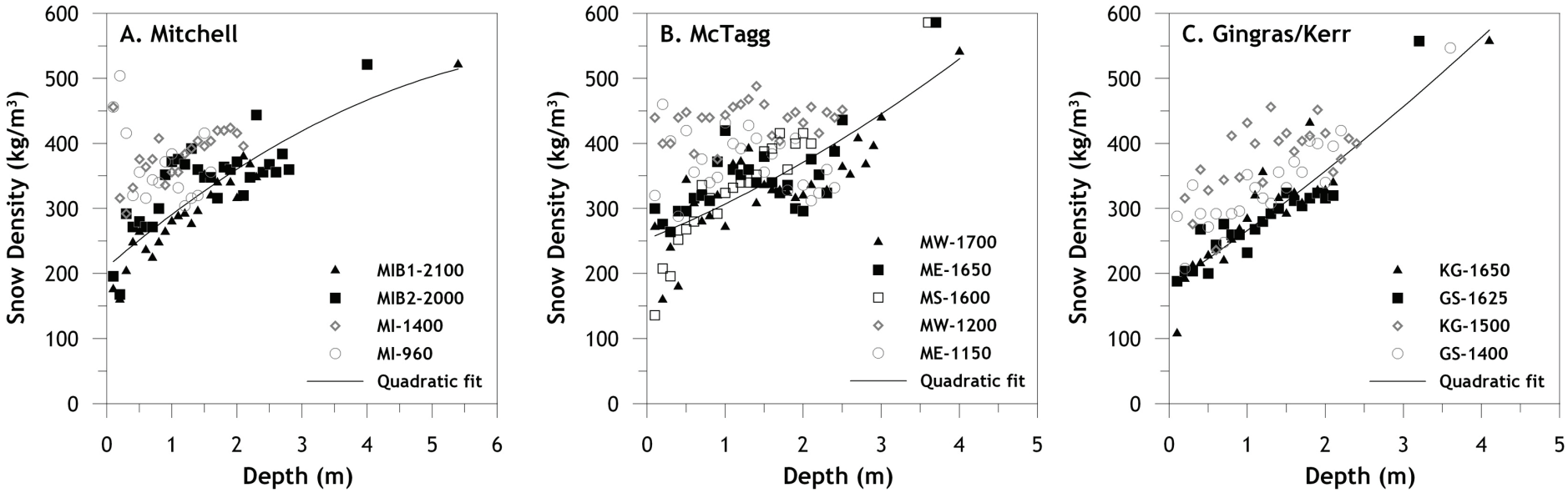

Figure 4.2-7

SEABRIDGE GOLD
KSM PROJECT

Snow Density Change with Depth, April 2011

Figure 4.2-7

Rescan™ Engineers & Scientists

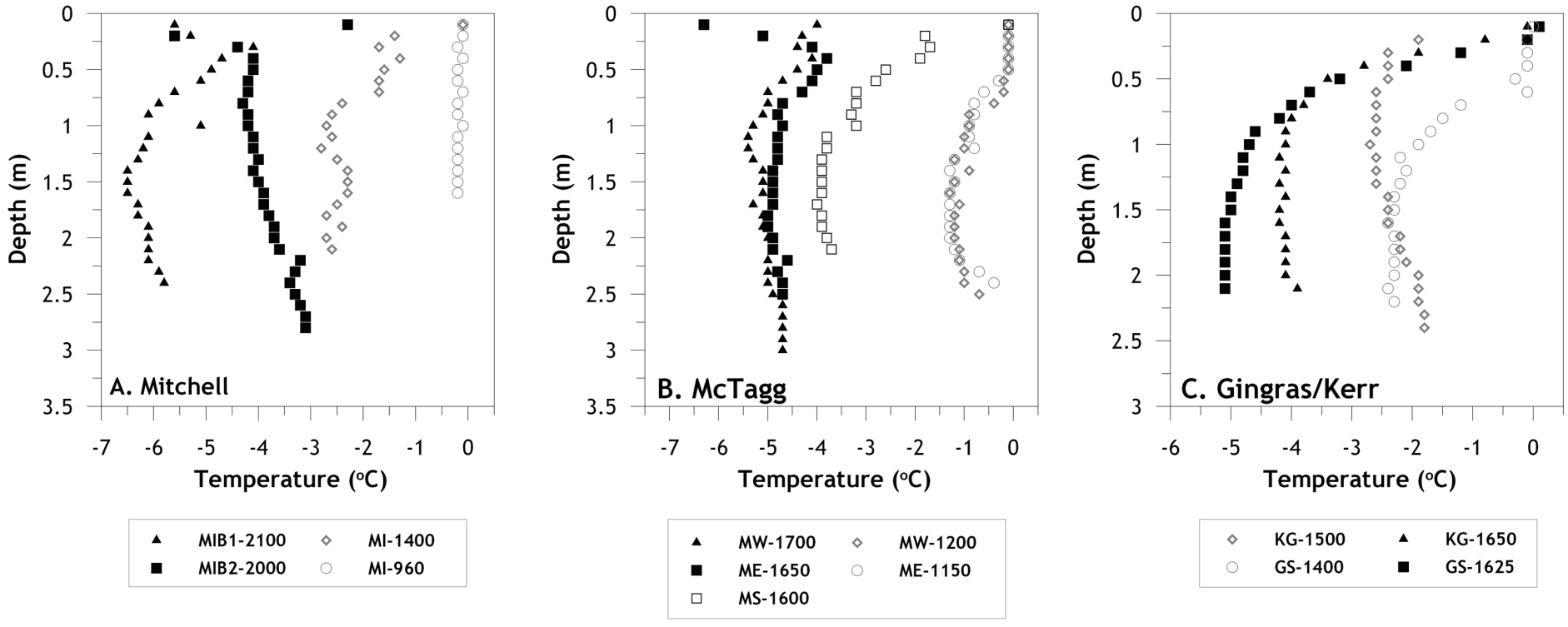

Figure 4.2-8

SEABRIDGE GOLD
KSM PROJECT

Snow Pit Temperature Profiles, April 2011

Figure 4.2-8

Rescan™ Engineers & Scientists

As for the depth-elevation relationships, McTagg South and West and East glaciers are grouped, as are Gingras North and South and Kerr glaciers. The fitted parameters p_4, p_5 and p_6 for each dataset shown in Figure 4.2-7 are given in Table 4.2-4 along with the coefficient of determination (R^2) and the root mean squared error (RMSE).

Table 4.2-4. Quadratic Fits for Snow Depth-density Relationships

Glacier	p_4	p_5	p_6	R^2	RMSE (m)
Mitchell	-5.563	86.485	209.801	0.74	28.81
McTagg	5.077	48.983	252.976	0.63	37.22
Gingras and Kerr	3.660	80.759	181.741	0.84	63.08

4.2.2.2 Distributed Winter Balance

With elevation data extracted from the adjusted DEMs for each glacier, a distributed winter balance for each 20 x 20 m grid cell was estimated by: 1) calculating the snow depth based on the elevation-snow depth relationships (Equation [6] and Table 4.2-3), and 2) integrating Equation [7] to determine snow density (and hence SWE) for the depth of each snowpack. The integrated form of Equation [7] is:

$$SWE = (p_7 Z^3 + p_8 Z^2 + p_9 Z) * 0.001 \qquad [8]$$

The fitted parameters p_7, p_8 and p_9 for each dataset are given in Table 4.2-5.

Table 4.2-5. Fitted Parameters for the Integration of Equation 7

Glacier	p_7	p_8	p_9
Mitchell	-1.854	43.243	209.801
McTagg	1.692	24.492	252.976
Gingras and Kerr	1.220	40.380	181.741

Due to the either uniform of inconsistent densities with depth encountered in the lower-elevation snow pits (Figure 4.2-7), Equation [8] was applied to elevations:

1. above 1,400 masl elevation for Mitchell Glacier
2. above 1,200 masl for McTagg South and West Glacier and McTagg East Glacier, and
3. above 1,400 masl for Gingras North and South and Kerr Glaciers.

The average density of the snowpack at 960 masl on the Mitchell Glacier (366 kg/m^3) was used to determine SWE from measured snow depths below 1,160 masl. Between 1,160 masl and 1,400 masl, the average density from the 1,400 masl pit (366 kg/m^3) was used to calculate SWE. The elevation 1,160 masl was selected as it lies halfway between the 925 masl and 1,400 masl snow-pit locations, and it can be inferred that melt was well underway at the lower pit, and just beginning at the upper pit.

In the same manner, the mean density at MW-1200 was used to calculate SWE from the terminus to 1,200 masl on McTagg South and West and East glaciers (436 kg/m^3), and the mean density at GS-1400 (337 kg/m^3) was used to calculate the SWE from the terminus to 1,400 masl on Gingras North and South and Kerr glaciers.

Table 4.2-6 gives the range of estimated winter snow depths and b_w (equivalent to SWE from Equation [8]) across the surface of each glacier. The distributed 2010 to 2011 winter balance for Mitchell Glacier is shown in Figure 4.2-9 and for other glaciers in the study area in Appendix 1.

Table 4.2-6. Range of Estimated Winter Snow Depths and the Winter Balance for each Glacier

Glacier	Mitchell	McTagg South and West	McTagg East	Gingras	Kerr
Min. elevation (masl)	999	958	1,014	1,387	1,320
Max. elevation (masl)	2,464	1,997	1,899	2,113	2,054
Min.depth (m)	1.80	2.15	2.28	3.65	3.59
Max. depth (m)	5.61	4.68	4.44	6.85	6.41
Min. b_w (m w.e.)	0.66	0.94	0.85	1.23	1.35
Max b_w (m w.e.)	2.21	1.89	1.75	3.53	3.15

For Mitchell Glacier snow depths vary from 1.8 to 5.6 m and the winter balance ranges from 0.66 to 2.21 m w.e. The minimum snow depth in 2011 lies between the 2009 and 2010 values, which were 3.0 m and 0.7 m, respectively. The maximum depth is comparable to the 2009 and 2010 mass balance years, when maximum snow depths were estimated as 6.0 m and 5.3 m, respectively.

McTagg South and West Glacier and McTagg East Glacier have a lower range of snow depths and consequently winter balance compared to Mitchell Glacier (Table 4.2-6). This is primarily a function of the more limited elevation range of these glaciers but is, in part, also due to the lower slope of the snow depth-elevation curve used to predict snow depth at these glaciers (Figure 4.2-6).

Gingras North and South and Kerr glaciers have considerably higher estimated snow depths and winter balance totals than the other glaciers in the study area (Table 4.2-7). While they are located, on average, at higher elevations than the other sites, the observed and modelled snow depths on the Gingras and Kerr glaciers are also higher for a given elevation than the other glaciers. For example, for 1,400 masl, which is the lowest snow depth sampling location on Gingras and Kerr glaciers, snow depth is estimated (using the curves shown in Figure 4.2-6) to be 3.7 m, compared to 2.9 on Mitchell Glacier and 3.2 m on McTagg South and West or East glaciers. This also applies to measured April snow depths (Table 4.2-2). For the 1,400 - 1,850 masl elevation range of Gingras and Kerr glacier sampling sites, the mean April snow depth is 4.1 m, compared to 3.4 m on Mitchell Glacier and 3.7 m on McTagg South and West and East glaciers.

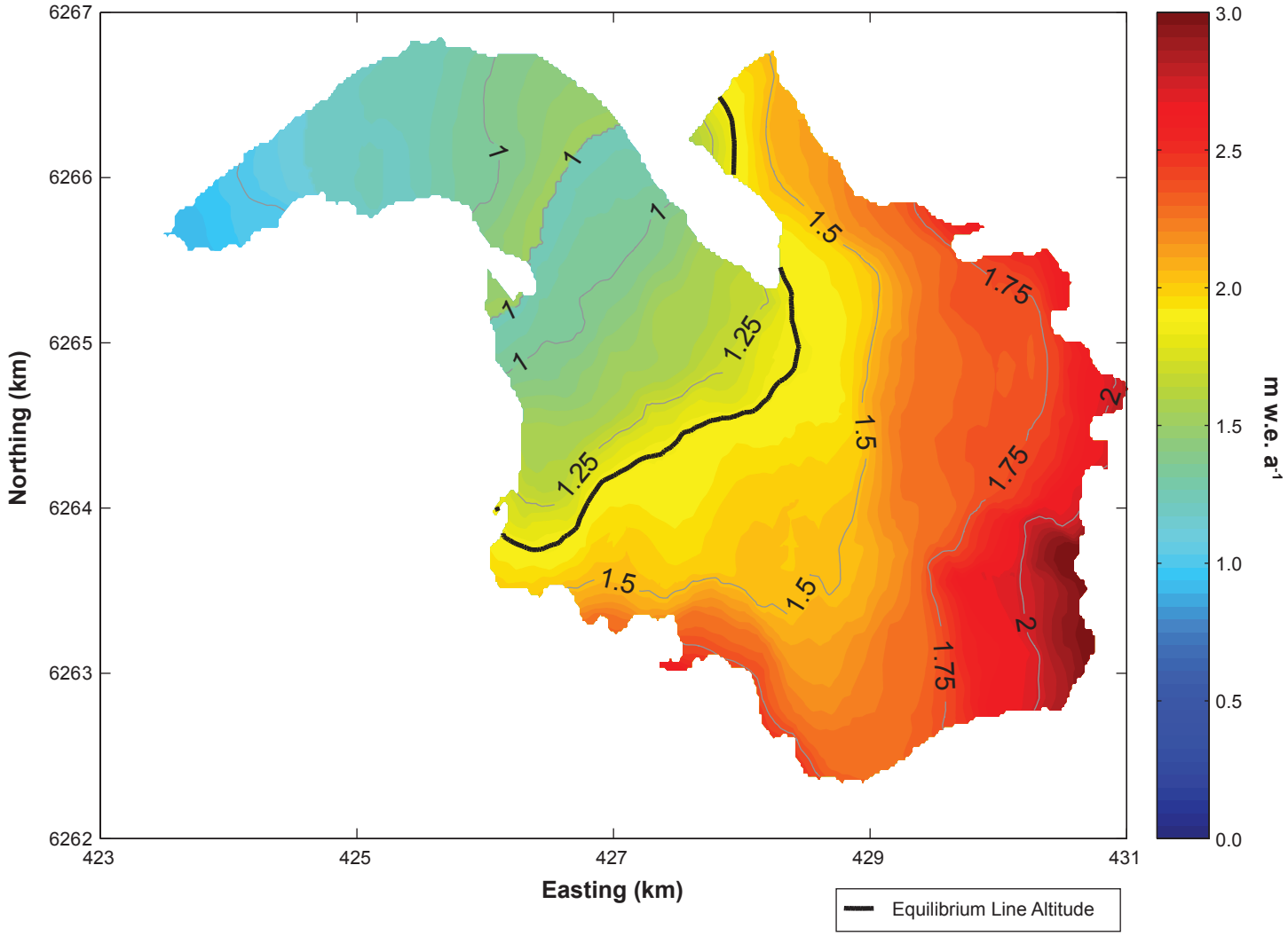

Figure 4.2-9

SEABRIDGE GOLD
KSM PROJECT

Mitchell Glacier Winter Mass Balance, 2010 to 2011

Figure 4.2-9

Rescan™
Engineers & Scientists

It appears from these results that Gingras North and South and Kerr glaciers are in more sheltered, topographically protected, basins and collect more winter snow accumulation than the other larger glaciers in the study region.

4.2.3 Summer Balance

4.2.3.1 Point Summer Balance

The summer mass balance calculation required three field visits to each site. In September 2010, ablation poles were drilled into the glacier and their height above the surface was recorded. Ablation poles below the transient snowline were then re-drilled in mid-summer (between late June and early August). Final changes in surface height were measured in September 2011 to provide a full year of ice melt measurements, and ablation stakes were re-drilled and reset in preparation for the 2012 ablation season. Snow depths and densities above the snowline were also sampled in April and September to provide estimates of the loss of snowpack during the summer melt season at high-elevation sites.

To estimate the summer balance b_s at each stake (Equation [5]), total snow melt M_s and ice melt M_i (in m w.e.) were calculated from field observations. Below the end-of-summer snow line, snow melt is assumed to equal the observed winter balance. Above the snow line, the remaining SWE in September was measured using a combination of snow depth probing and snow density measurements. Snow densities measured in two snow pits on Mitchell Glacier (at 2,000 and 2,100 masl) and one additional snow pit on the McTagg East Glacier (at 1,700 masl) in September 2011 were essentially uniform with depth, aside from layers with high densities due to ice lens formation. For this reason the mean density of 529 kg/m^3 was used to estimate the SWE of the remaining snowpack at snow-depth measurement sites.

Ice melt totals for stakes below the end-of-summer snow line were determined from the change in stake height between September 2010 and mid-summer (late June-early August 2011), and then again between mid-summer and September 2011, accounting for ablation stake re-drilling and extensions. Total ice surface height changes (Δd_i), observed through the stake height measurements, were converted to m w.e. following Equation [4]. Table 4.2-2 summarizes snow melt, ice melt, and summer balance calculated at each measurement site.

4.2.3.2 Distributed Summer Balance

To estimate melt totals over the surface of each glacier, a quadratic relation between summer balance (b_s) and elevation (Z) was developed (Figure 4.2-10):

$$b_s = p_{10} Z^2 + p_{11} Z + p_{12}. \qquad [9]$$

The fitted parameters p_{10}, p_{11} and p_{12} for Mitchell Glacier, McTagg South and West and East glaciers, and Gingras and Kerr glaciers are given in Table 4.2-7 along with the coefficient of determination (R^2) and the root mean squared error (RMSE).

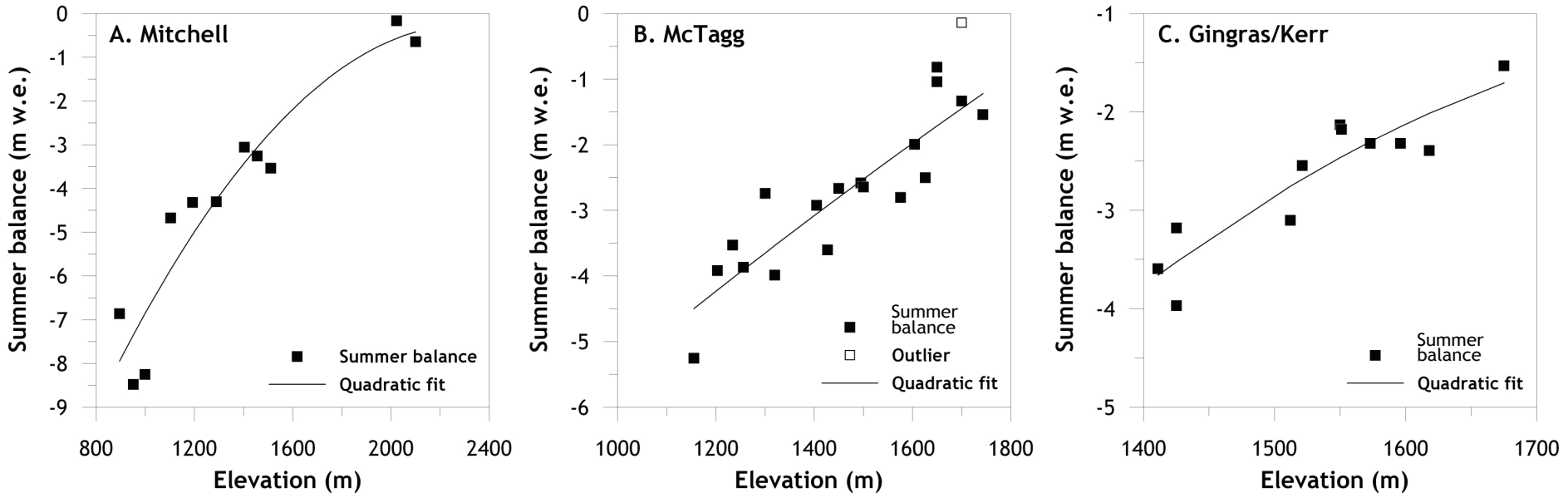

Figure 4.2-10

SEABRIDGE GOLD
KSM PROJECT

Summer Balance Variation with Elevation, 2011

Figure 4.2-10

Rescan™ Engineers & Scientists

Table 4.2-7. Quadratic Fits for Summer Balance-elevation Relationships

Glacier	p_{10}	p_{11}	p_{12}	R^2	RMSE (m)
Mitchell	-3.849×10^{-6}	1.777×10^{-2}	0.900	0.90	0.82
McTagg	1.892×10^{-6}	5.377×10^{-2}	0.789	0.79	0.57
Gingras and Kerr	-9.439×10^{-6}	3.654×10^{-2}	0.834	0.83	0.28

Equation [9] was applied to the adjusted DEM of each glacier to calculate the distributed summer balance, and Table 4.2-8 gives the range of estimated summer balances on each glacier. The distributed summer balance for Mitchell Glacier is shown in Figure 4.2-11 and for other glaciers in the study area in Appendix 2.

Table 4.2-8. Range of Estimated Summer Balance for each Glacier

Glacier	Mitchell	McTagg South and West	McTagg East	Gingras	Kerr
Min. elevation (masl)	999	958	1,014	1,387	1,320
Max. elevation (masl)	2,464	1,997	1,899	2,113	2,054
Max. b_s (m w.e.)	-6.87	-5.69	-5.35	-3.90	-4.64
Min b_s (m w.e.)	-0.34	0.06	-0.42	-1.36	-1.20

For Mitchell Glacier, combined snow and ice melt totals are estimated to range from 6.9 m w.e. at the lowest elevations of the glacier to 0.3 m w.e. in the higher areas of Mitchell Glacier (Table 4.2-8). Terminus melt for 2011 is lower than 2010 estimates (8.3 m w.e.), but the melt at high elevations in 2010 was also estimated to be 0.3 m w.e. (Rescan 2011). This indicates that, as for the 2010 mass balance year, the glacier experienced melt across its entire surface over the summer months.

For other glaciers, maximum summer ablation (snow and ice melt) ranged from 3.9 m w.e. on Gingras North and South Glacier to 5.7 m w.e. on McTagg South and West Glacier (Table 4.2-8). McTagg East Glacier has a slightly positive summer balances at high elevations. This is a result of the extrapolation of the elevation-summer balance curve (Figure 4.2-10) above the highest measurement site. Summer balance only becomes positive, however, at 1,990 m so this only affects a small area of the upper accumulation zone (~7 m of elevation) and has negligible effect on net mass balance calculations.

It is estimated that Gingras and Kerr glaciers experienced high melt rates across the entire surface, with summer balances of -1.4 m w.e. and -1.2 m w.e. at the highest elevations. However, it is of note that the highest monitoring site on these glaciers is at 1,675 masl while the highest elevation is ~2,100 masl. The extrapolation of the elevation-summer balance curve (Figure 4.2-10) approximately 400 m above the highest monitoring site therefore results in less certainty associated with b_s at high elevations.

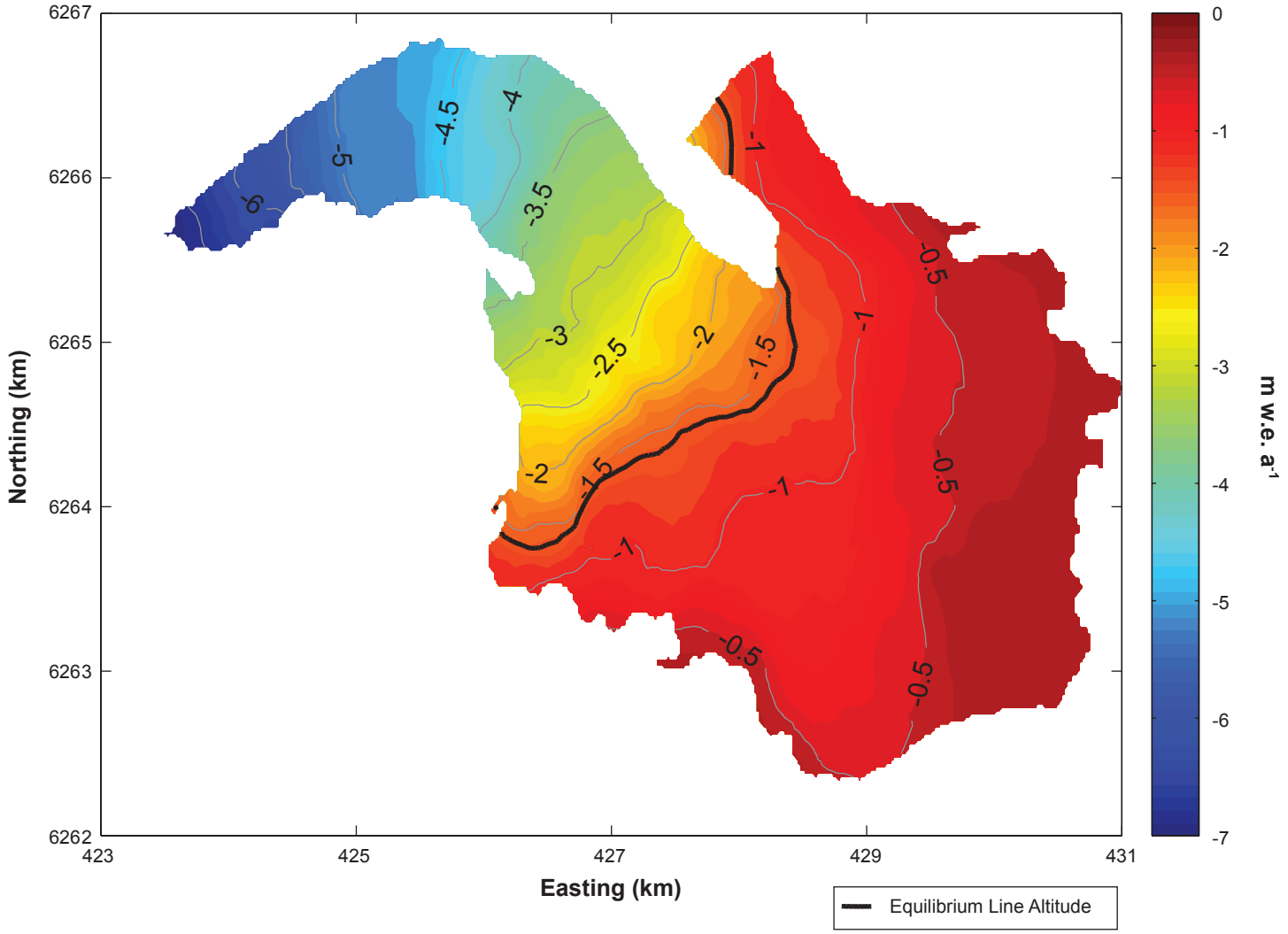

Figure 4.2-11

SEABRIDGE GOLD
KSM PROJECT

Mitchell Glacier Summer Mass Balance, 2011

Figure 4.2-11

Rescan™ Engineers & Scientists

4.2.4 Net Mass Balance

A specific net mass balance b_n for all monitoring sites was calculated as the sum of the estimated summer b_s and winter balance b_w. For sites in the accumulation area, net balance was set equal to the remaining SWE in September. Summaries of the winter, summer, and net mass balance are given in Table 4.2-2. The winter, summer, and net mass balance at each monitoring site as a function of elevation are shown in Figure 4.2-12.

Two methods could be used to estimate the net mass balance in each grid cell of the adjusted DEMs: 1) calculate a net balance in each grid cell as the sum of the estimated summer b_s and winter balance b_w in each grid cell, and 2) estimate net balance in each grid cell based on a quadratic relation between elevation and net balance at the monitoring sites. Both methods are equally appropriate (Braithwaite 2002), and should produce the similar results given identical input data in the form of field measurements. Any difference arises solely due to differences in the number and location of measurement sites that can be included in each calculation.

A relationship between net mass balance and elevation (Figure 4.2-12) was developed according to:

$$b_n = p_{13} Z^2 + p_{14} Z + p_{15}. \qquad [10]$$

The fitted parameters p_{13}, p_{14} and p_{15} for Mitchell, McTagg South and West and McTagg East glaciers are given in Table 4.2-9 along with the coefficient of determination (R^2) and the root mean squared error (RMSE). For Gingras and Kerr glaciers, the application of a quadratic fit to data shown in Figure 4.2-12 results in anomalously high maximum b_n values. As discussed in relation to the summer balance calculations, this is the result of limited data at high elevations. For this reason, a linear model ($b_n = p_{13} Z + p_{14}$) is chosen for b_n calculations at these sites, as it produces more realistic maximum b_n values. The addition of additional high-elevation monitoring sites in the 2011 mass balance year will help constrain the model at high elevations.

Table 4.2-9. Fits for Net Balance-elevation Relationships

Glacier	p_{13}	p_{14}	p_{15}	R^2	RMSE (m)
Mitchell	-2.958 x 10-6	1.644 x 10-2	-19.848	0.93	0.83
McTagg	2.956 x 10-6	1.488 x 10-3	-5.716	0.88	0.48
Gingras and Kerr*	0.010	-16.263	N/A	0.85	0.37

*** linear fit.**

These relationships explain 85-93% of the observed variation in net mass balance (R^2 = 0.85 - 0.93), and hence are considered strong predictors of net mass balance at all sites. It is also worth noting that the quadratic equations developed in 2011 to estimate the winter, summer and net balances on Mitchell Glacier are very similar to those used in 2009 and 2010. From this similarity, it can be inferred that the influence of elevation on accumulation and melt processes is consistent between the years that mass balance measurements have been conducted. Future mass balance measurements on the other glaciers in the study region will enable the inter-year consistency to be assessed at these sites.

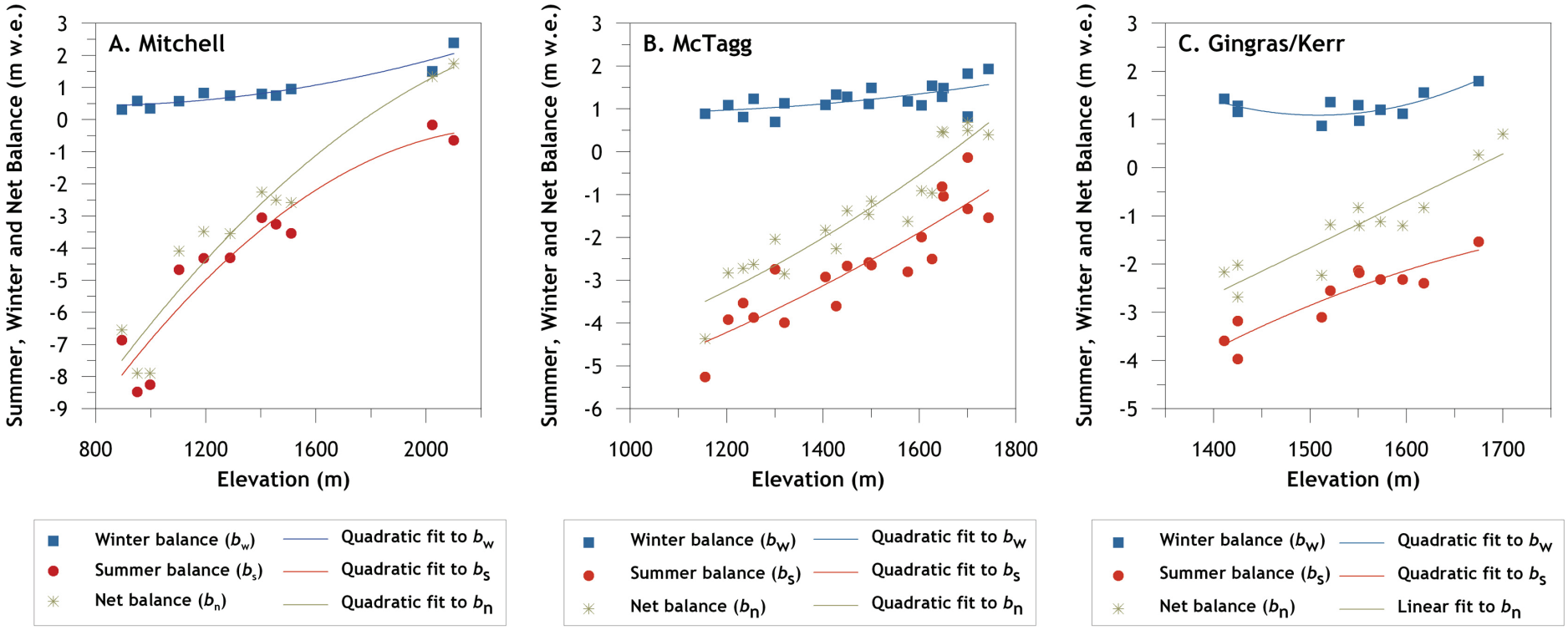

Figure 4.2-12

SEABRIDGE GOLD
KSM PROJECT

Calculated Winter, Summer and Net Balance at Different Elevations, 2010-2011

Figure 4.2-12

Rescan™ Engineers & Scientists

The distributed net mass balance on Mitchell, McTagg South and West, McTagg East, Gingras and Kerr glaciers are shown in Figure 4.2-13 to 4.2-17. The minimum and maximum net mass balance for each glacier from the distributed model is summarized in Table 4.2-10.

Table 4.2-10. Range of Elevations and Estimated Net Balance for Each Glacier

Glacier	Mitchell	McTagg South and West	McTagg East	Gingras	Kerr
Min. elevation (masl)	999	958	1,014	1,387	1,320
Max. elevation (masl)	2,464	1,997	1,899	2,113	2,054
Min. b_n (m w.e.)	-6.38	-4.43	-4.19	-2.81	-3.46
Max. b_n (m w.e.)	2.71	3.10	2.12	4.24	3.66

For Mitchell Glacier the distributed net mass balance (Figure 4.2-13) shows that mass was lost at lower elevations and gained at the higher elevations. The minimum net balance of -6.4 m w.e. near the terminus (Table 4.2-10), is comparable to the measured net balance of -6.5 m w.e. at the lowest measurement site, MI-900 (Table 4.2-2). A maximum net balance of 2.7 m w.e. is estimated for the highest elevations on Mitchell Glacier. This is approximately 1 m w.e. more than for the 2010 mass balance year. However, for two high-elevation sites where net mass balance data was measured directly (MIB2-2000 and MIB1-2100), b_n values of 1.3 to 1.7 m w.e. are much higher than for 2010 when b_n was between 0.3 and 0.4 m w.e. This suggests that the model is producing reliable results at high elevations on Mitchell Glacier and that the additional ~1 m w.e. in 2011 reflects high late-winter snow accumulation totals compared to the previous year.

McTagg South and West Glacier has a minimum estimated net balance of -4.4 m w.e. and a maximum of 3.1 m w.e. As this is calculated using the same quadratic fit as the McTagg East Glacier, b_n values for these sites are comparable, with a lower maximum b_n on McTagg East Glacier resulting simply from a lower maximum elevation. The maximum estimated net balance of between ~2 and 3 m w.e. is greater than the measured values at the highest-elevation monitoring sites. At ME-1750, for example, b_n was 0.5 m w.e. (Table 4.2-2; Figure 4.2-12), suggesting that extrapolation of the elevation-b_n curve to high elevations may overestimate b_n in the upper accumulation zone.

Estimates of net mass balance on Gingras and Kerr glaciers are in line with observations at other sites at the lower end of the elevation range, with minimum b_n values of -2.4 and -2.5 m w.e. on Gingras and Kerr glaciers respectively. However, as for McTagg South and West and East glaciers the extrapolation of the b_n curve shown in Figure 4.2-12 above the elevation of the highest monitoring site (1,700 masl) results in high b_n values. At site GS-1600B, b_n was -0.8 m w.e., and on Kerr Glacier b_n increased from 0.3 m w.e. to 0.7 m w.e. between KG-1675 and KG-1700 (Table 4.2-2). However, maximum modelled b_n is between 3.7 and 4.7 m w.e. at these sites.

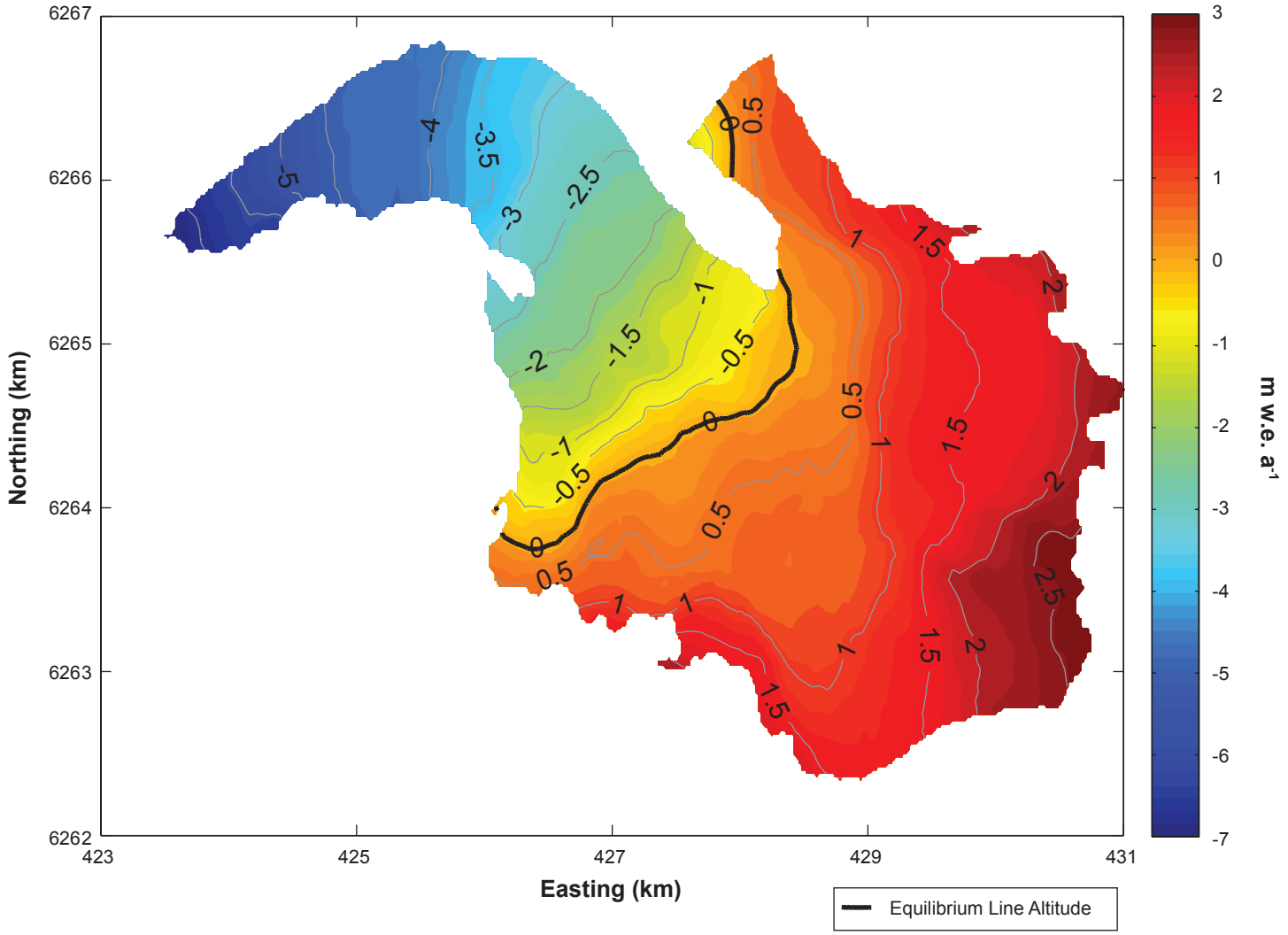

Figure 4.2-13

SEABRIDGE GOLD
KSM PROJECT

Mitchell Glacier Annual Mass Balance, 2010 to 2011

Figure 4.2-13

Rescan™ Engineers & Scientists

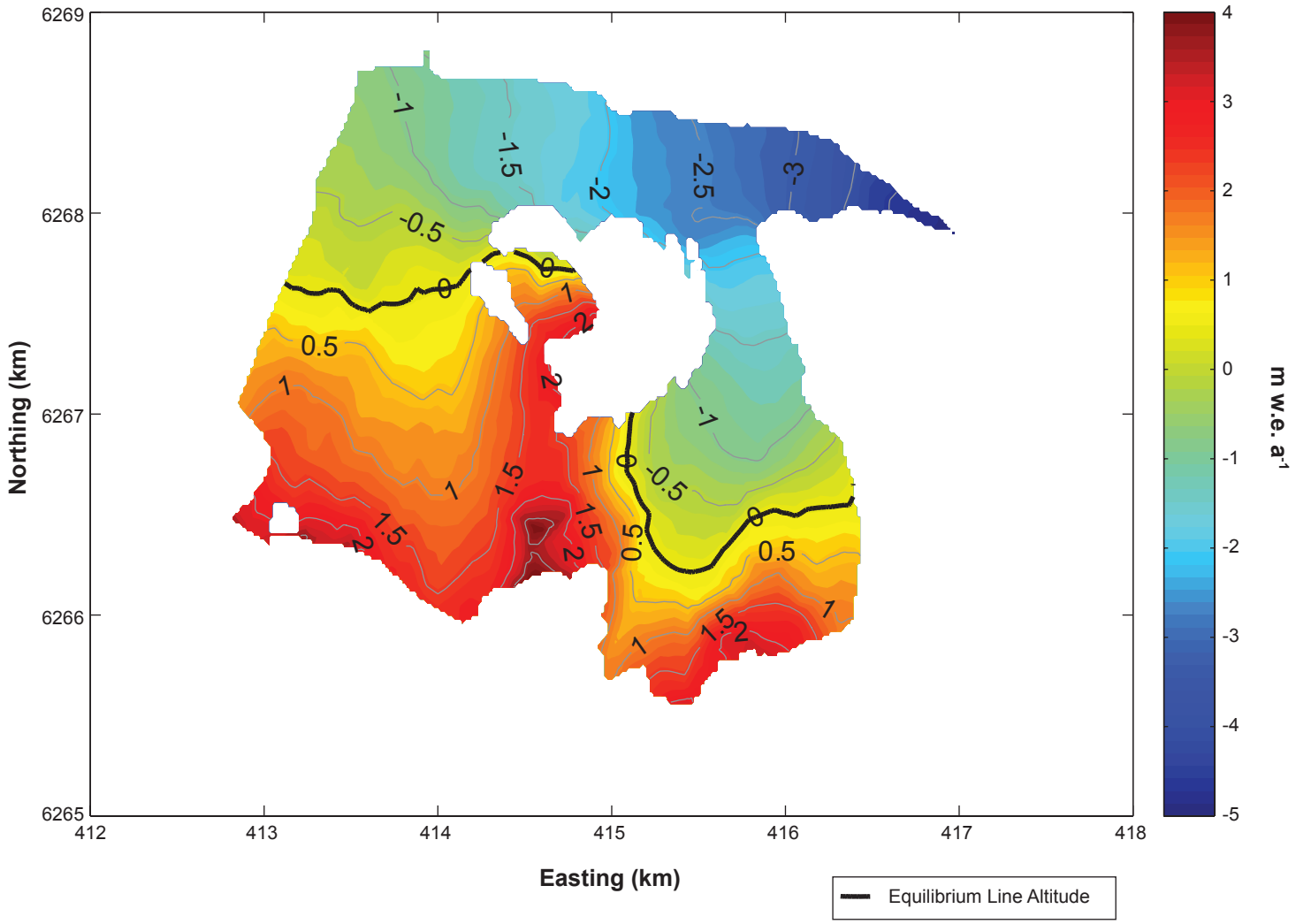

Figure 4.2-14

SEABRIDGE GOLD
KSM PROJECT

McTagg South and West Glacier
Annual Mass Balance, 2010 to 2011

Figure 4.2-14

Rescan™
Engineers & Scientists

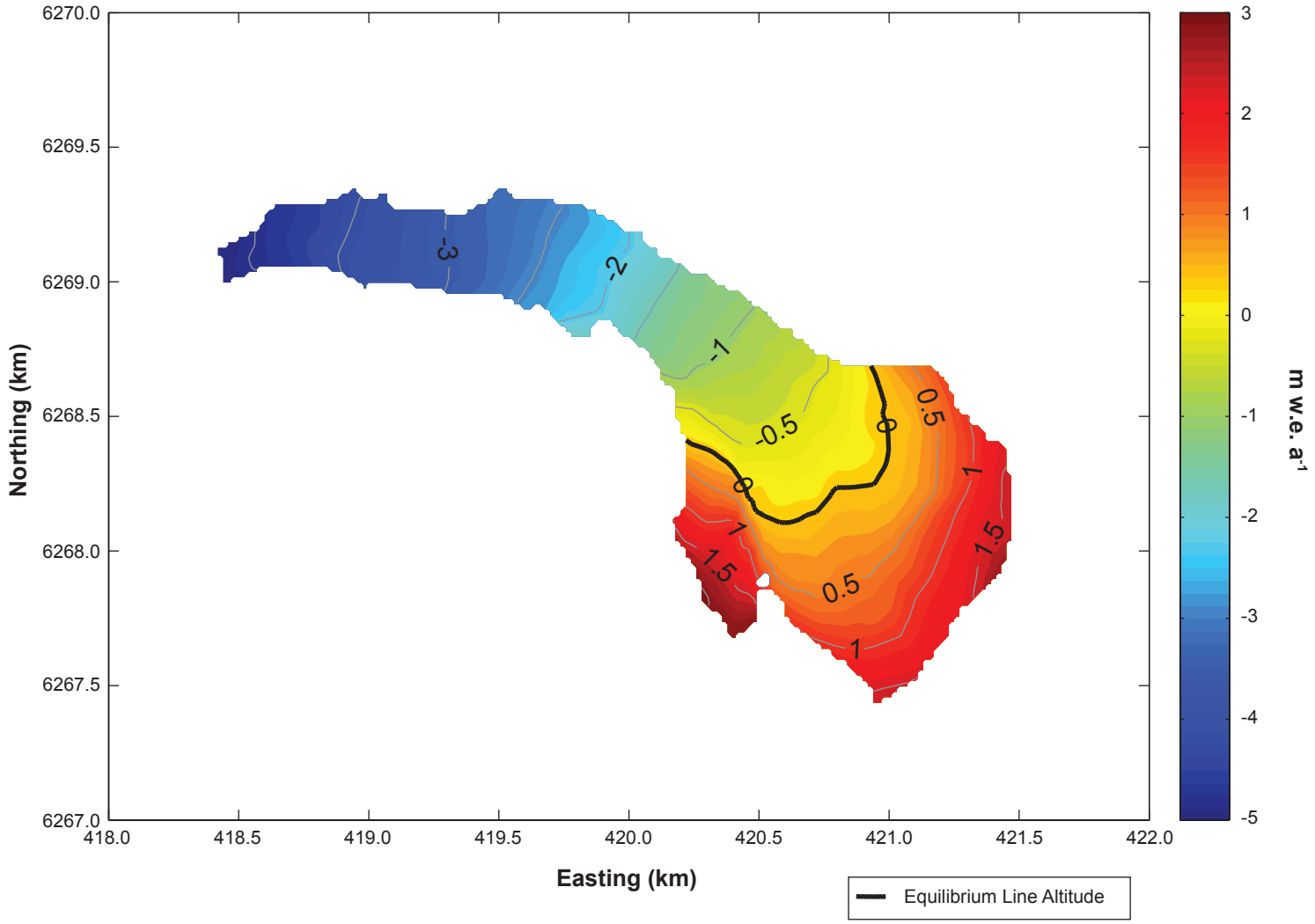

Figure 4.2-15

SEABRIDGE GOLD
KSM PROJECT

McTagg East Glacier Annual Mass Balance, 2010 to 2011

Figure 4.2-15

Rescan™ Engineers & Scientists

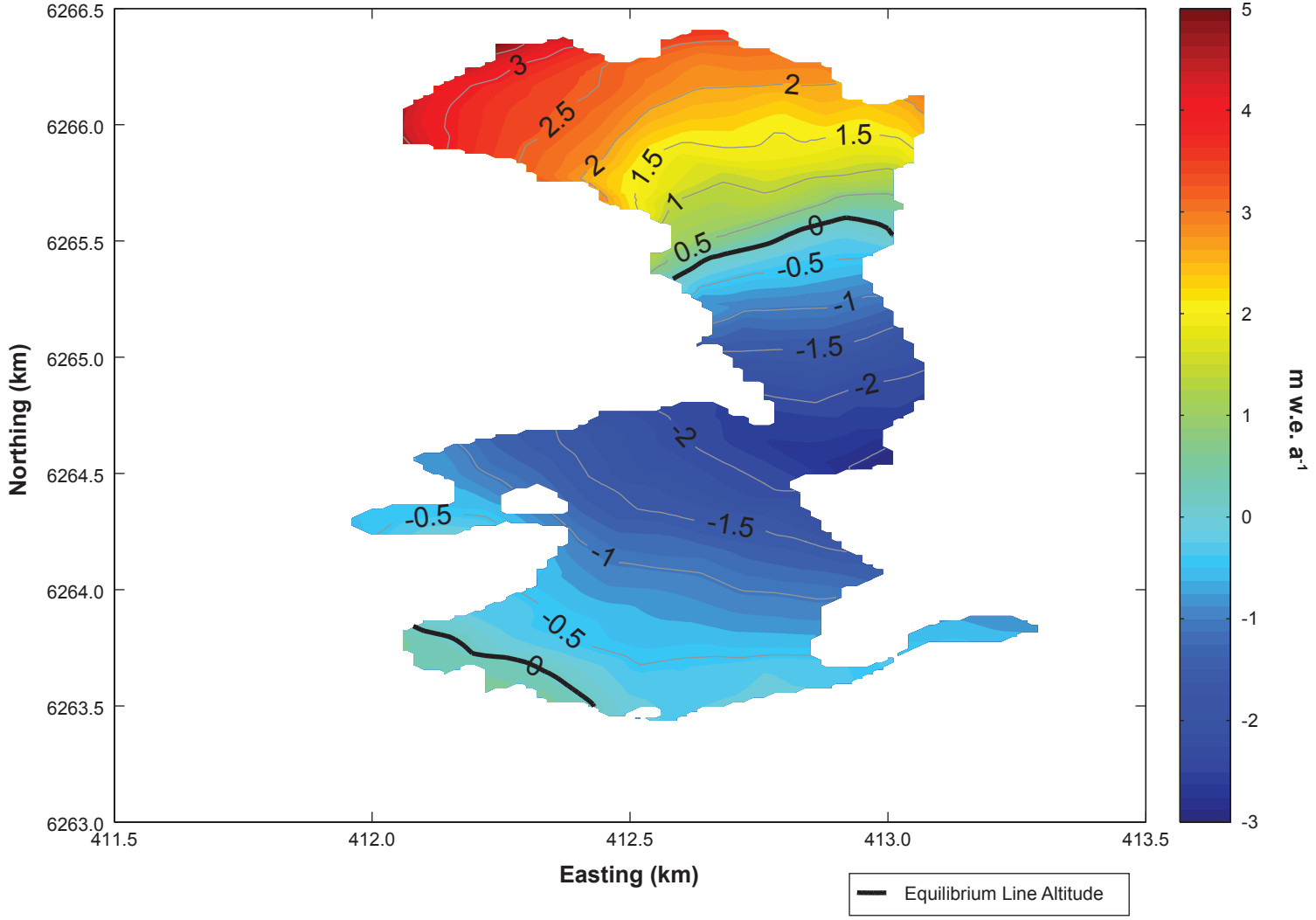

Figure 4.2-16

SEABRIDGE GOLD
KSM PROJECT

Gingras North and South Glacier
Annual Mass Balance, 2010 to 2011

Figure 4.2-16

Rescan™ Engineers & Scientists

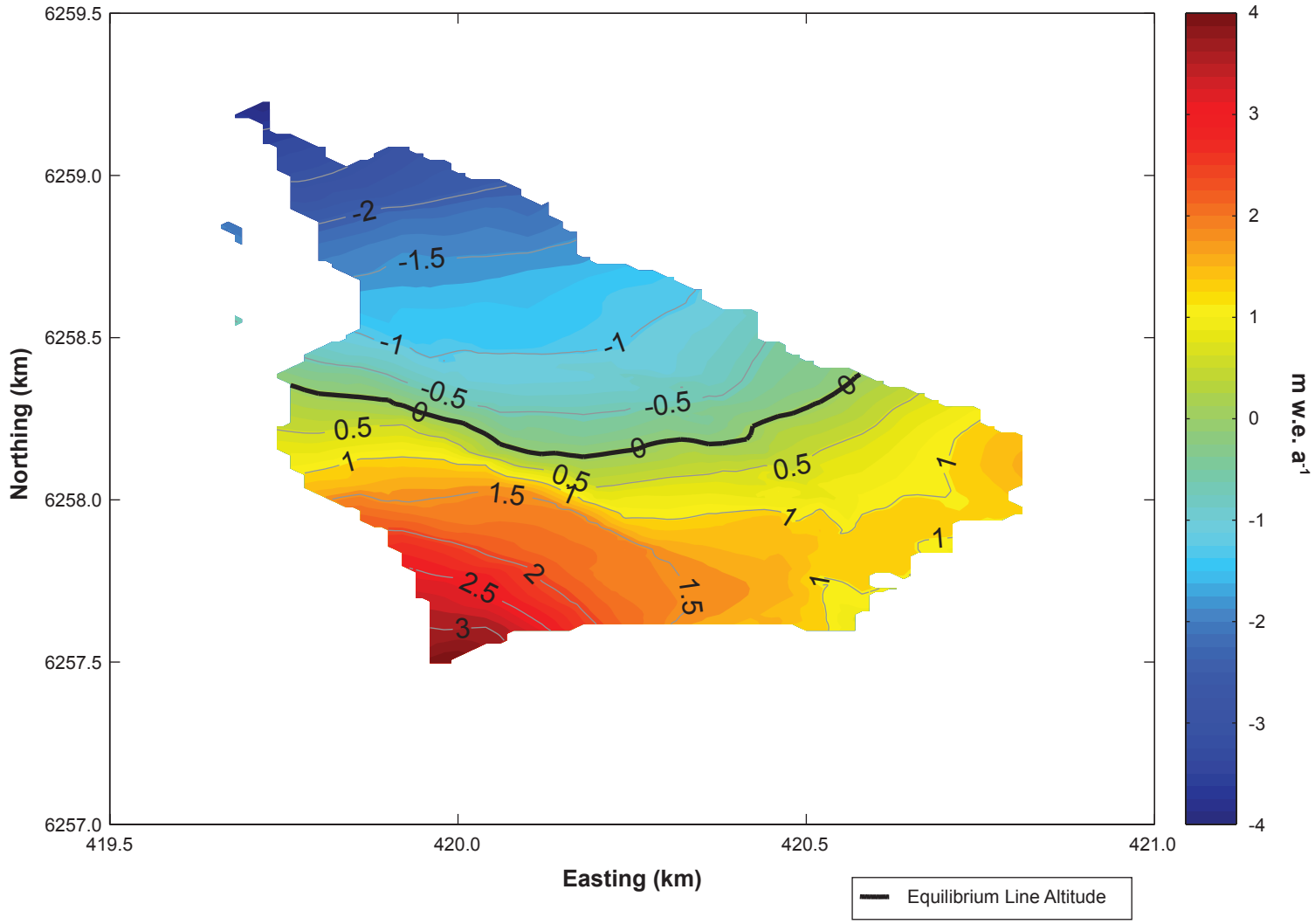

Figure 4.2-17

SEABRIDGE GOLD
KSM PROJECT

Kerr Glacier Annual Mass Balance, 2010 to 2011

Figure 4.2-17

Rescan™
Engineers & Scientists

The 2011 equilibrium line altitude (ELA), defined as the elevation where $b_n = 0$, is estimated to be 1,772 masl on Mitchell Glacier in 2011 (Table 4.2-11) compared to 1,976 masl in 2010 and 1,742 in 2009. It is important to note that due to the complex surface topography of Mitchell Glacier, the ELA is discontinuous and has been observed to span a 500 m elevation range (Rescan 2011). The ELA on the other glaciers in the monitoring program is estimated to be slightly lower than for Mitchell Glacier in 2011, with elevations of 1,665 masl for the McTagg South and West and East glaciers and 1,677 masl for Gingras and Kerr glaciers (Table 4.2-11).

Table 4.2-11. Accumulation Area Ratios and Equilibrium Line Altitude for Each Glacier

Glacier	Mitchell	McTagg South and West	McTagg East	Gingras	Kerr
Area (km^2)	16.36	7.61	2.15	2.05	1.14
$+b_n$ area (km^2) 2009	10.47	2.77	0.55	0.63	0.50
$+b_n$ area (km^2) 2010	5.27	0.00	0.00	0.07	0.02
$+b_n$ area (km^2) 2011	10.17	3.83	0.93	0.80	0.65
ELA (m)	1,772	1,665	1,665	1,677	1,677
AAR 2009	0.64	0.37	0.26	0.31	0.44
AAR 2010	0.33	0.00	0.00	0.03	0.20
AAR 2011	0.62	0.50	0.43	0.36	0.55

Note: 2009 and 2010 values for McTagg South and West, McTagg East, Gingras and Kerr glaciers are derived by applying Mitchell Glacier mass balance relationships to these sites (Rescan 2011).

Knowledge of the ELA can be used to calculate the accumulation area ratio (AAR), or the proportion of glacier area which experiences a positive net mass balance in a given year:

$$AAR = \frac{A_{b_n>0}}{A} \approx \frac{A_{ELA}}{A} \qquad [11]$$

where $A_{b_n>0}$ is the area with net balance (b_n) greater than zero and A is the total glacier area.

In cases where b_n is calculated as a function of elevation only, $A_{b_n>0}$ is equivalent to the area above the ELA (A_{ELA}). An *AAR* of 1.0 indicates that no ice melt occurred, while an *AAR* of 0 indicates that the entire ice surface was exposed to ice-melt. Glaciers in steady-state conditions have *AAR*s between 0.5 and 0.8, depending on the local climate. The quantities $A_{b_n>0} \approx A_{ELA}$ and A were calculated from the glacier DEMs and are given in Table 4.2-11 along with Mitchell Glacier values for 2009 and 2010.

For 2011, AAR values range from 0.36 to 0.62 for all glaciers (Table 4.2-11). McTagg East and Gingras glaciers have AAR values of less than 0.5, indicating that these glaciers were in a state of disequilibrium (negative mass balance) in 2011. The AAR for McTagg South and West Glacier and Kerr Glacier indicates that 50-55% of the glaciers' area accumulated mass over this time period. The 2011 AAR for Mitchell Glacier is comparable to the 2009 year, indicating that

~60% of the glacier experienced a net mass gain. However, in 2010 Mitchell Glacier had a lower AAR value of 0.33, illustrating the interannual variability in the glacier mass balance regime.

4.2.5 Glacier Averaged Mass Balance

Glacier-averaged mass balances (B_w, B_s, B_n) calculated from the distributed winter, summer, and net balances are shown in Table 4.2-12 and correspond to the total estimated mass gained or lost by the glacier over one mass balance year. The 2009 and 2010 values for Mitchell Glacier are also given as a comparison. As mentioned above, the estimated net balance based on Equation [10], B_n, yields similar results to the sum of the summer and winter balances (B_n* in Table 4.2-12), but is less reliable when some sites are measured inconsistently.

Table 4.2-12. Glacier-averaged Winter, Summer and Net Mass Balance

Glacier	Year	B_w	B_s	B_n	$B_n^* = B_w + B_s$	Diff B_n-B_n*
Mitchell	2009	1.95	-2.03	-0.04	-0.08	0.04
	2010	0.98	-2.33	-1.33	-1.35	0.02
	2011	1.41	-1.71	-0.22	-0.30	0.08
McTagg South and West	2011	1.41	-1.82	-0.15	-0.40	0.26
McTagg East	2011	1.33	-2.21	-0.66	-0.87	0.21
Gingras	2011	1.75	-1.98	-0.07	-0.23	0.16
Kerr	2011	1.79	-1.83	0.13	-0.04	0.17

Note: All values in metres of water equivalent (m w.e.) and B_n values are based on distributed b_n.

Considering the range of b_n values, and the magnitude of the estimated summer and winter balances, B_n and B_n* are in good agreement for all sites, and particularly Mitchell Glacier. This consistency between methods and years is an encouraging result given the challenges associated with weather, snow, and surface conditions that affect data collection in the field. For consistency with previous years, we take B_n to be the best estimate of the glacier-averaged mass balance.

Mitchell Glacier had a negative overall mass balance in 2011, but the value of -0.22 m w.e. is higher than for the 2010 year, when B_n was -1.33 m.w.e. This is a result of less summer melt (B_s was -2.3 m w.e. in 2010 and -1.7 m w.e. in 2011) and higher snow accumulation and B_w values (1.0 m w.e. in 2010 compared to 1.4 m w.e. in 2011).

McTagg South and West, McTagg East and Gingras North and South glaciers also had negative mass balances of between -0.07 and -0.66 m w.e. Kerr Glacier is the only site with a slightly positive net mass balance. However, as discussed above, extrapolation of the elevation-b_n curve in Figure 4.2-12 could result in an overestimation of b_n at high elevations, and this would bias the glacier-averaged mass balance. However, as B_n* has a similar value, (though slightly negative), this potential bias does not seem to have a major impact on the calculation of B_n.

4.3 Glacier Dynamics

The first full year of the glacier dynamics program was completed on Mitchell Glacier in 2010. In addition, stakes installed on the McTagg South and West, McTagg East, Gingras North and South, and Kerr Glaciers now enables surface velocity estimates to be calculated for the 2010 - 2011 mass balance year on these glaciers.

It should be noted that the discrepancies between the DGPS data and the Trim data are related to mapping accuracy in the field versus remote methods. Field mapping will usually include parts of the terminus that are debris covered, which could be extensive for some glaciers. This is very difficult to delineate using satellite imagery and so remotely-mapped extents are usually limited to debris free sections, for which the mapper has higher confidence. For field surveys of the glacier termini in this study, we include debris-covered ice if it is actively flowing and connected to the main body of the glacier.

4.3.1 Terminus Positions

4.3.1.1 Mitchell Glacier

Differential GPS surveys of the terminus of Mitchell Glacier, collected in the September of 2008, 2009, 2010 and 2011 are shown in Figure 4.3-1. The 2008 terminus was located between 100 and 250 m east of the 2004 terminus digitized from remotely sensed imagery. This represents a retreat rate of approximately 25 to 50 m/y. The average retreat rate between September 2009 and September 2010 was approximately 35 m/y and the retreat rate at the easternmost point of the terminus was approximately 100 m/y, twice that noted in 2009. For September 2010 to September 2011, the average retreat rate at the terminus increased to 48 m/y, with a maximum rate of 93 m/y at the easternmost point. This likely reflects the negative mass balance of the previous (2010) year (Table 4.2-12) Note that the glacier itself does not retreat (i.e., the ice does not flow uphill); rather the rate of melt is greater than the rate of advance, causing the glacier terminus to melt back from its position. Furthermore, this retreat rate is highly variable, and is difficult to quantify because the shape of the terminus is irregular and the retreat rate is not uniform along the length of the terminus.

4.3.1.2 McTagg, Gingras and Kerr Glaciers

DGPS terminus surveys of the McTagg South and West (Figure 4.3-2), McTagg East (Figure 4.3-3), Gingras North and South (Figure 4.3-4) and Kerr glaciers (Figure 4.3-5) were conducted in September 2010 and will be updated in September 2012. Definition of the ice terminus and glacial extent proved difficult where debris covered ice, ice-cored moraines, seasonal snow cover and debris complicated the survey boundaries (Plates 4.3-1 to 4.3-3). This was especially the case for McTagg South and West and McTagg East glaciers. These problems are commonly encountered during remote classification work, and are summarized by Paul et al. (2004).

PROJECT # 0868-016-06-01 GIS No. KSM-10-159 November 22, 2012

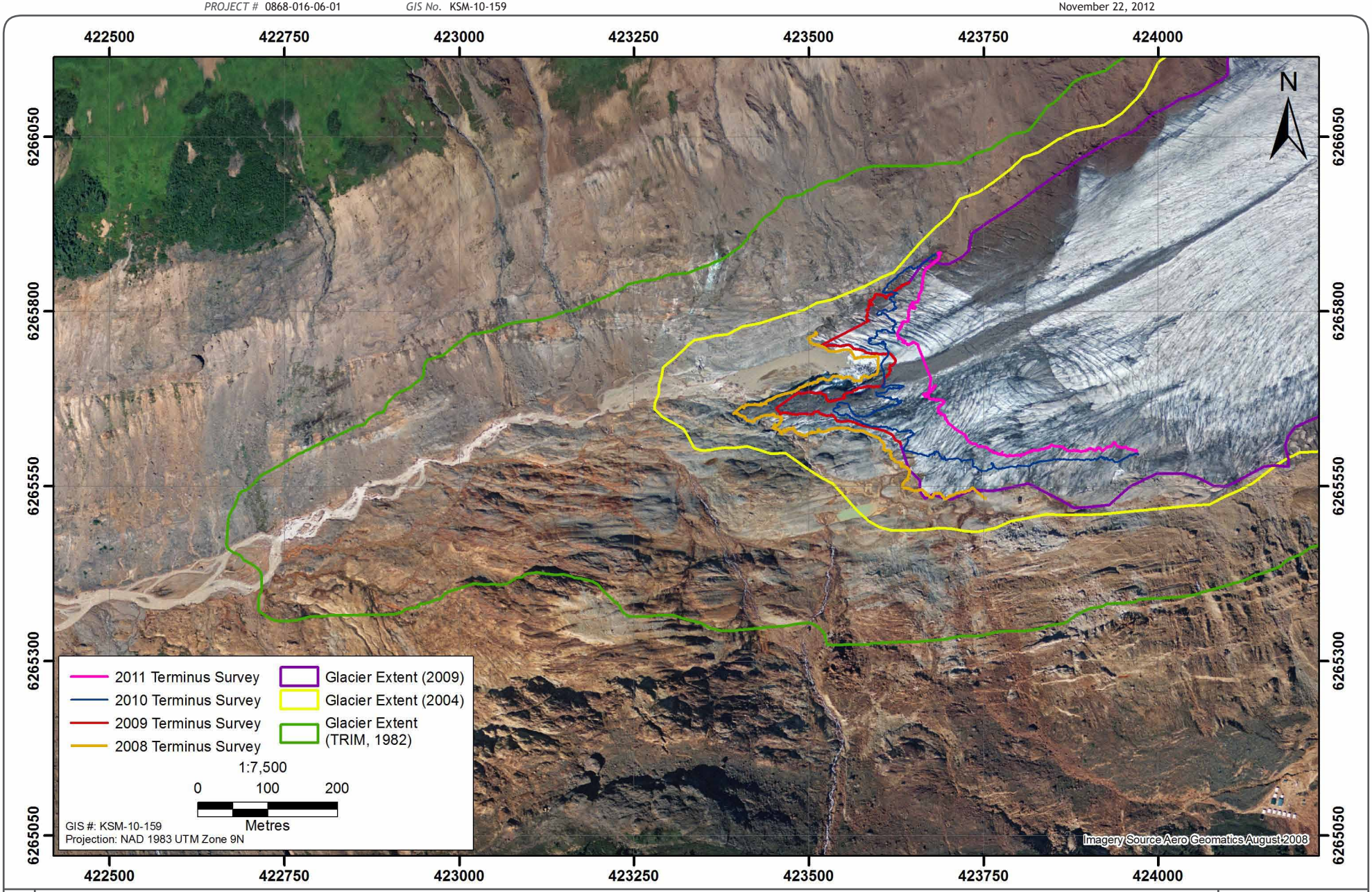

Figure 4.3-1

SEABRIDGE GOLD
KSM PROJECT

DGPS Survey of the Mitchell Glacier Terminus

Figure 4.3-1

Rescan
Engineers & Scientists

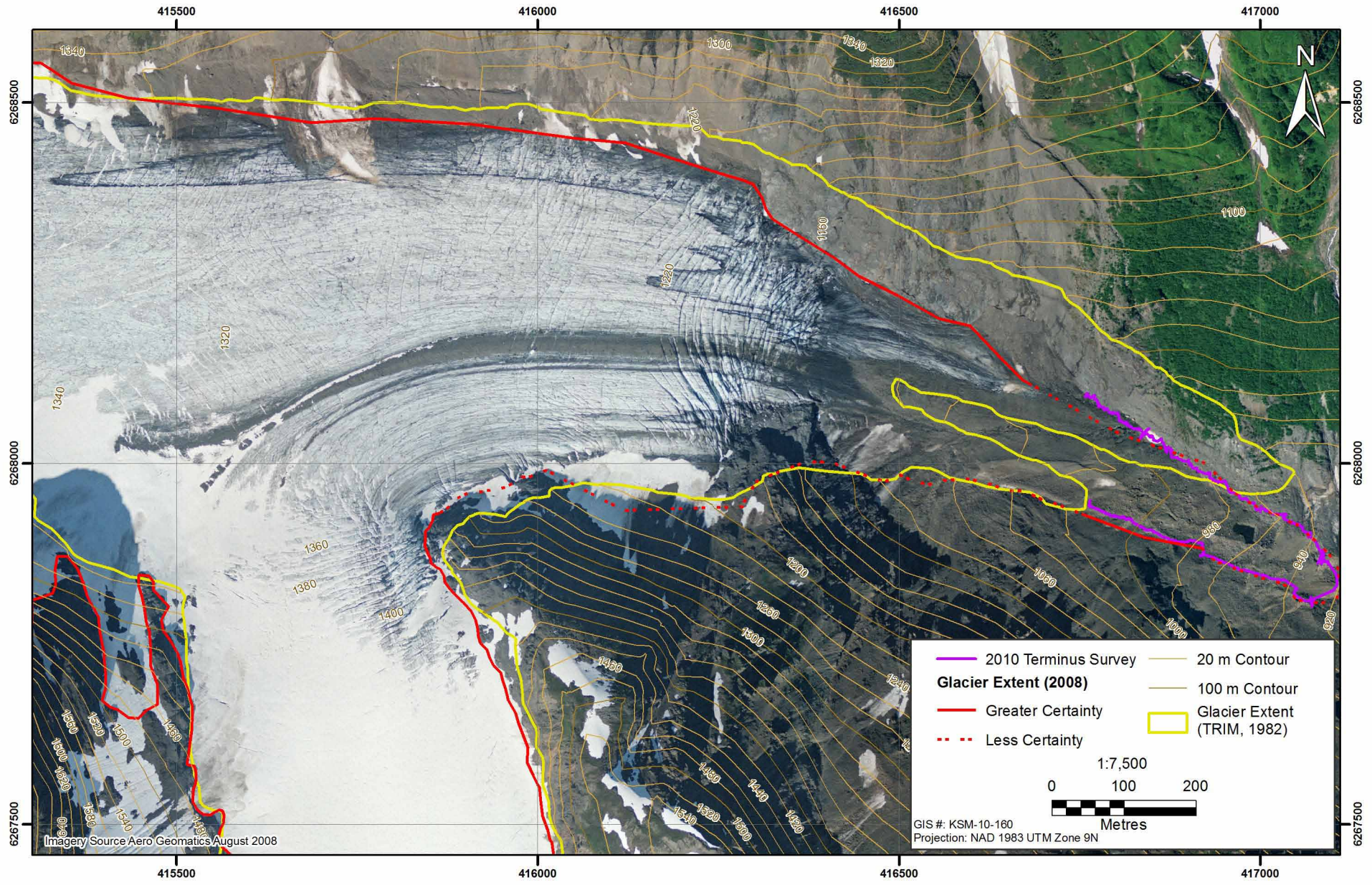

Figure 4.3-2

SEABRIDGE GOLD
KSM PROJECT

DGPS Survey of the McTagg South and West Glacier Terminus

Figure 4.3-2

Rescan
Engineers & Scientists

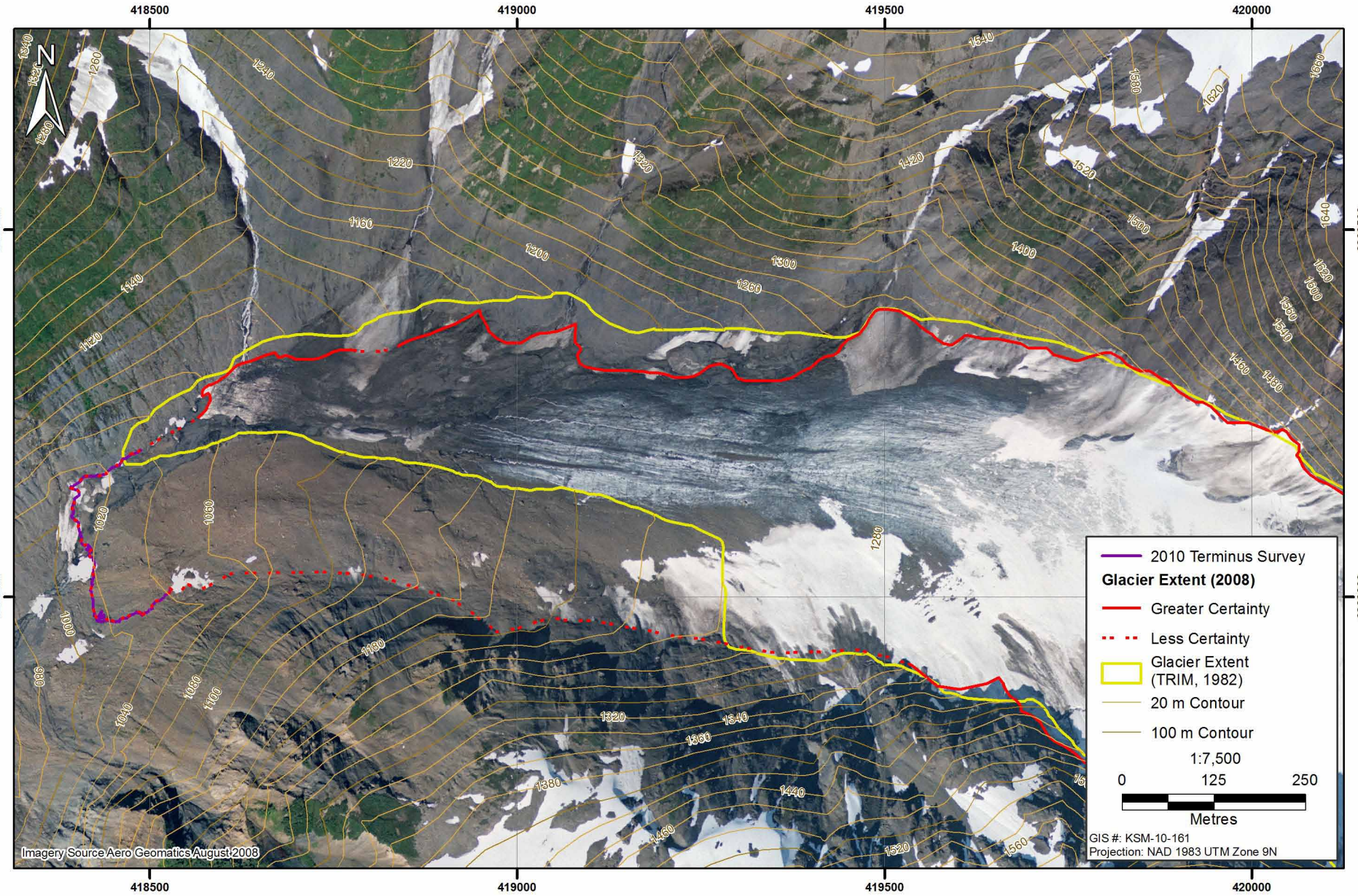

Figure 4.3-3

SEABRIDGE GOLD
KSM PROJECT

DGPS Survey of the McTagg East Glacier Terminus

Figure 4.3-3

Rescan
Engineers & Scientists

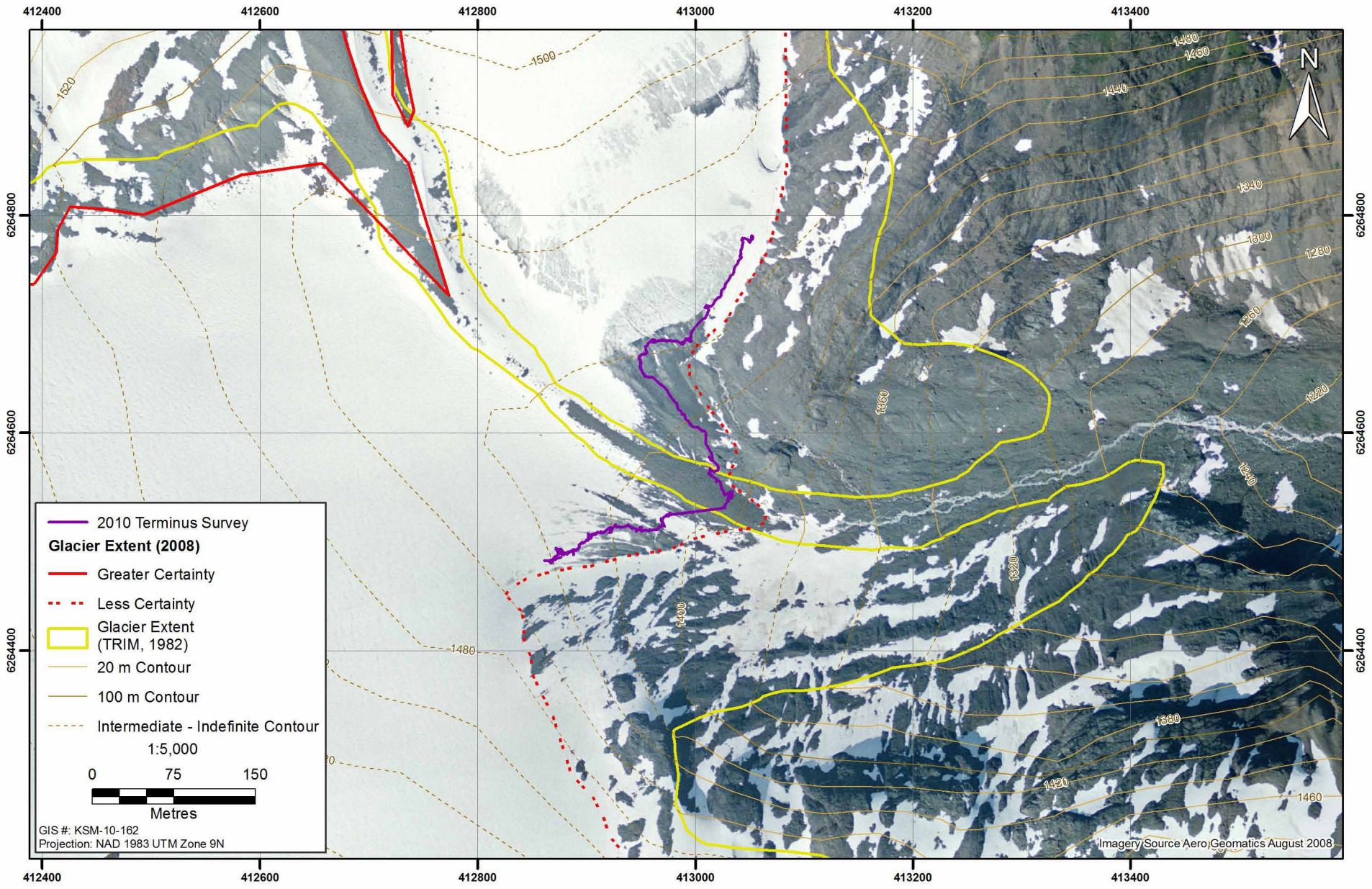

Figure 4.3-4

SEABRIDGE GOLD
KSM PROJECT

DGPS Survey of the Gingras North and South Glacier Terminus

Figure 4.3-4

Rescan
Engineers & Scientists

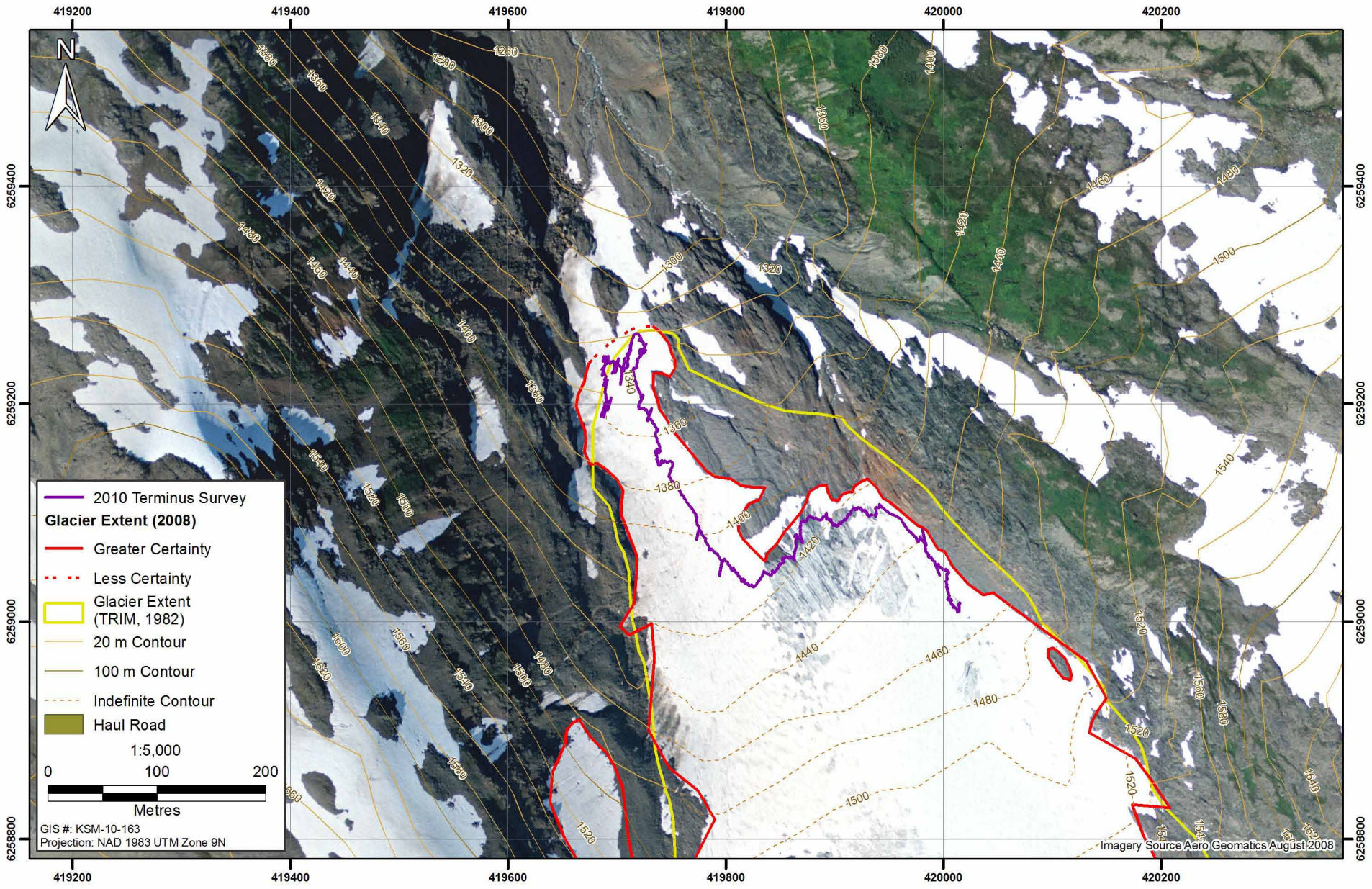

Figure 4.3-5

SEABRIDGE GOLD
KSM PROJECT

DGPS Survey of the Kerr Glacier Terminus

Figure 4.3-5

Rescan
Engineers & Scientists

Plate 4.3-1. Terminus of McTagg South and West Glacier, September 2010.

Plate 4.3-2. Terminus of McTagg East Glacier, September 2010.

Plate 4.3-3. Aerial view of the Terminus of Gingras North and South Glacier, September 2010. The north arm is to the right of the image, and the south arm is at the top of the image.

4.3.2 Surface Velocity

Glacier surface velocity was estimated from repeat surveys of ablation stakes drilled into the ice. The positions of all stakes were tracked between September 2010 and September 2011 and data were used to estimate the total horizontal (xy) and vertical (z) displacement and surface velocities (equivalent to the three dimensional displacement; xyz) for 2010 - 2011. These calculations are shown for Mitchell Glacier in Table 4.3-1 alongside values for the 2010 mass balance year. Velocities at ablation stake sites for 2010 and 2011 are very close, with a maximum difference of 6.1 m at MI-1400. This illustrates the dominant role of topography, rather than inter-annual differences in mass balance, in controlling surface velocities.

Table 4.3-1. Displacement and Velocity of Ablation Stakes on Mitchell Glacier for 2009 and 2010 Mass Balance Years

	September 2009 - September 2010			September 2010 - September 2011		
	Displacement		Velocity	Displacement		Velocity
Site	xy (m)	z (m)	(m/yr)	xy (m)	z (m)	(m/yr)
MI-900				8.9	-19.8	21.7
MI-960	17.5	-10.8	20.6	14.4	-17.0	22.3
MI-1000	25.8	-8.1	27.1	23.0	-16.7	28.4
MI-1100	47	-7.2	47.6	45.7	-19.5	49.7
MI-1200	65	-11.9	66.1	55.8	-25.5	61.3
MI-1300	85	-13.3	86	84.0	-28.1	88.5
MI-1400	100	-12.4	100.8	105.1	-19.3	106.9
MI-1450	45.3	-3.5	45.5	45.0	-14.2	47.2
MI-1525	64	-11.9	65.1	63.3	-22.7	67.2

xy = the horizontal plane and z = the vertical plane.

A vector plot of the changes in stake location (Figure 4.3-6) shows the magnitudes and directions of ice flow observed at Mitchell Glacier. This indicates that the glacier is well-nourished at high elevations, leading to relatively rapid downslope flow, with the highest velocities measured at MI-1400 (107 m/y). Near the terminus, a downslope velocity of 22 m/y was observed at MI-900 and MI-960. Given the observed average terminus retreat rate of 48 m/yr, this suggests that ablation at the terminus is only partially offset by ice flow to the lower portions of the glacier. In this situation, downwasting may become the dominant mode of glacier wastage at the terminus, as opposed to ice cliff calving. A pattern of decreasing velocities towards the terminus is furthermore consistent with previous studies of warm-based alpine glacier dynamics (e.g., Kaab 2005).

In addition to the glacier motion evidenced by repeat DGPS surveys of several ablation stakes, the presence of numerous heavily-crevassed zones, as well as field observations of large cracks and shifts in the ice indicates that Mitchell Glacier is characterized by an active flow regime (Plate 4.3-4). Other evidence for the motion of the Mitchell Glacier can be inferred from the characteristics of ice at the glacier margins. Plate 4.3-5 illustrates a boundary between bottom-ice (sediment-laden) and surface ice (clean and blue). The evidence for motion at the base suggests that the entire depth of the glacier is in motion, but that ice at the surface is travelling faster than ice at the base, resulting in this discontinuity.

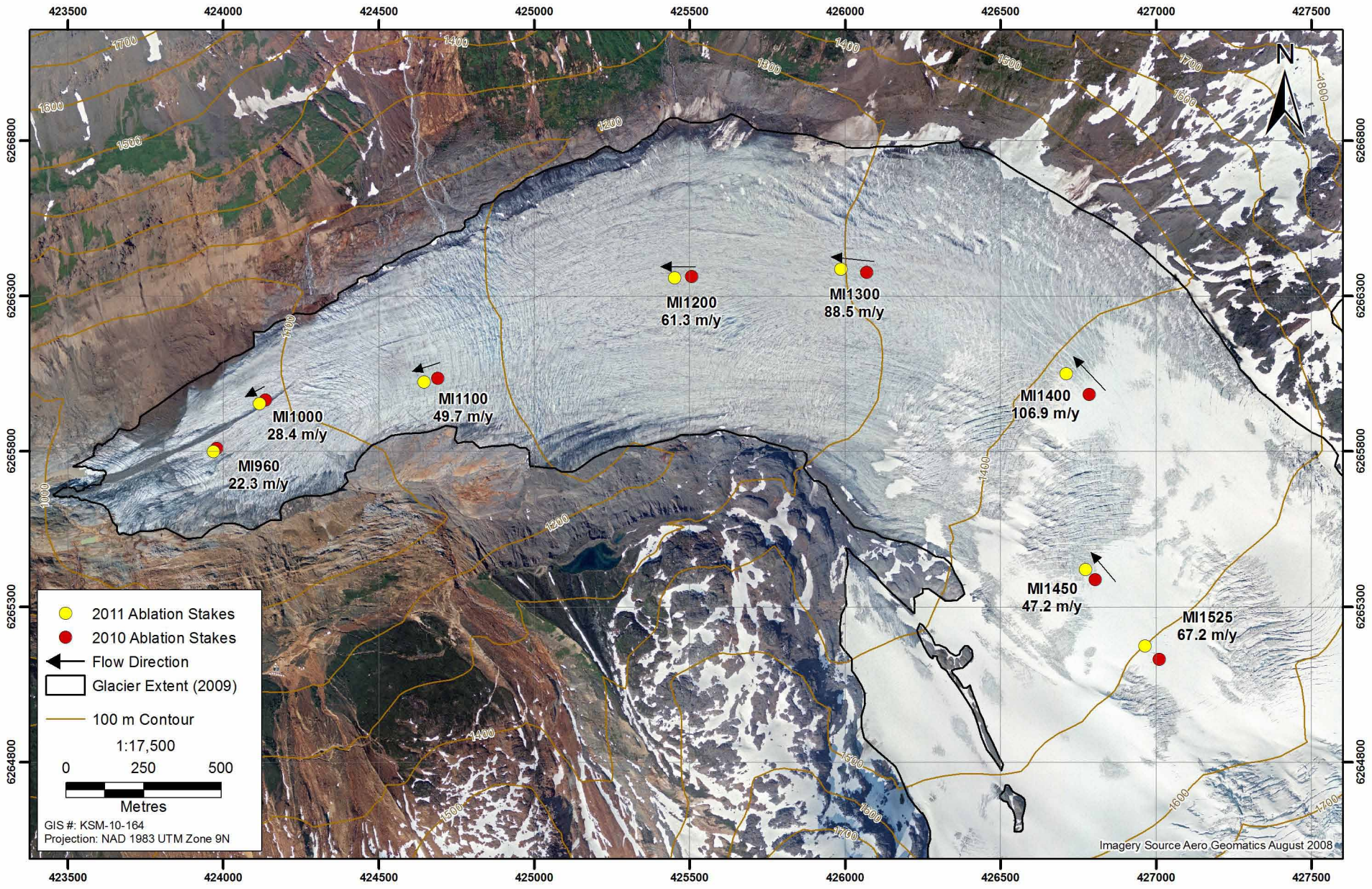

Figure 4.3-6

SEABRIDGE GOLD
KSM PROJECT

Mitchell Glacier Surface Velocities, September 2010 to September 2011

Figure 4.3-6

Rescan
Engineers & Scientists

Plate 4.3-4. Aerial view looking southward down the Mitchell Glacier, September 2010.

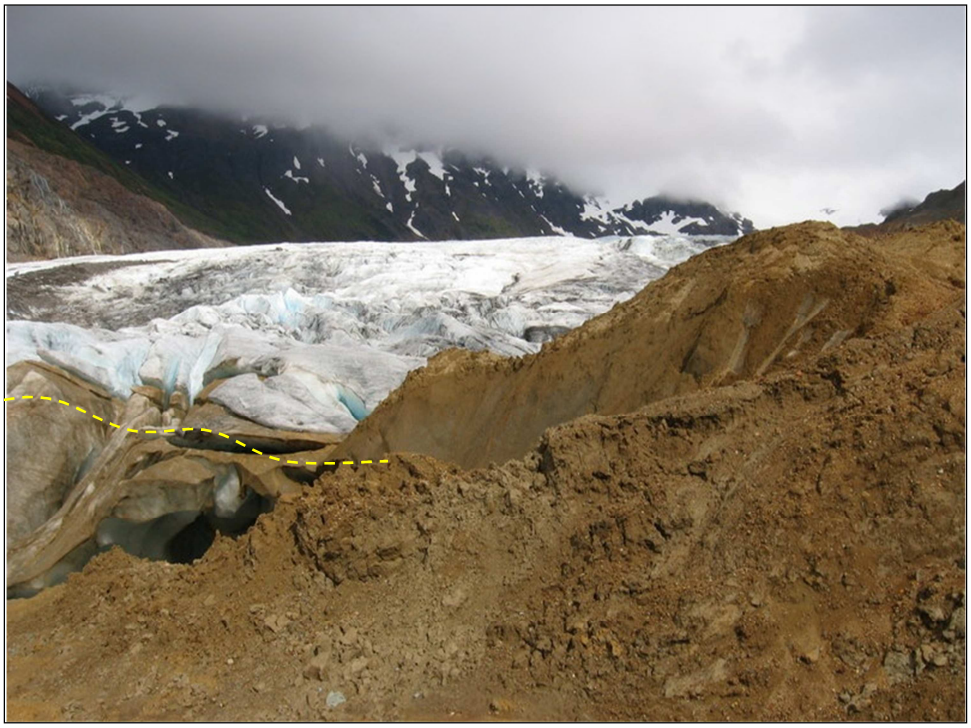

Plate 4.3-5. Discontinuity (see dashed line) between bottom ice (sediment-laden) and surface ice, which appear to be flowing at different speeds.

Table 4.3-2 gives estimates of surface displacement and velocity for McTagg South and West, McTagg East, Gingras and Kerr glaciers. McTagg South and West Glacier has surface velocity range (17 to 104 m/yr) comparable to velocities at Mitchell Glacier (22-107 m/yr). Like Mitchell Glacier (Table 4.3-1), the highest velocity does not occur at the terminus, but at MI-1625. However, the velocity at a low-elevation site, MW-1040, is relatively high (99 m/yr) compared to the velocity of 28 m/yr observed at ~1,000 masl on Mitchell Glacier. It is possible that the terminus of McTagg South and West Glacier responds more rapidly to the input of summer meltwater and that basal sliding is more dominant at this site compared to Mitchell Glacier. By comparison, McTagg East, Gingras North and South and Kerr glaciers have low surface velocities at all elevations, with a maximum of 36 m/yr observed at McTagg East Glacier and 10 and 14 m/yr for the Gingras North and South Glacier and Kerr Glacier, respectively.

Table 4.3-2. Displacement and Velocity of Ablation Stakes on McTagg South and West, McTagg East, Gingras North and South and Kerr Glaciers

		September 2010 - September 2011		
		Displacement		Velocity (m/yr)
Glacier	Site	xy (m)	z (m)	
McTagg South and West	MW-1040	53.2	-83.8	99.2
	MW-1200	20.5	-2.6	20.7
	MW-1250	19.0	-1.9	19.1
	MW-1325	22.4	-13.0	25.9
	MS-1440	17.4	-11.7	21.0
	MW-1440	27.5	-26.0	37.9
	MS-1500	9.6	-14.5	17.4
	MW-1500	30.5	-10.3	32.2
	MW-1575	19.6	-11.0	22.5
	MW-1625	104.1	-8.9	104.4
McTagg East	ME-1150	7.1	-7.8	10.5
	ME-1225	11.8	0.0	11.8
	ME-1300	25.4	-9.9	27.3
	ME-1400	33.7	-12.5	35.9
	ME-1550	N/A	N/A	N/A
	ME-1600	16.6	-10.5	19.7
Gingras North and South	GS-1400	4.4	-9.2	10.2
	GN-1425	3.4	-5.5	6.4
	GS-1500	6.8	-5.7	8.9
	GS-1600A	3.7	-9.0	9.7
	GS-1600B	1.2	-8.1	8.2

(continued)

Table 4.3-2. Displacement and Velocity of Ablation Stakes on McTagg South and West, McTagg East, Gingras North and South and Kerr Glaciers (completed)

Glacier	Site	September 2010 - September 2011		
		Displacement		Velocity (m/yr)
		xy (m)	z (m)	
Kerr	KG-1425	9.4	-4.0	10.2
	KG-1500	5.1	-9.5	10.8
	KG-1575	8.4	-11.1	13.9
	KG-1650	6.3	-8.7	10.7

xy = the horizontal plane and z = the vertical plane.

4.4 Conclusions

Measurements of glacier mass balance and dynamics at Mitchell, McTagg South and West, McTagg East, Gingras North and South and Kerr glaciers were conducted between September 2010 and September 2011 (Plates 4.4-1 and 4.4-2). This is the third consecutive year of mass balance measurements at Mitchell Glacier and the first year of monitoring at the other sites. A glacier-averaged net mass balance of -0.22 m w.e., calculated from point observations made at 27 sites, indicates that Mitchell Glacier was in disequilibrium, (i.e., negative mass balance) in 2011. This value is more positive than for the 2010 mass balance year (-1.33 m w.e.) and closer to the 2009 glacier-averaged mass balance (-0.04 m w.e.).

Plate 4.4-1. Travelling across the ablation zone of Mitchell Glacier during the 2011 mass balance survey.

Plate 4.4-2. Accumulation zone of Gingras North Glacier, surveyed for snow depth and density in April 2011.

At high elevations, Mitchell Glacier gained mass, with a maximum measured net balance of 1.8 m w.e. at 2,100 masl. The AAR suggests that 66% of the glacier experienced mass gain between September 2010 and September 2011. However, net mass balances of -7.9 m w.e. at the glacier terminus (1,000 masl) indicate that the glacier continued to lose mass at low elevations. Relatively low flow velocities indicate that this is primarily due to downwasting of the glacier surface rather than fast flow resulting from the input of summer melt water and basal sliding.

Evidence suggests that Mitchell Glacier is actively flowing, but low terminus velocities and downwasting of the glacier surface are sufficient to cause a retreat rate of approximately 48 m/y from September 2010 to September 2011. This rate is greater than the average 2004 - 2008 retreat rate estimated from satellite imagery, and the observed 2009 and 2010 rates of 25 m/y and 35 m/yr, respectively.

McTagg East Glacier had the lowest net mass balance of all glaciers in the monitoring program in the 2010 mass balance year (-0.66 m w.e.), with an AAR of 0.43, which suggests that less than half of the glacier gained mass. This is the result of high terminus ablation, with maximum measured values of -4.4 m w.e. near the terminus (at 1,150 masl). As for Mitchell Glacier, surface velocities are relatively low near the terminus of this glacier, suggesting that this loss of mass occurred primarily due to downwasting of the ice surface.

McTagg South and West, Gingras and Kerr glaciers all had glacier-averaged net mass balances close to neutral (ranging from -0.15 to 0.13 m w.e.), with AAR values of between 0.36 and 0.55. Measured ice loss at low elevations was less at these sites than at Mitchell and McTagg East

glaciers, with a net balance of -2.8 m w.e. at McTagg South and West Glacier (at 1,200 masl); -2.7 m w.e. at Gingras North and South Glacier (at 1,425 masl) and -2.0 m w.e. at Kerr Glacier (at 1,425 masl). Gingras North and South and Kerr glaciers have considerably higher snow depths and winter balance totals than the other glaciers in the study area, which contributes to the more positive net mass balance.

Ablation stake velocities were calculated for these glaciers between September 2010 and September 2011. McTagg South and West Glacier has high surface velocities, ranging from 21 to 104 m/yr, which is comparable to Mitchell Glacier. However, unlike Mitchell Glacier, it also has high terminus velocities, which suggests that this glacier responds rapidly to the input of summer melt water, which would lubricate the bed and cause basal sliding. Gingras North and South and Kerr glaciers have low surface velocities, with maximum speeds of only 10 - 14 m/yr.

References

Benn, D.I. and D. J. A Evans. 1998. *Glaciers and Glaciation*. John Wiley & Sons, New York, NY.

Bolch, T., B. Menounos, and R. Wheate. 2010. Landsat-based inventory of glaciers in Western Canada, 1985-2005. Remote Sensing of Environment 114: 127-137.

Braithwaite, R. J. 2002. Glacier mass balance: the first 50 years of international monitoring, Progress in Physical Geography, 26, pp. 76-95.

Clarke, G. K. C. 1991. Length, width, and slope influences on glacier surging, *Journal of Glaciology*, 37(126): 236-246.

Copland, L., M. J. Sharp, and J. Dowdeswell. 2003. The distribution and flow characteristics of surge-type glaciers in the Canadian High Arctic, *Annals of Glaciology*, 76:73-81.

Josberger, E. G., W. R. Bidlake, R. S. March, and B. W. Kennedy. 2007. Glacier mass-balance fluctuations in the Pacific Northwest and Alaska, USA. *Annals of Glaciology*, Volume 46, Number 1, October 2007, pp. 291-296(6)

Kaab, A. 2005. Combination of SRTM3 and repeat ASTER data for deriving alpine glacier flow velocities in the Bhutan Himalaya. *Remote Sensing of the Environment* 94(4):463-474. Moore, R.D., 2004. Introduction to salt dilution gauging for stream flow measurement: Part 1. *Streamline Watershed Management Bulletin*, 7(4), 20-23.

Østrem, G., and M. Brugman. 1991. *Glacier mass balance measurements: a manual for field and office work.* National Hydrology Research Institute, Inland Waters Directorate, Environment Canada, Saskatoon, Saskatchewan.

Paul, F., C. Huggel, and A. Kääb. 2004. Combining satellite multispectral image data and a digital elevation model for mapping debris covered glaciers. *Remote Sensing of Environment*, 89(4): 510-518.

Province of BC. 1998. *Standard for Developing Digital Data Specification Standards Documents.* Prepared by the Digital Data Working Group Resources Inventory Committee.

Raymond, C. F. 1987. How do glaciers surge? A review, *Journal of Geophysical Research*, 92(B9): 9121-9134.

Rescan. 2009. *Kerr-Sulphurets-Mitchell Project 2008 Baseline Study Report*. Prepared for Seabridge Gold by Rescan Environmental Services Ltd.

Rescan. 2010. *Kerr-Sulphurets-Mitchell Project 2009 Glacier Monitoring Baseline Report*. Prepared for Seabridge Gold by Rescan Environmental Services Ltd.

Rescan. 2011. *Kerr-Sulphurets-Mitchell Project 2010 Glacier Monitoring Baseline Report*. Prepared for Seabridge Gold by Rescan Environmental Services Ltd.

Shea, J. M., S. J. Marshall, and F. S. Anslow. 2005. Hydrometeorological relationships on Haig Glacier, Alberta, Canada. *Annals of Glaciology* 40, 52-60

Willis, I. C. 1995. Intra-annual variations in glacier motion: a review. *Progress in Physical Geography*, 19(1), pp. 61-106

APPENDIX 1
DISTRIBUTED SUMMER MASS BALANCE FOR MCTAGG SOUTH AND WEST, MCTAGG EAST, GINGRAS AND KERR GLACIERS

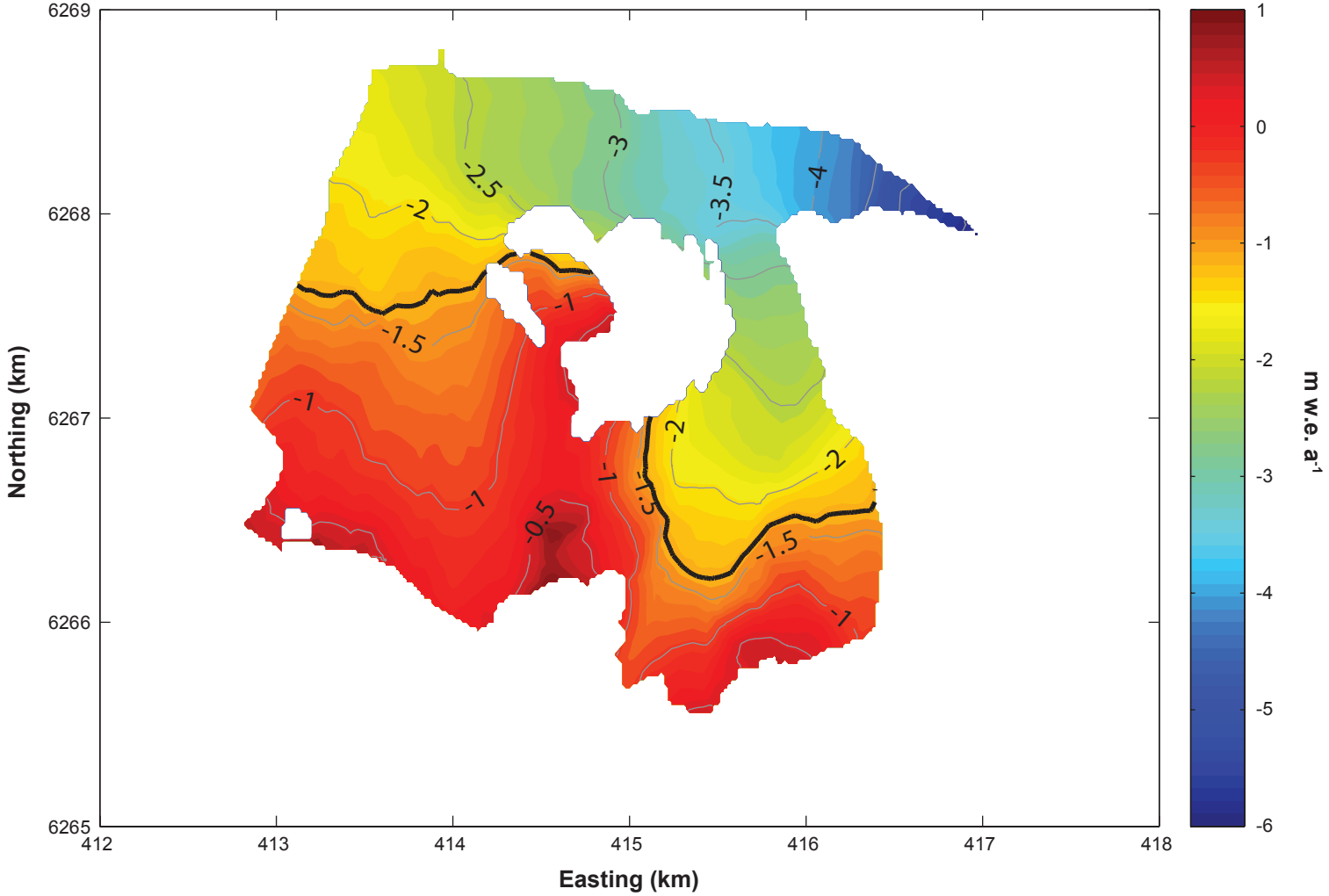

Figure A1-1

SEABRIDGE GOLD
KSM PROJECT

Distributed Summer Mass Balance for McTagg South and West

Figure A1-1

Rescan™ Engineers & Scientists

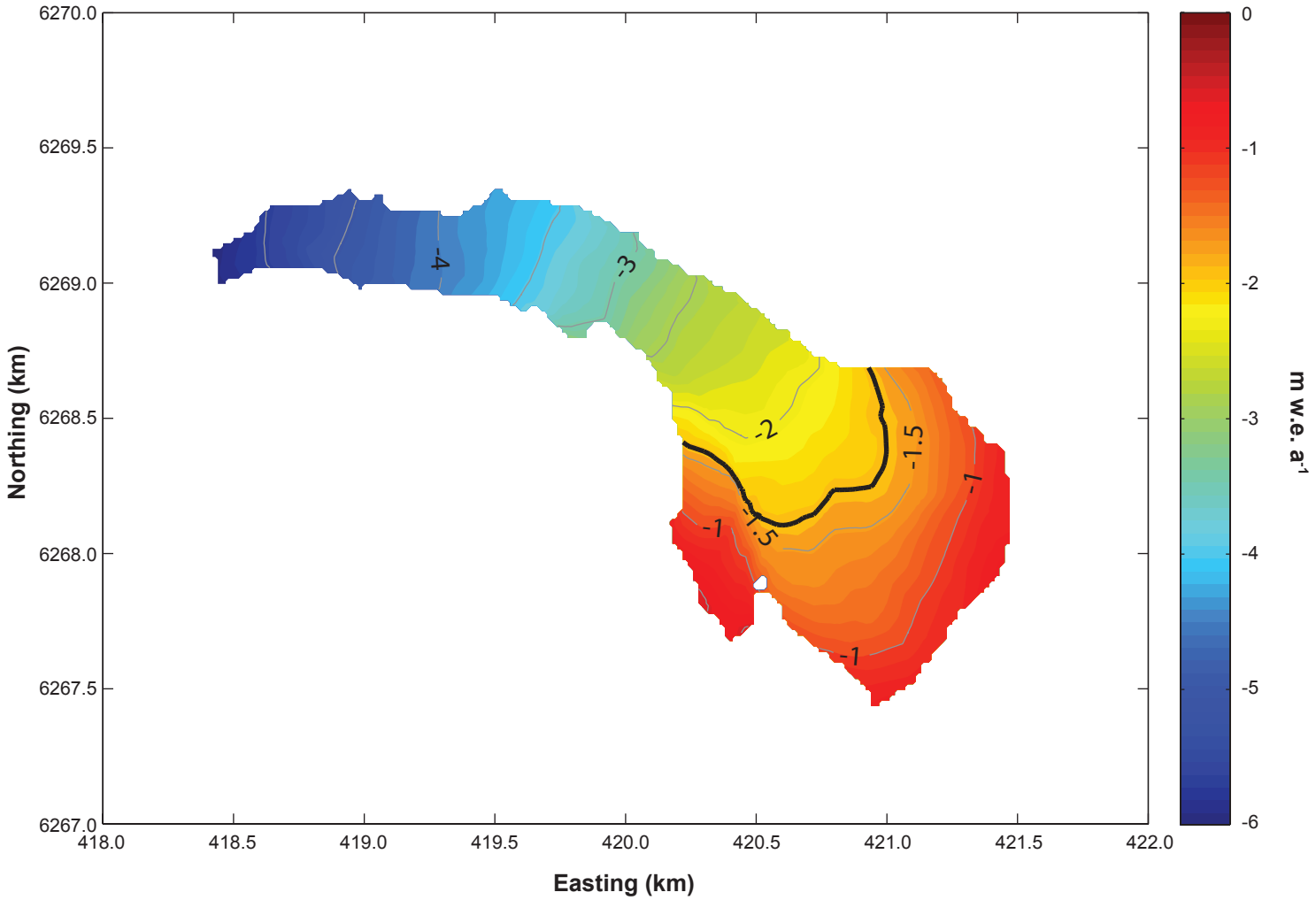

Figure A1-2

SEABRIDGE GOLD
KSM PROJECT

Distributed Summer Mass Balance for McTagg East

Figure A1-2

Rescan™ Engineers & Scientists

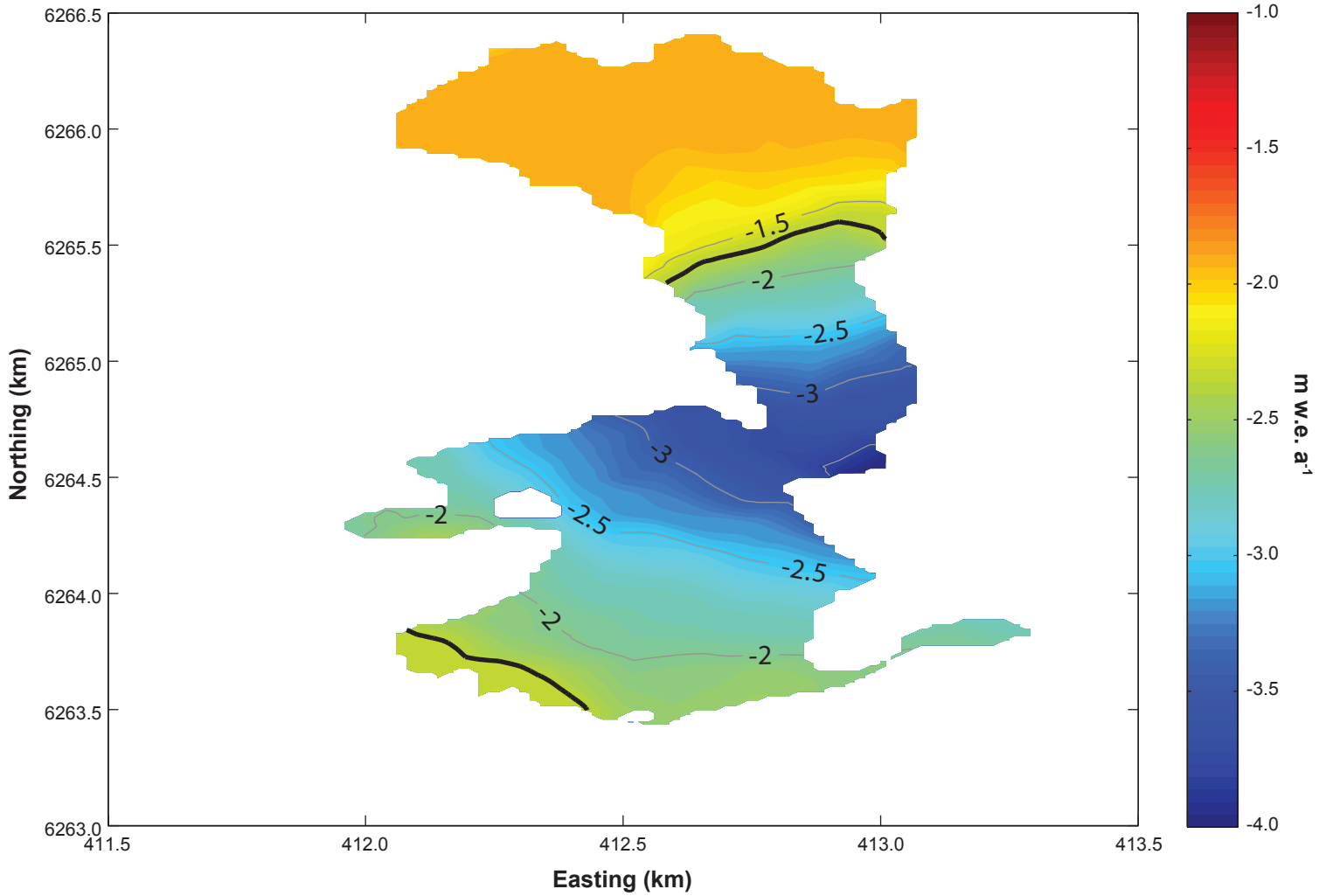

Figure A1-3

SEABRIDGE GOLD
KSM PROJECT

Distributed Summer Mass Balance for Gingras

Figure A1-3

Rescan™ Engineers & Scientists

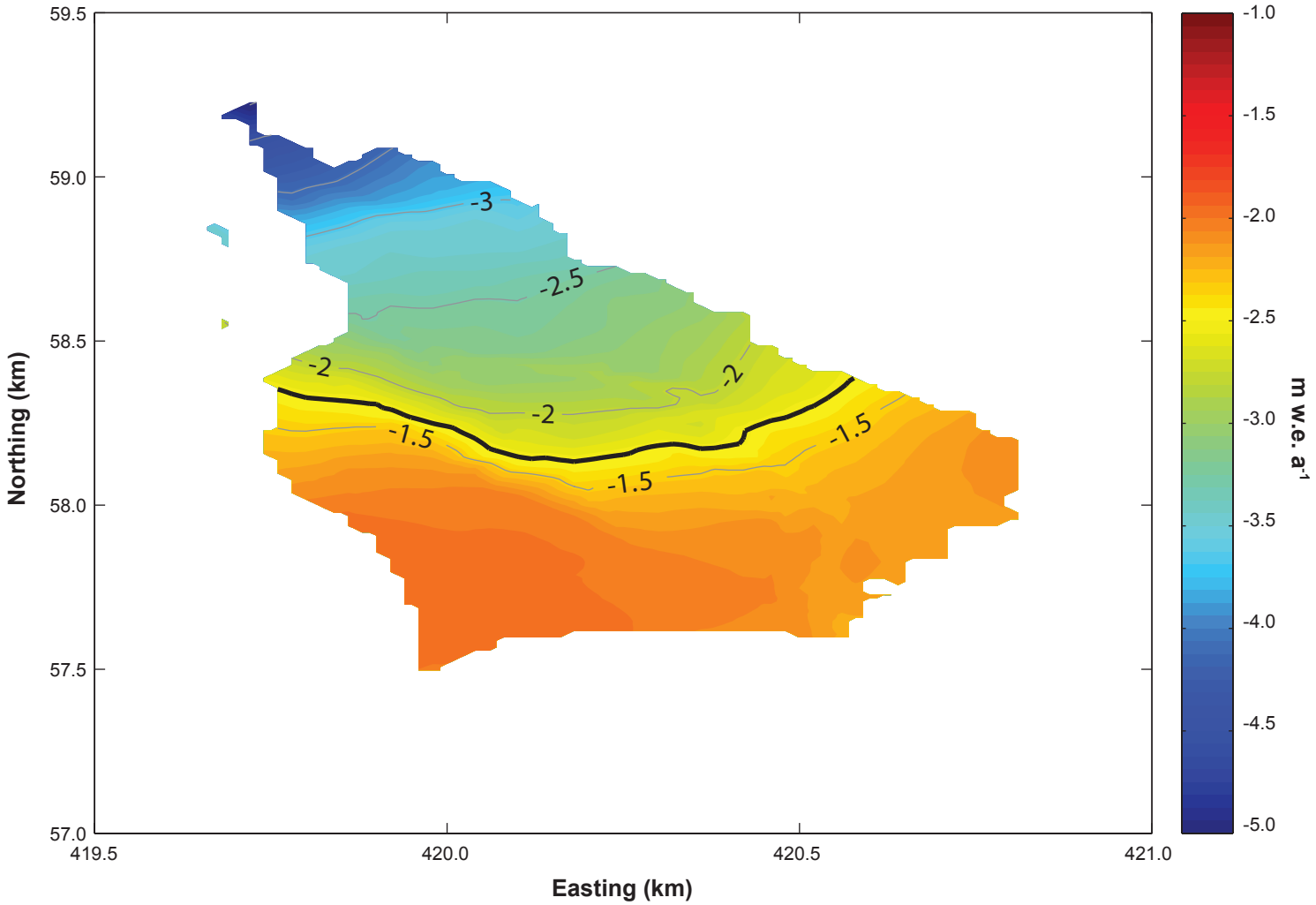

Figure A1-4

SEABRIDGE GOLD
KSM PROJECT

Distributed Summer Mass Balance for Kerr

Figure A1-4

Rescan™ Engineers & Scientists

APPENDIX 2
DISTRIBUTED WINTER MASS BALANCE FOR MCTAGG SOUTH AND WEST, MCTAGG EAST, GINGRAS AND KERR GLACIERS

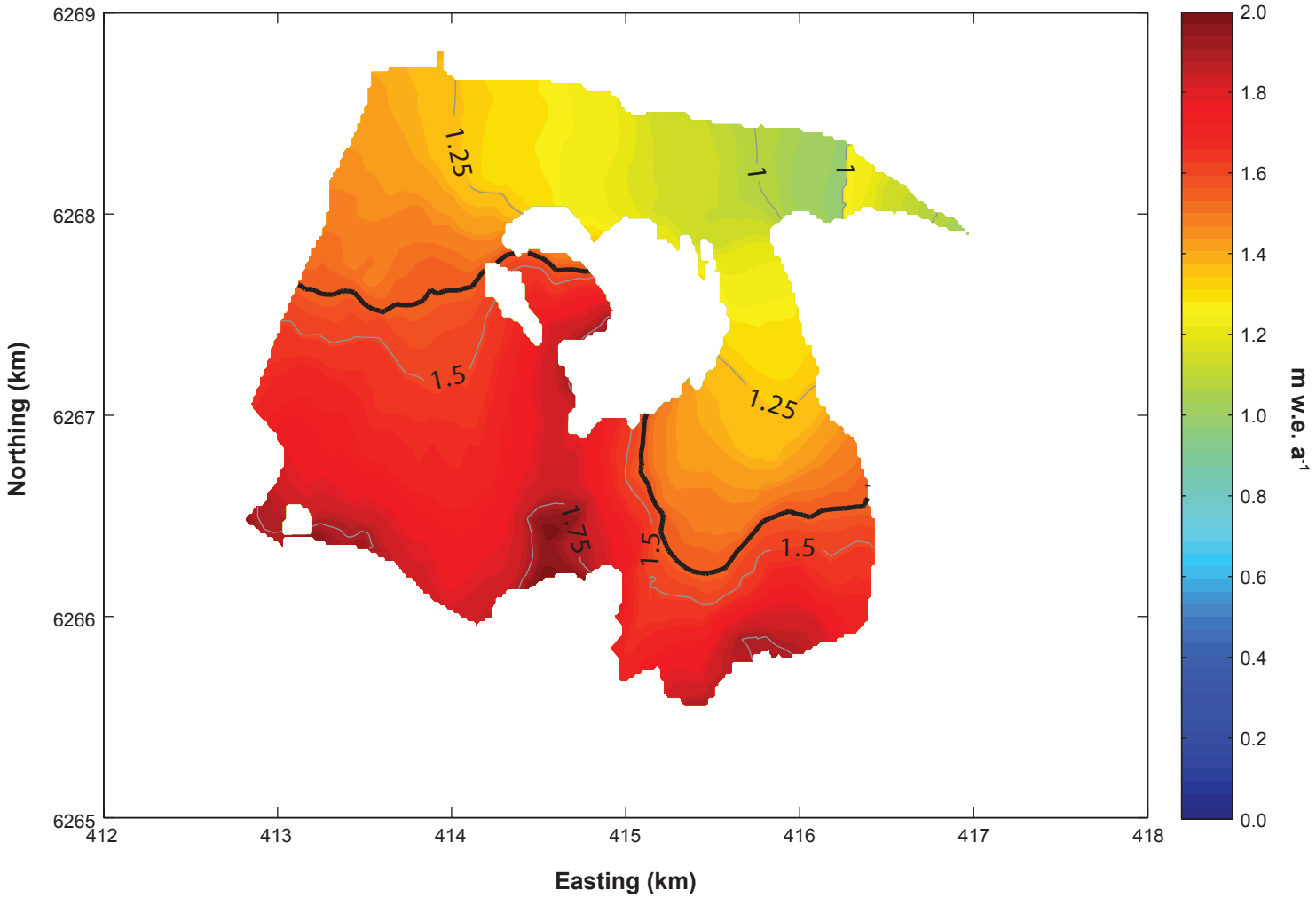

Figure A2-1

SEABRIDGE GOLD
KSM PROJECT

Distributed Winter Mass Balance for McTagg South and West

Figure A2-1

Rescan™ Engineers & Scientists

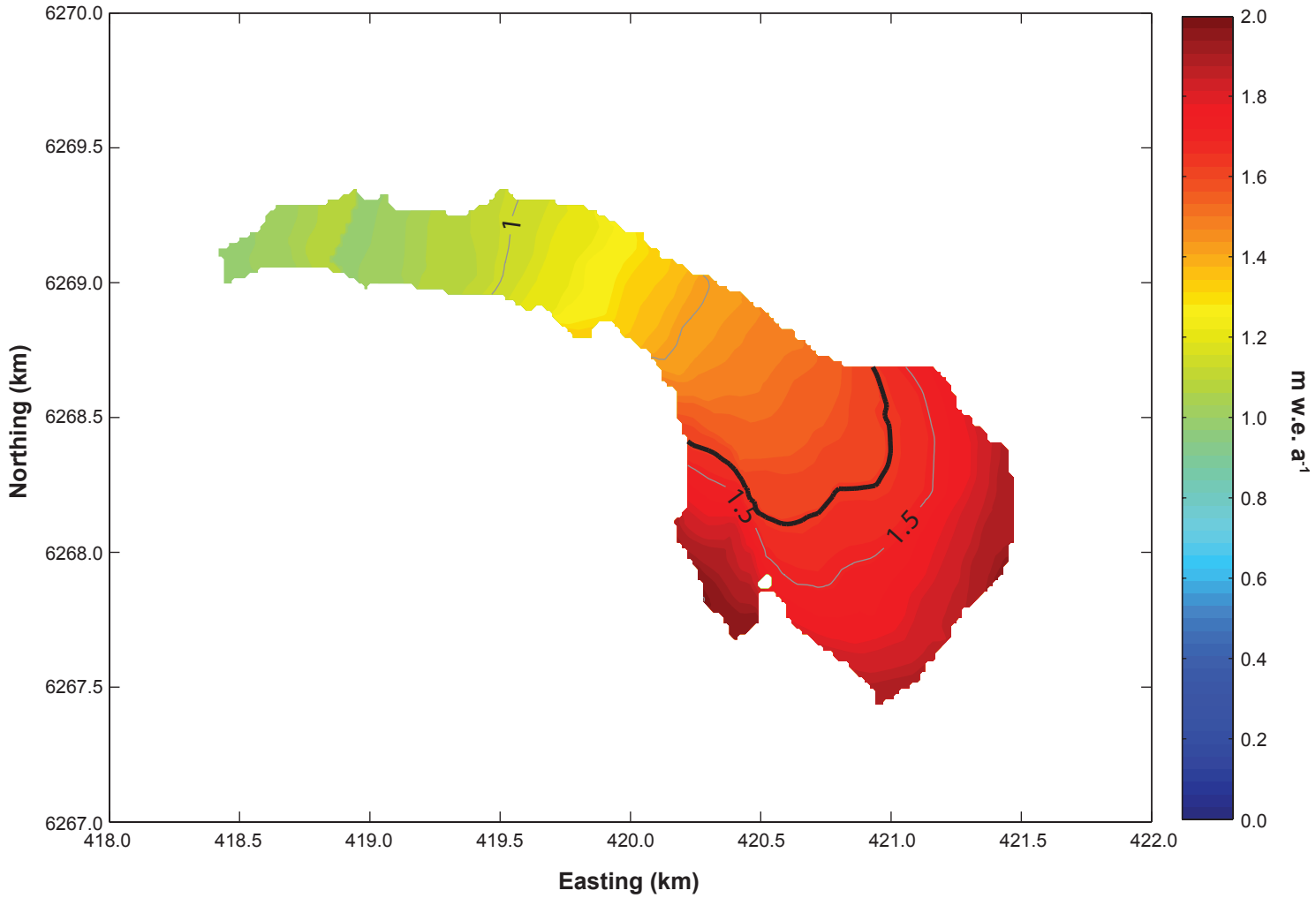

Figure A2-2

SEABRIDGE GOLD
KSM PROJECT

Distributed Winter Mass Balance for McTagg East

Figure A2-2

Rescan™ Engineers & Scientists

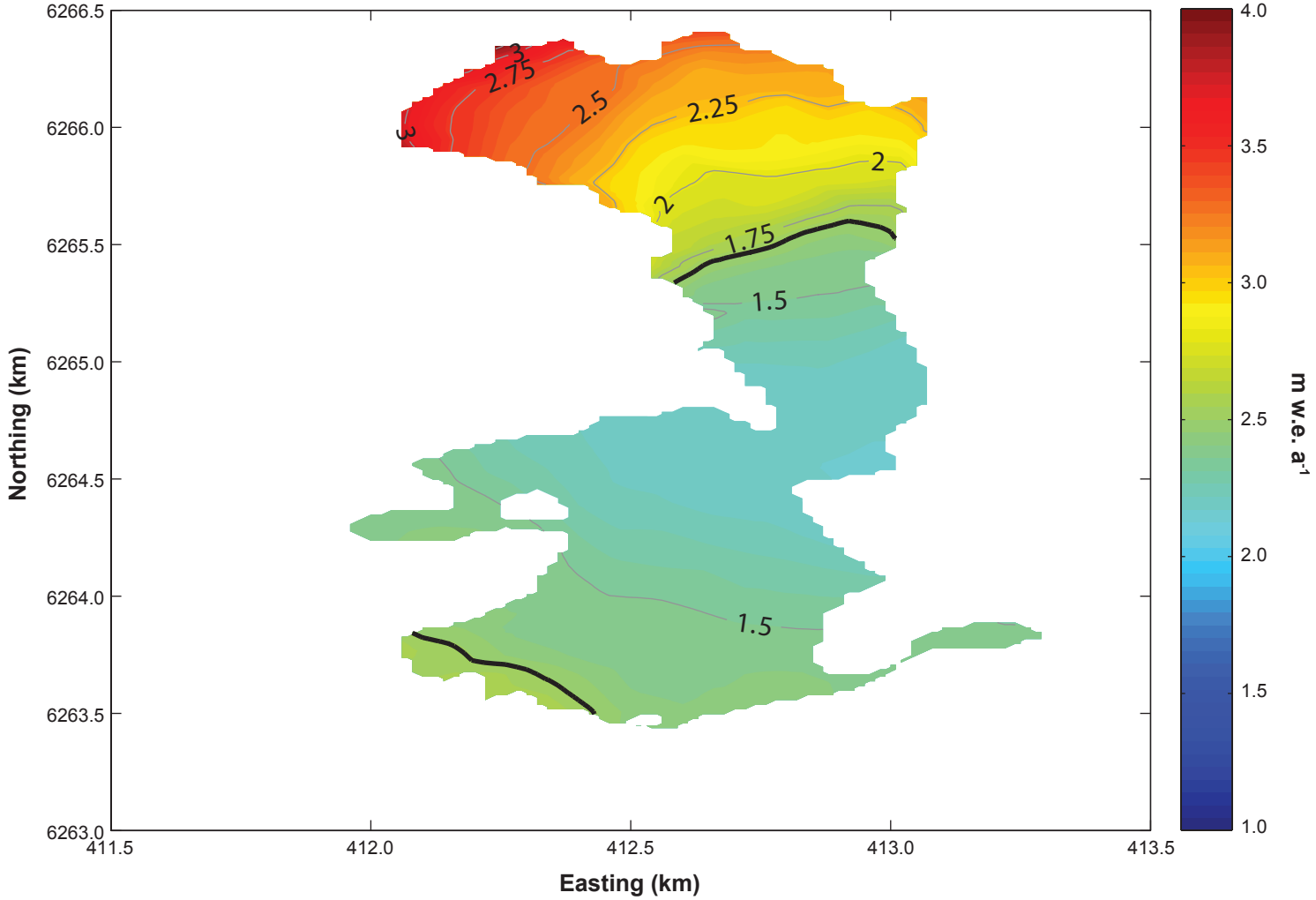

Figure A2-3

SEABRIDGE GOLD
KSM PROJECT

Distributed Winter Mass Balance for Gingras

Figure A2-3

Rescan™ Engineers & Scientists

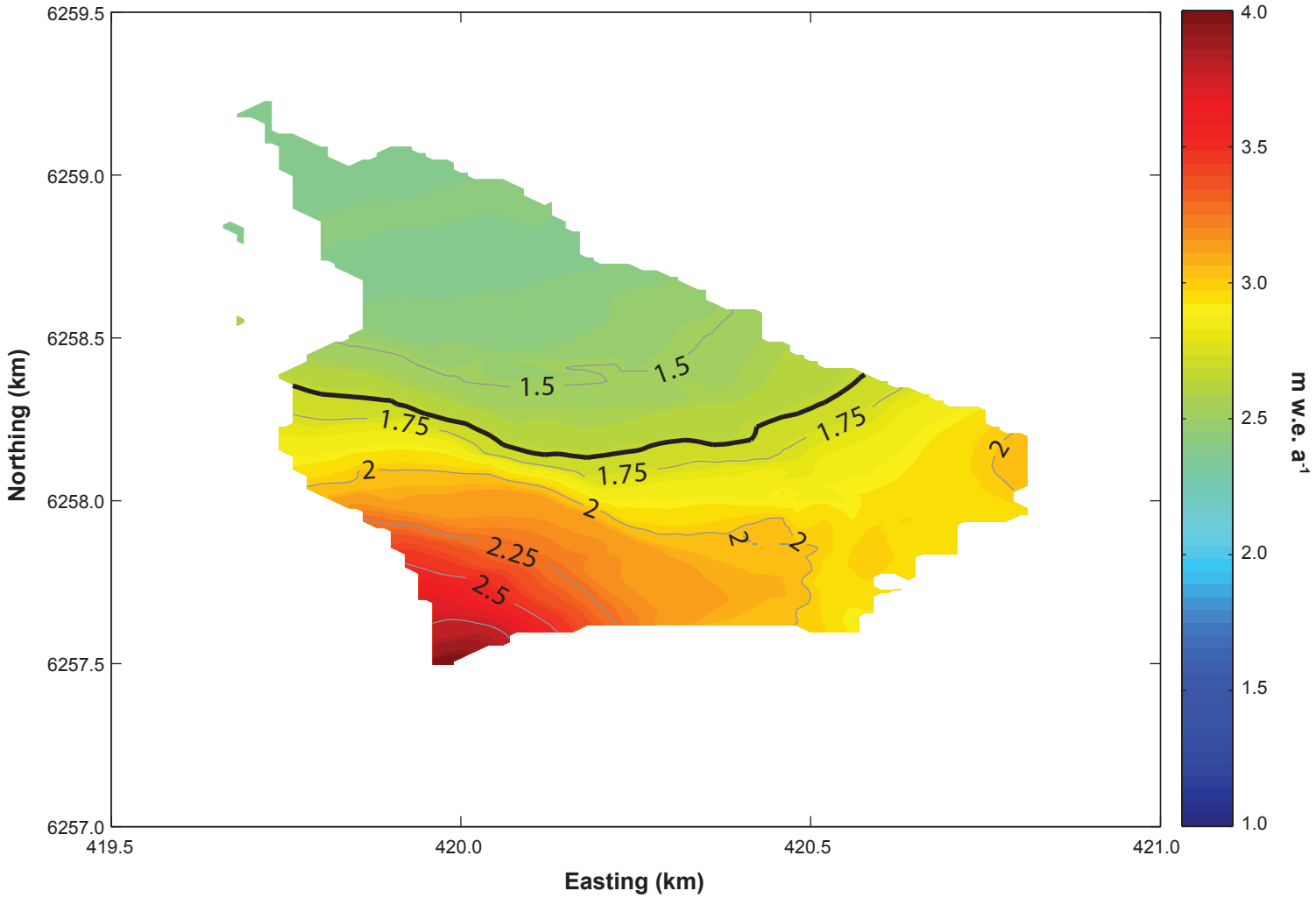

Figure A2-4

SEABRIDGE GOLD
KSM PROJECT

Distributed Winter Mass Balance for Kerr

Figure A2-4

Rescan™ Engineers & Scientists